University of Modena and Reggio Emilia

International Doctorate School in Clinical and Experimental Medicine
Cellular and Molecular Pathophysiology

XXVIII cycle

Effects of Lon protease silencing or inhibition on mitochondria of cancer cells

Author: Regina Bartolomeo

Tutor: Prof. Andrea Cossarizza

Co-Tutor: Prof. Marcello Pinti

Director of the school: Prof. Giuseppe Biagini

Academic year 2014-2015

1 INTRODUCTION 5

1.1 MITOCHONDRIA 5

1.1.1 Structure 5

1.1.2 Mitochondrial DNA 6

The replication of mtDNA 7

The transcription of mtDNA 8

1.1.3 Mitochondrial respiratory chain 9

1.1.4 Free radical generation 11

1.2 MITOCONDRIAL PROTEASE 13

1.3 THE LON PROTEASE 18

1.3.1 Structure 18

1.3.2 Functions 20

1.3.3 Regulation of Lon expression in physiological and pathological conditions 24

1.4 CANCER METABOLISM AND MITOCHONDRIA 27

1.4.1 Cancer metabolism: the Warburg effect and mitochondria 27

1.4.2 Lon protease and cancer 31

1.4.3 Inhibitors of Lon 34

2 AIM OF THE WORK 38

3 MATERIALS AND METHODS 39

3.1 CELL CULTURE 39

3.2 TISSUE SAMPLES AND PROTEIN EXTRACTION 40

3.3 CONSTRUCTS, RETROVIRUS PREPARATION, AND INFECTION 41

3.4 QUANTITATIVE REAL TIME PCR 43

Quantification of mitochondrial transcripts 43

Quantification of mtDNA 44

3.5 SDS-PAGE AND WESTERN BLOTTING 46

3.6 IMMUNOFLUORESCENCE ANALYSIS OF MITOCHONDRIAL MORPHOLOGY 47

3.7 TRANSMISSION ELECTRON MICROSCOPY 48

3.8 TWO-DIMENSIONAL GEL ELECTROPHORESIS (2-DE) 48

Sample preparation 48

Protein identification by MALDI-ToF/ToF-MS 49

Protein identification by LC–MS/MS analysis 50

3.9 ISOLATION OF MITOCHONDRIA 51

3.10 FLOW CYTOMETRY 51
Apoptosis and mitochondrial O_2^- 52
Cellular H_2O_2 53
Mitochondrial membrane potential (MMP) 53
MitoTracker 54
Caspase-3 activation 54
3.11 ATP QUANTIFICATION 54
3.12 GLUTATHIONE QUANTIFICATION 55
3.13 OXYGEN CONSUMPTION RATE (OCR) 55
3.14 IMMUNOHISTOCHEMICAL ANALYSIS 55
3.15 STATISTICAL ANALYSIS 56
4 RESULTS 57
4.1 LON EXPRESSION IS MODULATED IN HUMAN CANCER CELL LINES 57
4.2 LON DOWNREGULATION INCREASES CELL SUSCEPTIBILITY TO APOPTOSIS 58
4.3 LON DOWN-REGULATION STRONGLY AFFECTS MITOCHONDRIAL PROTEOME 61
4.4 LON DOWNREGULATION IMPAIRS MTDNA TRANSCRIPTION AND STEADY STATE LEVELS OF OXPHOS COMPLEXES 65
4.5 LON DOWNREGULATION IMPAIRS ATP SYNTHESIS AND MITOCHONDRIAL RESPIRATION 66
4.6 LON DOWNREGULATION ALTERS REDOX STATUS OF RKO CELLS 68
4.7 LON DOWNREGULATION ALTERS MITOCHONDRIAL MORPHOLOGY 69
4.8 LON IS OVEREXPRESSED IN CRC EX-VIVO CELLS 72
4.9 CDDO AND CDDO-ME DECREASE PROLIFERATION, INDUCE APOPTOSIS IN CANCER CELLS, AND INCREASE MITOCHONDRIAL HYDROGEN PEROXIDE AND MITOCHONDRIAL SUPEROXIDE ANION 75
4.10 CDDO AND CDDO-ME INDUCE MITOCHONDRIAL DEPOLARITATION 85
4.11 LON INHIBITION RESULTS IN ALTERED MORPHOLOGY OF MITOCHONDRIA 87
4.12 LON OVEREXPRESSION PROTECT CELLS FROM APOPTOSIS INDUCED BY CDDO AND CDDO-ME 89
5 DISCUSSION 91
6 REFERENCES 97

Summary

Lon is a nuclear-encoded, mitochondrial ATP-dependent protease that assists protein folding, degrades oxidized or damaged proteins preventing their accumulation, and participates in maintaining mitochondrial DNA (mtDNA) levels. It is induced by different stressors, and its expression and activity are modulated in different pathologies. Lon is up-regulated in several human cancer cells, and its down-regulation causes profound alterations of mitochondrial proteome and function, and cell death. Lon enzymatic activity is activated by ATP, and inhibited by the triterpenoid 2-cyano-3,12-dioxooleana-1,9-dien-28-oic acid (CDDO), or by its C-28 methyl ester derivative (CDDO-Me).

In order to clarify the role of Lon protease in cancer cells, we analyzed the effects of Lon down-regulation in RKO colon cancer cells, in which Lon could be conditionally silenced by RNA interference. We studied the impact of Lon down-regulation on cellular apoptosis, mtDNA and mtRNAs levels, mitochondrial functionality and mitochondrial morphology. Furthermore, we evaluated the effects of pharmacological inhibition of Lon, using CDDO or CDDO-Me, on mitochondria of three different cancer cell lines (RKO human colon cancer cells, HepG2 hepatocarcinoma cells and MCF7 breast carcinoma cells). We paid a particular attention to parameters such as membrane potential, mass, morphology, dynamics and ROS content, and Lon proteolytic activity.

Mitochondria of Lon-silenced cells displayed low levels of mtDNA transcripts, reduced levels of several subunits of oxidative phosphorylation complexes (Complex I being the most affected), a marked reduction of oxygen consumption rate, and impaired capability to synthetize ATP. Higher levels of hydrogen peroxide and mitochondrial superoxide anion could also be observed. Mitochondrial network appeared fragmented, with mitochondria heterogeneous in size and shape, dilated *cristae*, vacuoles and electrondense inclusions. In addition, we found that CDDO and CDDO-Me were potent stressors for mitochondria in cancer cells, rather than in normal non-transformed cells, being able to induce higher levels of ROS and altered mitochondrial morphology. In particular, these compounds caused depolarization of mitochondrial membrane, altered mitochondrial mass, and led to intrinsic apoptosis. The

overexpression of Lon could reduce apoptotic of cells treated with CDDO and CDDO-Me.

In conclusion, Lon can be considered a protein that does not initiate tumourigenesis *per se*, but it is important for cancer cell survival. Its pharmacological inhibition could represent a possible new anticancer strategy.

1. INTRODUCTION

1.1 Mitochondria

1.1.1 Structure

Mitochondria are membrane-enclosed organelles found in eukaryotic cells. Mitochondria are usually described as the “powerhouse unit” of the cell, because they contain the molecular machinery that governs many distinct metabolic pathways by which chemical energy (coming from carbohydrates, lipids, and proteins) is converted into ATP. Indeed, it is in this organelle that pyruvate oxidation, fatty acid β-oxidation, Krebs cycle and oxidative phosphorylation (OXPHOS) take place. The essential role of mitochondria in bioenergetic aspects of the cell is supported by the dynamics of this organelle, which is controlled by fusion and fission events. In addition, eukaryotic cells have the ability to initiate adaptative responses to different environmental stimuli, such as modifications in energy demands, cell growth, cell death or cell differentiation, by altering the number of mitochondria (enhanced or reduced mitochondrial biogenesis), changing their morphology, or remodeling the organization and distribution of mitochondria within the cell (1).

Mitochondria are bounded by two membrane systems, the inner and outer mitochondrial membranes which occasionally come together, rather like gap junctions, to form junctional complexes or contact sites. The inner mitochondrial membrane is largely impermeant and forms the major barrier between the cytosol and the mitochondrial matrix. It is organized in folds called *cristae*, which expand the surface area and contain mitochondrial respiratory chain complexes (figure 1). The space between the two membranes is referred to as the intermembrane space and is characterized by the presence of a large number of proteins, which play major roles in cell physiology, in mitochondrial energetics and in cell death most notably perhaps cytochrome c and creatine kinase. The outer membrane is relatively permeant to small molecules and ionic species, but recent studies suggest that it might form a more important and potentially regulated barrier (2). It contains several transport proteins, which allow large molecules to enter because the vast majority of mitochondrial

proteins are synthetized in the cytosol. They are characterized by a pre-sequence and other targeting sequences that direct proteins to the mitochondrial matrix, intermembrane space and inner or outer membranes via specialized import system (3).

Macroscopically, mitochondria exist as discrete and independent structures or form highly dynamic and interconnected networks depending on the tissue and on the cell status. The formation of a continuous *reticulum* might permit the diffusion of soluble messengers, such as calcium, that are essential for intracellular signaling (4). Indeed, mitochondria importance is not limited to cell metabolism, but during last decades has emerged its role as a master regulator controlling cell-wide stress responses and cell death.

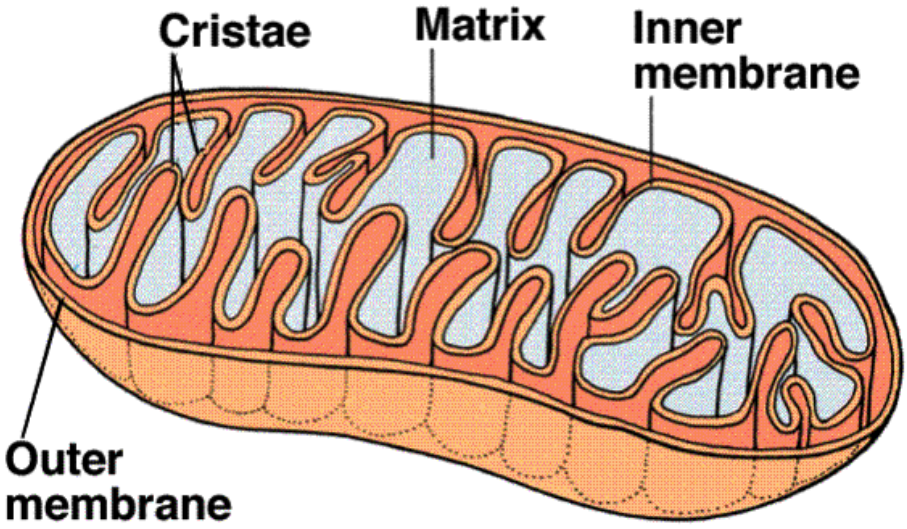

Figure 1: Schematic representation of mitochondrial structure principal components: outer membrane, inner membrane, cristae and matrix. Adapted from: J. Vander, J.H. Sherman, D.S. Luciano, Human Physiology: The Mechanisms of Body Function, 7th edition, McGraw-Hill Education, 1998.

1.1.2 Mitochondrial DNA

Each cell may contain thousands of copies of mtDNA. The primary remaining evidence of their independent bacterial origin is the presence of mitochondrial DNA (mtDNA),

a simple circular genome that has structural characteristics very similar to the circular DNA of primitive bacteria (5). Mitochondria and chloroplasts are the only structures in cells to possess their own DNA, which is distinct from the somatic DNA of the nucleus. Mitochondrial DNA (mtDNA) is a covalently closed circle with features very similar to the circular DNA of primitive bacteria. Indeed, the presence of mtDNA is consistent with the hypothesis that mitochondria have evolved from a bacterial progenitor, which was endosymbiont within some ancestral type of eukaryotic cell (6). Remarkably, phylogenetic analyses have revealed that the progenitor of Rickettsia prowazekii, the causative agent of epidemic typhus, is the closest ancestor of mitochondria (7). Interestingly, mitochondrial DNA encodes only a fraction of the proteins that are fundamental for mitochondrial function, while the vast majority of proteins required to build mammalian mitochondria are encoded in the nucleus and transported to the mitochondria where they become components of the mitochondrial transport machinery and regulatory system. Human mtDNA is a circle of only 16,569 bp double stranded DNA with a heavy (H) chain and a light (L) chains, which are guanine- and cytosine-rich, respectively. It contains 37 genes, thirteen of them encoding for proteins, which are all components of the respiratory chain. In addition, some 24 other genes are present on the mtDNA, encoding two rRNAS and 22 tRNAs required in turn to synthesise the 13 proteins (2, 8). Several specific proteins and enzymes are involved in mitochondria replication and translation processes, such as DNA polymerase γ (pol-γ), mitochondrial single-stranded DNA-binding protein (mtSSB), mtDNA helicase (Twinkle), and a number of accessory proteins and transcription factors, including the mitochondrial transcription factor A (TFAM) and the mitochondrial transcription specificity factors (TFB1M and TFB2M) (9).

Despite the knowledge of working principles of this machinery is almost exhaustive, the fine regulation of this mechanism in response to cell metabolic needs is still largely unknown.

The replication of mtDNA

Several specific proteins and enzymes are involved in mitochondria replication and translation processes, such as DNA polymerase γ (pol-γ), mitochondrial single-

stranded DNA-binding protein (mtSSB), mtDNA helicase (Twinkle), and a number of accessory proteins and transcription factors, including the mitochondrial transcription factor A (TFAM) and the mitochondrial transcription specificity factors (TFB1M and TFB2M) (9). Polymerase γ (pol-γ), is solely responsible for DNA replication and repair in mitochondria. Human pol-γ is an asymmetric heterotrimer composed of one catalytic subunit of 140 kDa (p140) and two 55 kDa accessory subunits (p55) that form a dimer. The catalytic subunit possesses confers enzyme processivity and tight binding of polS complex to mtDNA (10). The exonuclease activity preferentially removes mismatched nucleotides from the 3' end of a duplex DNA and is not active toward DNA with matched 3' ends (11). An efficient proofreading by the intrinsic exonuclease acitivity, along with high nucleotide selectivity and slow mismatch extension, assure the high base substitution fidelity of wild type human pol-γ. Conversely, proofreading-deficient pol-γ synthesizes DNA with substantially reduced fidelity, thus predicting high mutation rate which leads to a mutator phenotype in vivo (12).

Two models of mtDNA replication have been proposed, a displacement replication model and a symmetric bidirectional replication model (13). In both models DNA synthesis is catalized by pol-γ. The displacement model proceeds with single-stranded replication of the Hstrand with further expansion and displacement of the D loop. The intermediates are called expanded D-loops. After two-thirds of the nascent H strand is replicated, the L-strand origin (OL) is exposed, allowing subsequent synthesis of the new L strand in the opposite direction. The asymmetry of strand synthesis leaves one segregated daughter molecule with an incompletely synthesized L strand, called a gapped circle (GpC). In the strand-coupled or symmetric model both strands are synthesized bidirectionally as the double-stranded replication forks proceed through the length of the mtDNA (13, 14).

The transcription of mtDNA

The transcription of mtDNA depends essentially on the mitochondrial RNA polymerase (POLRMT), and other accessory proteins, including TFAM, TFB1M and TFB2M. TFAM is essential for transcription activation, TFB1M works as a transcription factor and TFB2M is responsible for rRNA methylation. The mechanisms of mtDNA

transcription are well established. In human cells mtDNA contains three promoter regions for transcription initiation: the light strand promoter (LSP) and the heavy strand promoter (HSP)-1 and -2 (15). Transcription from the mitochondrial promoters produce polycistronic precursor RNAs which are then processed to produce mRNA, tRNA and rRNA molecules. The H strand transcription produces two polycistronic molecules; when transcription is initiated from HSP1 two rRNA genes and 12mRNA-encoding genes are transcribed whereas when transcription is initiated from HSP2 two rRNA genes and 16S rRNA-encoding gene are transcribed (15). These polycistronic precursor rRNAs are then processed to produce the individual tRNA and mRNA molecules (16). All of the proteins and rRNA genes are immediately flanked by at least one tRNA gene whereas excision of tRNA molecules from the polycistronic transcripts is used to produce mature mRNA and rRNA molecules (15).

Despite the knowledge of mtDNA transcription is almost exhaustive, the fine regulation of this mechanism is largely unknown. It has been reported that several transcription factors, including the tumour suppressor p53, retinoid-X receptor a (RXRa) and the thyroid hormone receptor (TR), might directly influence mtDNA transcription (15). TR binds directly to regulatory regions in mtDNA and it modulates mitochondrial RNA levels and the mRNA/rRNA ratio by influencing the transcriptional rate (17). 9-cis retinoic acid induces RXRa translocation into MT and increases levels of mtDNA transcription and translation (18).

1.1.3 Mitochondrial respiratory chain

The mitochondrial respiratory chain is formed by a series of protein complexes responsible for the OXPHOS process. It is organized in four multisubunit enzymes embedded in the mitochondrial inner membrane, namely complex I, II, III and IV. These complexes are also indicated as NADH dehydrogenase, succinate dehydrogenase, ubiquinol-cytochrome c reductase and cytochrome c oxidase, respectively (2). In addition, two diffusible factors that function as electron shuttles within the mitochondrial intermembrane space take part to the system: coenzyme Q, which is a lipophilic quinone, and cytochrome c, which is an hydrophilic heme protein localized on the external surface of the inner membrane (19). It has been calculated

that approximately 80 proteins make up the respiratory chain and about 16% of these proteins are encoded by mtDNA, whereas all the other by nuclear DNA (nDNA) (20). Complex II, coenzyme Q, and cytochrome c are exclusively encoded by nDNA. Conversely, complexes I, III, IV and V contain some subunits encoded by mtDNA (20). It has been demonstrated that mitochondrial complexes do not exist as physically separated entities within the inner mitochondrial membrane, but rather co-assemble into higher-ordered structures referred to as "supercomplexes" (21). All these mitochondrial complexes form an electron transport chain that transfer electrons from a donor, e.g. reduced NADH accumulated during metabolic processes (tricarboxylic acid cycle, pyruvate oxidation, fatty acid and amino acid catabolism) to an acceptor, i.e. molecular oxygen (O_2), thus reducing it to water. The free energy decrease accompanying electron transfer is exploited to create an electrochemical gradient by proton translocation from the matrix to the intermembrane space (22). The proton gradient is then used as a source of energy to synthesize ATP from adenosine diphosphate (ADP) and inorganic phosphate (P**i**) by the ATP synthase complex or complex V. The synthesized ATP is moved to the cytoplasm in exchange with ADP by the ATP/ADP translocase. The process of electron transport and consequent ATP synthesis is shown in figure 2.

Mitochondrial respiratory function can be negatively affected by multiple factors, including mutations in mitochondrial DNA, malfunction of the electron transport chain, aberrant expression of enzymes involved in energy metabolism, and insufficient oxygen available in the cellular microenvironment. It is known that mtDNA contains a displacement loop, and the coding gene sequence for thirteen important protein components of the mitochondrial respiratory complexes without introns. Mutations in mtDNA are likely to cause alterations of the encoded protein and compromise the respiratory chain function. Thus, the frequent mtDNA mutations observed in a variety of human cancers are thought to contribute to respiratory malfunction in cancer cells (23, 24). The constant generation of reactive oxygen species within the mitochondria and the increased free radical stress in cancer cells may cause further damage to both mtDNA and the electron transport chain, thus amplifying respiratory malfunctions and dependency on glycolysis (25, 26).

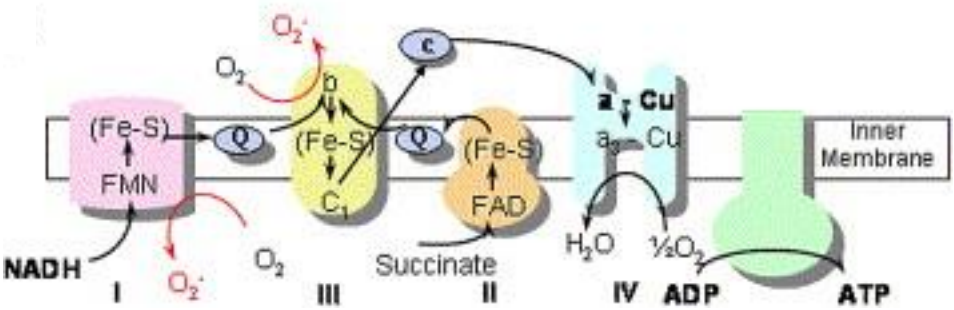

Figure 2: Representation of mitochondrial respiratory chain complexes. Electrons are transferred to coenzyme Q (Q) through Complex I and II. Q shuttles electrons to Complex III. Then cytochrome c (Cyt c) shuttles electrons to Complex IV. These reactions are also associated with the transfer of protons across the mitochondrial inner membrane, from matrix into the intermembrane space, to establish an electrochemical proton gradient that determine the phosphorylation of ADP to ATP by complex V or F_1F_0-ATP synthase. Adapted from: Duchen MR. Mitochondria in health and disease: perspectives on new mitochonbdrial biology. Mol Aspects Med, 25(4):365–451, 2004.

1.1.4 Free radical generation

In most cell types, mitochondria appear to represent one of the major sources of generation of free radicals or reactive oxygen species (ROS), in particular because of the generation of unpaired electron during the oxidative phosphorylation. The interaction of these electrons with O_2 results in the generation of superoxide ions, highly reactive free radical species. These are readily interconverted to other radical species, such as hydroxyl ions (OH^-) and H_2O_2 (27, 28). Endogenous ROS can be produced by different reactions that take place in mitochondria; however, it is accepted that the major producers of superoxide anion (O_2^-) are complexes I and III of the respiratory chain (19). It is widely assumed that the major impact of such ROS generation is harmful although recently it has been suggested that mitochondrial ROS generation may play a significant physiological signaling role. Nevertheless, ROS may cause cellular damages which include DNA oxidation, protein carbonylation and lipid peroxidation. Mitochondria represent not only a major source of ROS generation, but also a major target of ROS induced damage. DNA is one of the major target of excessive ROS levels and mtDNA is even more susceptible to oxidative damage than nDNA, probably because of its close proximity to the site of ROS generation and lack of histones protection. Carbonylation reduces or abrogates the catalytic functions of

targeted proteins and may trigger the formation of potentially cytotoxic high-molecular-weight complexes (28). Lipid peroxidation reactions principally cause the formation of 4-hydroxy-nonenal which affects the functionality of several membrane proteins (29).

Cells have evolved several antioxidant defenses, including repair and detoxifying enzymes, and small scavenger molecules, such as reduced glutathione (GSH). The intracellular ROS-scavenging system includes superoxide dismutases (SOD), glutathione peroxidase GPx, peroxiredoxins, thioredoxins, glutaredoxins, and catalases. In mitochondria, O_2^- can be dismutated to H_2O_2 by two enzymes, namely copper-zinc superoxide dismutase (CuZnSOD) and manganese superoxide dismutase (MnSOD) that are present in the intermembrane space and in the mitochondrial matrix, respectively. Once generated, H_2O_2 is mostly decomposed by GPx in mitochondria or by catalase in the cytosol.

Another contribute to antioxidant defenses is the proteolytic degradation of damaged proteins after oxidative modifications. Rapid elimination of damaged proteins is crucial to prevent the formation of large aggregates and ensures a physiologic protein turnover. In mammalian cells, the most important proteolytic system is represented by the proteasome in the cytoplasm, nucleus and endoplasmic reticulum (30). However, this proteolytic complex is not present in mitochondria that, in turn, contain a proteolytic activity in the matrix (31). Severe oxidative stress can lead to mitochondrial DNA damage, which causes impaired electron transport chain (32) and dysfunction of mitochondrial proteins, resulting in functional impairment and even cell death (27). Thus, mitochondrial management of oxidative damage appears to be crucial in maintaining cellular homeostasis. Dysfunctional mitochondria and elevated production of free radical species have been associated with numerous diseases and with the aging process (33, 34).

1.2 Mitocondrial protease

Mitochondria are cell organelles involved in the processes of cell life and death and therefore also in tumoral transformation. Functional integrity and rapid and appropriate responses to physiological and pathophysiological stimuli are required for mitochondria to meet cellular energy demands. In addition, mitochondria participate in cellular Ca^{2}+ homeostasis, signaling cascades.

The mitochondrial respiratory chain is one of the main sources of endogenous ROS and mitochondrial proteins represent targets for oxidative modification and loss in function. An important factor for protein maintenance in the presence of oxidative stress is enzymatic reversal of oxidative modifications and/or protein degradation.

Mitochondrial proteases degrade misfolded and non-assembled polypeptides, thus performing quality control surveillance in the organelle (31).

For many years, mitochondrial proteases were thought to be mainly involved in the degradation of misfolded and damaged proteins as part of a quality control system, as well as in the processing of proteins that have been imported into mitochondria. However, it is becoming increasingly clear that mitochondrial proteases are highly specific and perform highly regulated proteolytic reactions. Thus, these enzymes modulate many biochemical activities that are essential for mitochondrial function.

Mitochondrial proteases are a highly diverse group of multifunctional enzymes that share a mitochondrial location, being located either exclusively in mitochondria or in both the mitochondrial and cytosolic compartments. They are all encoded by nuclear genes, which are translated in the cytoplasm and then permanently or temporarily translocated to mitochondria; and regulate mitochondrial functions, both in healthy and stressed or damaged mitochondria. (35)

Human mitochondrial proteases consist of twenty-five proteins that can be classified into three different categories, according to their location, function, and structural and proteolytic characteristics. Each category can be divided into three subcategories depending on catalytic class: that is, cysteine, metallo and serine proteases.

The first group is formed by the “intrinsic” mitochondrial proteases, which function mainly in the mitochondrion. This group comprises all proteolytic enzymes that localize to the different mitochondrial compartments, as well as proteases that reside

in both the cytosol and in mitochondria but mainly function in mitochondria. The second group includes the “pseudo” mitochondrial proteases that have structural similarity to proteases but lack some key residues for catalysis. These can regulate the activity of homologous proteases or perform completely different functions. They can regulate the activity of homologous proteases, such as mitochondrial-processing peptidase subunit-α (PMPCA; also known as α-MPP), or they may perform completely different functions, for example, cytochrome b–c_1 complex subunit 1 (UQCRC1) and UQCRC2, which are part of the respiratory chain. Finally, the third group comprises proteases that are known as “transient” because they translocate to mitochondria only under certain circumstances to perform additional proteolytic activities (figure 3) (35).

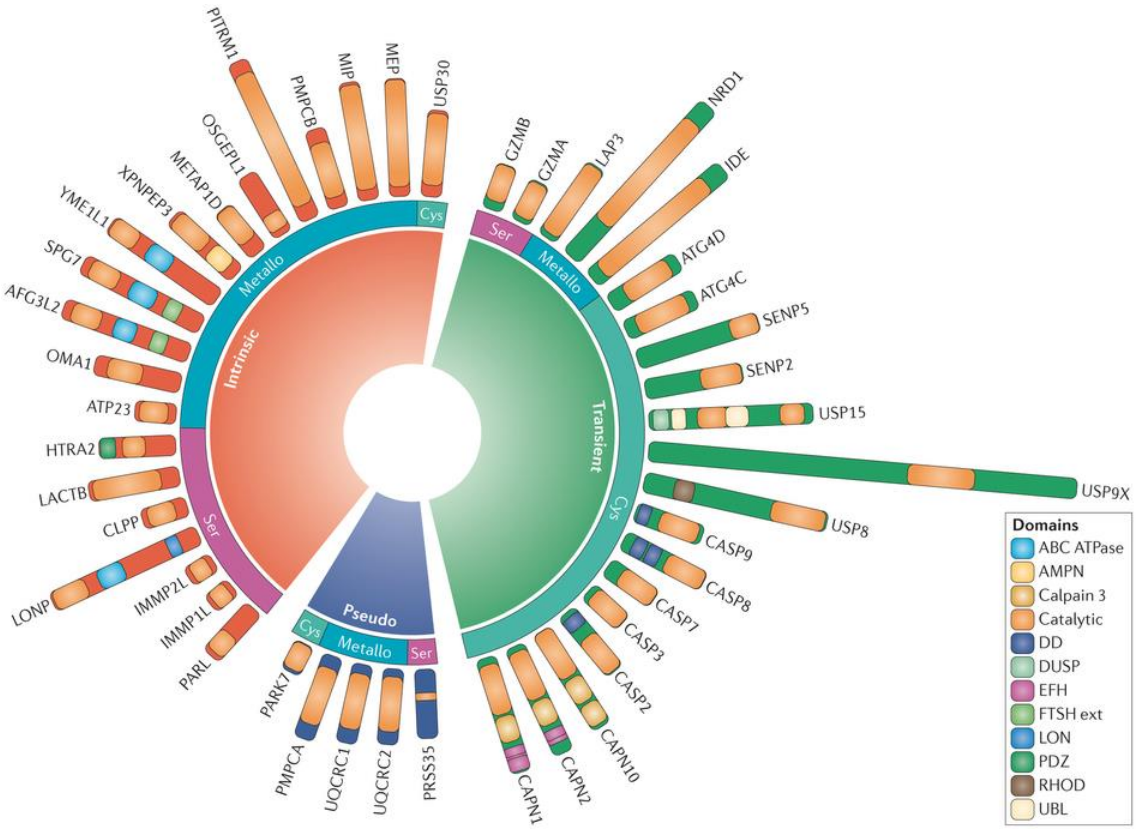

Figure 3: Classification of human mitoproteases. Human mitoproteases are classified into three different categories, according to their location, function, and structural and proteolytic characteristics. The first group is formed by 20 "intrinsic" mitochondrial protease that function mainly in the mitochondrion. The second group includes five "pseudo" mitochondrial protease that have structural similarity to proteases but lack some key residues for catalysis. These can regulate the activity of homologous proteases or perform completely different functions. The third group comprises at least 20 proteases that are known as "transient". These transiently translocate to mitochondria to perform additional proteolytic activities. Each category is also divided into three different subcategories depending on catalytic class: cysteine, metallo and serine proteases. Mitochondrial protease are represented around the circle with their amino termini oriented towards the centre. The relative length of each mitoprotease in the figure corresponds to the size of the protein in amino acids. The catalytic core domain and additional ancillary domains are shown in different colours. ABC ATPase, predicted ATPase of the ABC class domain; AFG3L, AFG3-like protein; AMPN, aminopeptidase P, N-terminal domain; calpain 3, calpain large subunit, domain 3; CAPN, calpain catalytic subunit; CASP, caspase; CLPP, ATP-dependent Clp protease proteolytic subunit; DD, death domain; DUSP, domain in ubiquitin-specific proteases; EFH, EF-hand, calcium binding motif; FTSH ext, FTSH extracellular domain; GZM, granzyme; IDE, insulin-degrading enzyme; IMMP, mitochondrial inner membrane protease subunit; LACTB, Ser protease β-lactamase-like protein; LAP3, leucyl aminopeptidase; LON, ATP-dependent protease La domain; LONP, Lon protease homologue; MEP, mitochondrial oligopeptidase M; METAP1D, Met aminopeptidase 1D; MIP, mitochondrial intermediate peptidase; NRD1, nardilysin; OSGEPL1, O-sialoglycoprotein endopeptidase-like protein 1; PARK7, DJ-1; PARL, presenilins-associated rhomboid-like protein; PITRM1, presequence protease; PMPC, mitochondrialprocessing peptidase subunit; PRSS35, inactive Ser protease 35; RHOD, rhodanese homology domain; SENP, sentrin-specific protease; SPG7, paraplegin; UBL, ubiquitin-like domain; UQCRC, cytochrome *b*–*c*1 complex subunit; USP, ubiquitin carboxyl-terminal hydrolase; XPNPEP3, X-Pro aminopeptidase 3; YME1L1, ATP-dependent zinc metalloprotease YME1L1. Adapted from: Quiros M., et al., New roles for mitochondrial proteases in health, ageing and disease. Nat Rev Mol Cell Biol, 16(6):345-59, 2015.

Mitochondrial intrinsic protease contribute to several process that are essential for mantaining mitochondrial function and homeostasis. Indeed they act mainly in mitochondria and the identification of disease-causing mutations in genes encoding

mitochondrial proteases, and the recent development of loss-of-function mouse models for several of these enzymes, have provided interesting information about their involvement in various biological processes.

Together with chaperones (which recognize unfolded polypeptides and contribute to their stabilization and solubility), participate in the import and trafficking of proteins from the cytosol into mitochondria, as well as being involved in the folding and activation of the imported proteins. They also act as “protein quality control” being involved in the degradation of non-assembled proteins and proteins that are misfolded or damaged as a result of reactive oxygen species. Finally, they mediate the processing of proteins involved in mitochondrial fusion and fission, regulating mitochondrial dynamics (35).

Mitochondrial protease-mediated quality control is the first line of defence against mitochondrial damage. In the inner membrane, protein quality control is mainly exerted by the intermembrane ATPases associated with diverse cellular activities (AAA) protease (iAAA protease) and matrix AAA (mAAA) protease. In humans, the mAAA protease can be composed of two different subunits, AFG3-like protein 2 (AFG3L2) and paraplegin (SPG7), which form heterooligomers, or alternatively can be a homo-oligomeric AFG3L2 complex, whereas the iAAA protease is composed entirely of an ATP-dependent zinc metallo protease YME1L1 subunit (36). AAA proteases exert quality control functions by degrading membrane-spanning and membrane-associate subunits of the electron transport chain that are damaged or non-assembled. Therefore, in the absence of any of these proteases, defective oxidative phosphorylation (OXPHOS) complexes accumulate (36). In addition, they promote mitochondrial protein synthesis, dynamics and calcium homeostasis.

LON protease is a highly conserved serine peptidase that has an important role in degrading misfolded, oxidized and damaged proteins in the mitochondrial matrix, which supports cell viability under different stress conditions (35). In addition to LON protease, the mitochondrial matrix contains serine protease CLPP, which forms the CLPXP complex with the chaperone ATP-dependent Clp protease ATP-binding subunit ClpX-like (CLPX). The function of CLPP is not yet clear, but it has been implicated in the degradation of misfolded proteins (37). It has been shown that CLPP is induced in response to unfolded protein stress in mammalian cells. Furthermore, homozygous

deletion of the gene encoding CLPP in mice results in the accumulation of CLPX and mtDNA, which leads to infertility, hearing loss and growth retardation (37).

Other ATP-independent proteases participate in the protein quality control that takes place in the intermembrane space. HTRA2, also known as OMI, which is highly conserved from bacteria to mammals, forms trimers in the mitochondrial intermembrane space and has key roles in the degradation of oxidized proteins. Loss of HTRA2 induces a decrease in both mitochondrial mass and mitochondrial membrane potential, which eventually results in ATP depletion. HTRA2 has also been associated with mtDNA maintenance, on the basis of mtDNA mutations that have been found in HTRA2-deficient mouse cells (35). In addition, HTRA2 exerts important coordinated roles during programmed cell death and several reports links HTRA2 dysregulation with cancer (31).

Many human diseases are caused by defects or mutations in these proteolytic enzymes. Mitochondrial proteases have been implicated in the maintenance of mitochondrial proteostasis and in the regulation of mitochondrial shape and function, which are crucial processes in cellular homeostasis. Mitochondrial proteases also modulate the ageing process, both negatively and positively, by controlling mitochondrial proteostasis or triggering stress responses that promote longevity.

Recent works have emphasized the functional importance of mitochondrial proteases in various stages of the development and progression of cancer.

Lon protease has a key role in tumour cells, inducing their metabolic reprogramming and protecting them from senescence.

Several studies have consistently reported that down-regulation of Lon protease in cancer cells decreases their tumorigenic properties, whereas up-regulation protects the cells from various stress conditions and increases their oncogenic potential (35).

1.2 The Lon Protease

1.2.1 Structure

The Lon protease family is the most widespread family of ATP-dependent proteases, which are highly conserved throughout all phylogenetic kingdoms from archaea, eubacteria, fungi to mitochondria and peroxisomes of lower and higher eukaryotes (38-40). Prokaryotic Lon protease is a key enzyme with a protein quality control and regulatory function by degrading unfolded and damaged proteins and numerous cellular regulatory proteins, respectively (41). Lon protease it is up-regulated under stress conditions; it is essential for cellular homeostasis, for survival from DNA damage and developmental changes in response to numerous stresses, through the control of protein machinery and the regulation of metabolism (42). Finally, bacterial Lon is able to bind DNA, in a sequence specific manner (43).

Eukaryotic Lon proteases exhibit similar functions especially in mitochondria and endoplasmic reticulum. Mitochondrial Lon protease shares the majority of properties with bacterial Lon, including the capacity to bind DNA and the essential role in protein quality control system by eliminating abnormal proteins (38). Although it is still not clear whether the mitochondrial Lon of *eukarya* has the same functions as bacterial Lon in regulating gene expression of certain specific proteins, observation made on the forms expressed by the filamentous fungus *Pseudosporaanserina* (PaLon) and by the plant *Arabidopsis thaliana* (AtLon), suggest that Lon can exert some important regulatory functions. Indeed, PaLON1 is essential in extreme growth conditions (high and low temperatures), in ascospore germination and sexual reproduction, two regulated developmental steps (44), and mutated forms of PaLON1 impact plant development (45).

The importance of both prokaryotic and eukaryotic Lon proteases has been demonstrated in yeast cells, in which the disruption of a functional PIM1 gene, encoding for the yeast Lon protease, determines the accumulation of electron-dense inclusions in the mitochondrial matrix and the alteration of mtDNA, thus leading to mitochondrial functionality impairment (46, 47). Because mitochondria are a major source of free radical generation in cells, and the loss of Lon results in damaged mitochondria, this might contribute to a vicious cycle of ROS generation within the

cell.

Human Lon protease is an ATP-dependent mitochondrial matrix protease. The majority of Lon protease is soluble in the matrix whereas a small fraction is associated with the inner membrane, where mitochondrial nucleoids are present (48). Lon is encoded by the nuclear PRSS15 gene, which is located in the region p13.2 of Chr 19 and is approximately 29,000 base pairs long (49). The encoded protein is initially synthesized in the cytosol as a precursor carrying an amino-terminal mitochondrial targeting sequence (MTS). After being imported into the matrix, the MTS is cleaved leaving the mature form of the protein (with a molecular weight of approximately 100 kDa) (48, 50).

Lon cDNA is approximately 3,500 bp long and it is characterized by a 61-bp 5' -terminal fragment, a 2,814-bp open reading frame and a 518-bp 3' -UTR with three potential polyadenylation signals (51). The aminoacid sequence includes 963 residues, more than 30% of which are identical with those of eubacterial Lon proteases; the N-terminal region is the most divergent in both amino acid composition and length whereas the middle and the C-terminal regions are pronouncedly conserved (48, 46). The LON protease is formed by three domains conserved along evolution (49). The N-terminal domain is responsible for interactions with protein substrates, the AAA+ module is involved in ATP binding and in ATP hydrolysis, and the third domain carries the aminoacidic residues necessary for catalyzing proteolysis (Figure 4) (53).

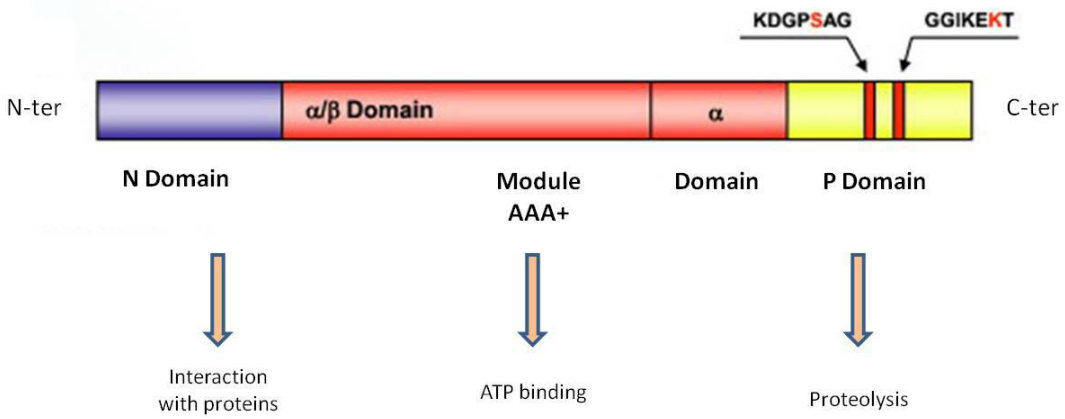

Figure 4: Schematic representation of domain organization of human Lon protease. Abbreviations: N, N-terminal domain (interaction with substrates); AAA, ATPase associated with various cellular activities; α/β domain, ATP binding site; α domain, ATP hydrolysis domain; P domain, proteolytic domain. Adapted from: Bulteau AL, Bayot A. Mitochondrial proteases and cancer. Biochim Biophys Acta, 1807(6):595–601, 2011.

Lon acts as a serine protease and, in most cases, does not recognize a specific consensus peptide sequence but prefers hydrophobic sequences adjacent to scissile bond (54). Its proteolytic activity is stimulated by ATP and inhibited by ADP, indicating regulation in response to the energy status of the cell (55, 56). Lon is expressed ubiquitously, with a certain degree of variability among different tissues and cells. High levels of Lon mRNA have been observed in brain, liver, heart, skeletal muscle, placenta, and lower but clearly detectable levels in lung, kidney and pancreas (49, 57). There are few compounds known to inhibit Lon, including coumarinic derivatives, proteasome inhibitors at very low levels (58) and the triterpenoid 2-cyano-3,12-dioxooleana-1,9-dien-28-oic acid (CDDO) or its C-28 methyl ester derivative (CDDO-Me) (59).

1.2.2 Functions

The Lon protease activity has been identified more than 30 years ago in *Escherichia coli* (60), and the gene encoding Lon was cloned in 1984; the human homologue (LONP1, best known as Lon or mitochondrial Lon) was identified in 1993 (49, 57), as a nuclear gene encoded mitochondrial protein of approximately 100 kDa (47), ubiquitously expressed in tissues and cells. Despite its strong conservation throughout evolution, relatively little attention has been paid to the role of Lon in the normal

physiology of mitochondria, and to its possible involvement in the pathogenesis of human diseases. However, in the last few years Lon has been gaining the centre of the scene as a fundamental component of mitochondrial quality control, and as an important factor in the mitochondrial alterations that can be observed in chronic diseases and cancer. In humans, Lon is involved in several aspects of mitochondrial biology. Lon belongs to the mitochondrial proteolytic systems, even if it is not part of the mitochondrial unfolded protein response. Mammalian LON displays several crucial properties, which include: binding and hydrolizing of ATP and protein substrate (i.e. misfolded and oxidatively damaged proteins for quality control or other proteins as a regulatory mechanism), chaperoning and mtDNA binding (figure 5) (61-63).

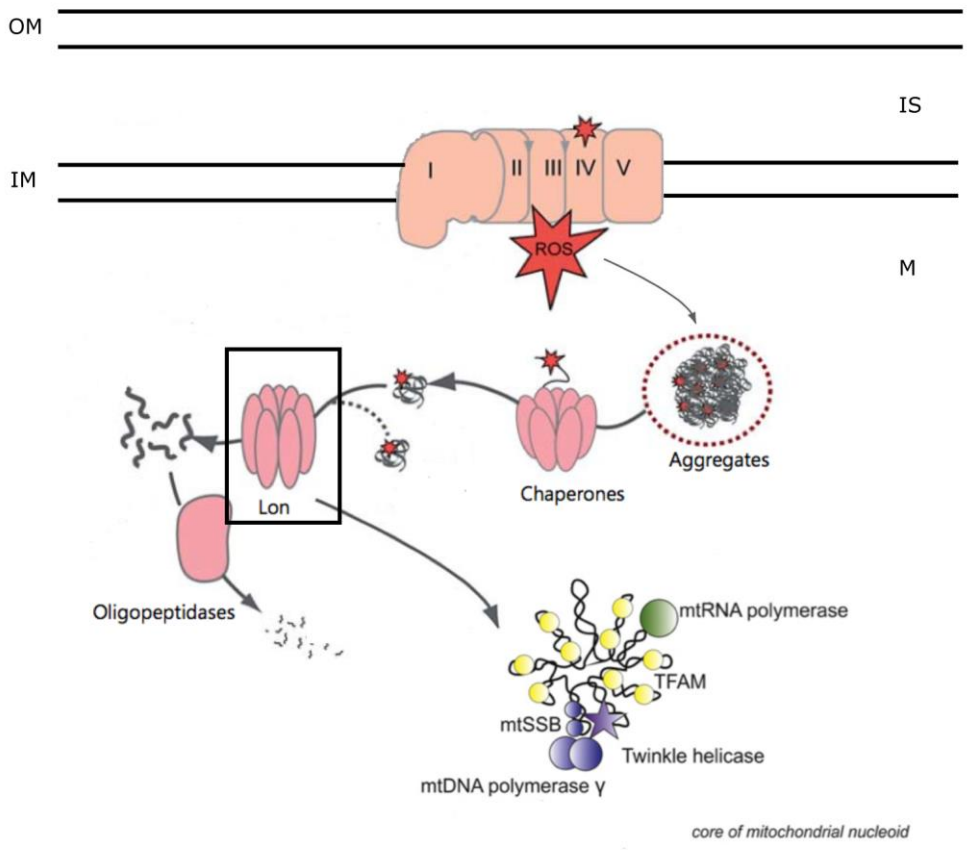

Figure 5: Schematic representation of Lon protease functions. First, Lon degrades aggregated protein damaged by reactive oxygen species (ROS) produced by oxidative phosphorylation complexes (I, II, III, IV, V). Second, it binds to mitochondrial nucleoids, composed of mtDNA and a series of proteins (mtDNA polymerase γ, mtSSB, Twinkle helicase, TFAM and mtRNA polymerase), to regulate mtDNA maintenance and transcription. Adapted from: Ambro, L., et al., The influence of ATP-dependent proteases on a variety of nucleoid-associated processes. J Struct Biol, 2012. Osiewacz H.D. and D. Bernhardt, Mitochondrial quality control: impact on aging and life span – a mini-review, Gerontology, 59(5):413-20, 2013.

Several reports indicate that Lon expression and/or activity increase in the presence of high levels of carbonylated proteins, as well as proteins modified by peroxidation and glycation (64, 65). Indeed, Lon primarily degrades misfolded and damaged proteins, and its down-regulation leads to profound alteration of mitochondrial proteome (66). However, the direct involvement of Lon in the degradation of putative proteins has been demonstrated only for aconitase (67), the 5-aminolevulinic acid synthase (ALAS-1) (68), the steroidogenic acute regulatory protein (StAR) (69), the mitochondrial transcription factor A (TFAM) (70), the glutaminase C (71) and the cystathionine β-synthase (CBS) (72). Interestingly, two out of six of these proteins participate directly or indirectly, in TCA cycle: aconitase catalyzes the isomerization of citrate to isocitrate, and is highy susceptible to mild oxidative damage (73), whereas glutaminase C catalyzes the conversion of glutamine to glutamate, which is not an intermediate of Krebs cycle but can be converted to α-ketoglutarate.

It has been hypotesized that, by degrading mildly oxidized proteins, LON protease may prevent more extensive oxidative damage, which could compromise mitochondrial functionality and cell viability. Indeed, the down-regulation of PRSS15 using morpholino oligonucleotides determines ATP depletion, impairment of mitochondrial respiration, decreased mitochondrial mass, and high sensitivity to apoptosis inhuman fibroblasts (74). Changes in the expression levels of several subunits of complex I and complex V were also reported by Quiros *et al.* (75) indicating that Lon modulation leads to changes in cell bioenergetics through the remodelling of OXPHOS subunits.

The link between Lon proteolytic activity and mitochondrial respiration is important also in the presence of hypoxia and oxidative stress. In hypoxic conditions, Lon is required for the degradation of cytochrome *c* oxidase (COX), subunit 4, isoform 1 (COX4-1) to optimize the efficiency of respiration at low O_2 concentration (76, 77). Mild oxidative modification in the aconitase results in increased exposure of hydrophobic residues and increased susceptibility to proteolysis by Lon (67). Taken together, these examples demonstrate that Lon plays a role in the regulation of mitochondrial and OXPHOS functions.

Lon does not recognize a specific consensus peptide sequence but prefers hydrophobic sequences adjacent to scissile bond (78). Its proteolytic activity is

stimulated by ATP and inhibited by ADP, indicating regulation in response to the energy status of the cell (79, 80). Nevertheless it has been observed that hydrophobicity does not appear to be an essential feature of the sequence element identified (81). Moreover, Lon could recognize proteins even in a folded functional state (79) in an ATP-powered process, indicating that its action is not limited to misfolded or damaged substrates, thus highlighting new aspects of the complex and still unclear mechanism of this protease (82, 83).

LON binding to mtDNA strongly depends on several factors, which include: i) the single stranded state of mtDNA; ii) the availability of mtDNA binding sites as they have to be free from other proteins; iii) the state of the cell. LON binds preferentially ssDNA with specificity for a G-rich consensus sequence (TTGGTAGGGGGATGA) either in vitro (61, 62) or in vivo (84). ATP, as well as its non-hydrolyzable analogs, blocks LON binding to ssDNA or ssRNA whereas the presence of a protein substrate increases binding affinity of LON to DNA of 2-6- fold (62). The DNA and RNA binding activity of LON provides a mechanism by which a protease can be recruited to mtDNA to degrade or process proteins involved in mtDNA replication and transcription (62). Indeed, LON interacts with pol-γ, the twinkle helicase, mtSSB and PDIP38 and it selectively degrades both TFAM and mtDNA pol-γ catalytic subunit A (pol-γA) when they are not bound to mtDNA (85). On the contrary, when pol-γA and TFAM are bound to DNA, they are resistant to LON proteolysis. The binding of LON to mtDNA strongly depends on the state of the cells as in the presence of oxidative stress and damaged proteins, LON binding to mtDNA is reduced. In this condition, Lon binds to its substrates and utilizes ATP to degrade proteins. Upon reduction of stress levels, LON binds ADP and mtDNA binding increases. Reduced binding may occur because DNA repair proteins, competing with LON, bind mtDNA or, in turn, because LON may be recruited in the matrix to degrade damaged proteins. Furthermore, when bound by LON, mtDNA becomes more sensible to damages by ROS (84). As a result, Lon modulates mtDNA copy number (86) and mitochondria biogenesis (87). The capability of LON to bind mtDNA, together with its ability to interact with pol-γ and twinkle, suggest that this protease plays a role in mitochondrial gene regulation and/or DNA replication.

1.2.3 Regulation of Lon expression in physiological and pathological conditions

Lon expression occurs physiologically at different levels in all human tissues (51, 49). The mechanisms regulating Lon transcription and expression in human cells have been only partially elucidated. Nevertheless is becoming clear that it is essentially modulated by several conditions of cellular stress, including endoplasmic reticulum stress, high levels of ROS and hypoxia (65, 76) in various cell lines and conditions (88-91). In hypoxic cells, Lon is up-regulated and is responsible for degrading COX4-1 to optimize the efficiency of respiration (76). Similarly, when cells are challenged with oxidative stress, Lon is involved in the degradation of misfolded, oxidized and carbonylated proteins, thereby preventing their accumulation and increases cell viability (92, 93).

In a model of endoplasmic reticulum stress, the overexpression of wild-type LON or proteolitically inactive LON enhance the assembly of COX II into COX I containing complexes, remarking the importance of the chaperone activity of this molecule (94). Interestingly, Lon levels appears not regulated by mtDNA copy number, even if Lon can bind and is involved in maintenance of mtDNA (92). Serum starvation and heat stress have also been shown to increase Lon protein levels (65).

Hypoxia is another major inducer of Lon. The up-regulation of Lon in hypoxic conditions has been observed in THP-1 (monocytic), HeLa (cervical cancer) and RKO (colon cancer) cells (75, 77), and has been shown to be determined by the stabilization of HIF-1α and its binding on the promoter of *PRSS15*. The observation that Lon is up-regulated by hypoxia at the mRNA and protein level has been further confirmed in an animal model, *i.e* in rat cultured astrocytes cultured in hypoxic conditions, and in rat ischemic brain (96). Finally, although no data are available in human cells, observations in rat Zajdelahepatoma cells, as well as in hyperthyroid rats suggest that Lon up-regulation is correlated with enhanced mitochondrial biogenesis (87). Taken together, these data indicate that Lon can be appears to be a stress-responsive protein, which expression can be stimulated to overcome accumulation of damaged (oxidized or carbonylated) proteins, thus providing transient protection to the cell. All these studies pointed out clear discrepancies among changes in PRSS15 gene transcription, levels of Lon mRNA, and the amount of proteins detected in

mitochondria, suggesting that a fine tuning in Lon expression exists at multiple levels (96), and that mechanisms related with protein stability are involved in Lon regulation. Lon is essential for cell survival, and its absence is lethal in mammalians at the gastrulation stage (75). However, modifications in Lon expression and activity have been reported in myoclonic epilepsy with ragged-red fibers (MERRF) and mitochondrial encephalomyopathy, lactic acidosis, and stroke-like episodes (MELAS), two well-known inherited mitochondrial diseases caused by mtDNA mutations (97-99). With regards to MELAS, immortalized B-cell line harbouring the A3243G mutation in mtDNA display increased levels of Lon protein that specifically accumulates in mitochondria holding the mutated genome and missing complex I subunit NDUFS3 (99). Similarly, MERRF cybrids are characterized by increased Lon expression, but lower Lon activity, if compared to wild-type cybrids (101). Lon accumulation in the presence of a reduced activity can be linked to the fact that Lon is somehow inhibited and increasing its expression could represent an attempt to stabilize mitochondrial respiratory chain complexes (102). Lon is also implicated in other diseases or disease models where its expression levels are either up- or down-regulated, e.g. neurodegenerative conditions like Friederich ataxia, amyotrophic lateral sclerosis (103), hereditary spastic paraplegia, and lypodystrophy as a side effect of highly active antiretroviral therapy (HAART) (95). Frataxin deficiency causes a significant up-regulation of Lon in the cardiac mouse model of Friedrich ataxia (104). Two mechanisms have been proposed to explain this upregulation: the presence of endoplasmic reticulum stress or the depletion of ATP, both occurring in tissues of patients with Friedreich ataxia (104). In this case, the increase of Lon is accompanied by increased proteolytic activity and a concomitant decrease in Fe-S subunits of complex I (NDUFS3), complex II (SDHB), and complex III (Rieske), which is related to the enzymatic deficiency of the respiratory chain (104). In lipodystrophic patients, Lon resulted to be up-regulated in adipose tissue, and its up-regulation was linked to oxidative stress but not to the mtDNA depletion caused by antiretroviral drugs, despite the crucial role of Lon in mtDNA maintenance (95). HAART related lipodystrophy is a disorder observed in HIV patients assuming antiretroviral drugs for long periods, and characterized by fat redistribution, metabolic alterations, quantitative and qualitative alterations of mtDNA, and chronic oxidative stress (105).

Expression and activity levels of LON are also modulated by aging. It is known that Lon protease expression and activity decline with aging, probably contributing to the accumulation of oxidative damaged proteins typical of this process (106). Ngo et al. suggest that the regulation of Lon could be biphasic: up-regulated during transient stress, while down-regulated during chronic stress and aging (78). Notably, they observed that protein levels were increased with only a minor elevation of the relative transcript, introducing the intriguing idea that Lon could be post-translationally regulated during stress.

Moreover, Lon levels are increased in different tumours and tumour cell lines (59, 107, 108). Interestingly, down-regulation of Lon in some tumour cells causes apoptosis and cell death (74), indicating a possible addiction of tumour cells to Lon function, as occurs with other intracellular proteases associated with cancer (109, 110, 75).

Accordingly, Lon expression and activity decrease in aged rats and mice, and are accompanied by the accumulation of oxidized and carbonylated proteins in the matrix together with a decrease in the activity of mitochondrial aconitase (111, 112). Mice deficient for Lon show a lethal phenotype during gastrulation, a period in which a well-fitted mitochondrial function is required to induce profound changes in embryo development. At this stage, Lon-null embryos display loss of mtDNA and growth arrest, which are features observed in mice deficient in OXPHOS complex subunits, like GRIM19 and SCO2 (113, 114), or in mtDNA-associated proteins, such as POLG, POLG2, and TFAM (115-117), that also exhibit embryonic lethality. In contrast, Lon-heterozygous mice develop normally and do not display any obvious pathological alterations, allowing to evaluate in vivo the functional and pathological relevance of Lon haploinsufficiency. Interestingly, Lon*+/-* mice are protected against chemically induced colorectal and skin tumours, suggesting an oncogenic function for this mitochondrial protease. Therefore, Lon is essential for in vivo and in vitro embryo development (75).

Aging is characterized by an exponential decline of mitochondrial capacity, which is linked to decreased mtDNA levels, mtRNAs and protein expression, increased oxidative stress, and increased accumulation of oxidatively modified proteins (118-120). Mitochondrial quality control, which operates to maintain mitochondrial quality, is also reduced with aging (121). Indeed, old mice show reduced Lon levels and activity

in skeletal muscle if compared to young mice (111), an effect that is exacerbated in MnSOD heterozygous mice. Lon levels increase with age in rat hearts, but Lon activity does change, suggesting that inactive Lon is progressively accumulated with aging (122), probably because of oxidative damage of the enzyme that reduces its activity (123).

1.3 Cancer metabolism and mitochondria

1.3.1 Cancer metabolism: the Warburg effect and mitochondria

The neoplastic transformation of normal cells into cancer cells is a multistep process that is first initiated by diverse genetic alterations, then enhanced by several oncogenesis-associated cellular stresses, that can be observed in many cancer cells, such as DNA damage and mitotic stress, as well as to metabolic, proteotoxic, and oxidative stress (124, 125).

In addition, it is well now well known that neoplastic diseases share several common traits, that govern the transformation of normal cells to cancer cells and are responsible for the progression of the disease. It includes sustaining proliferative signaling, evading growth suppressors, resisting cell death, enabling replicative immortality, inducing angiogenesis, and activating invasion and metastasis (125).

Cancer cells exhibit considerably different metabolic requirements than most normal differentiated cells as they must generate the energy required to support rapid cell division (127, 128). For example, in order to support their high rates of proliferation, cancer cells consume additional nutrients and divert those nutrients into macromolecular synthesis pathways. Metabolic pathways must therefore be rewired in such a way that balances biosynthetic processes with sufficient ATP production to support cell growth and survival (127). In addition to the ATP that is required to maintain normal cellular processes, proliferating tumour cells must function also generate the energy that is required to support rapid cell division (128).

The reprogramming of cellular metabolism is essential to support continuous cell growth and proliferation in a ‘cancer’ microenvironment that can differ from the

normal one, in term of oxygen and nutrient supplies. Indeed, cancer cells are often characterized by profound metabolic reprogramming, which involves changes in the regulation of glycolysis and mitochondrial functions. For istance, under aerobic conditions, cells can process glucose first to pyruvate and to CO_2 in mitochondria. Under anaerobic conditions, glycolysis is favoured and little pyruvate is consumed in mitochondria.

In 1920s, Otto Warburg first observed that cancer cells displayed anomalous energy metabolism. He observed that cancer cells, even under normal oxygen concentration, metabolize glucose by aerobic glycolysis at a surprisingly high rate compared to normal cells; therefore, aerobic glycolysis is a necessary adaptation to cope with a lack of ATP generation by oxidative phosphorylation (128). They secrete most of the glucose-derived carbon as lactate rather than oxidizing it completely by OXPHOS, a phenomenon known as the "Warburg effect" (129) (Figure 6). To explain this metabolic shift, he postulated that cancer originates from irreversible injury to mitochondrial respiration followed by an increase in glycolysis to replace ATP loss due to defective OXPHOS (130). Despite its lower efficiency in terms of ATP production if compared to OXPHOS, aerobic glycolysis can generate more ATP by producing it at a faster rate (132). However, it has been established that mitochondria are functional and still generate the majority of ATP in most tumour cells (132, 133). The advantage of high glycolytic activity is that glucose metabolism provides precursors needed for biosynthesis of macromolecules, for instance by the conversion of pyruvate via cytosolic and mitochondrial pathways (131, 134), and for the generation of reducing equivalents as antioxidant defences (135). Still remains the fact that utilization of glycolytic intermediates for biosynthesis and antioxidant activity accounts for less than 10% of the glycolytic rate. The rest of the glucose is converted to lactate that has the important role in maintaining NAD+/NADH balance for glycolysis to continue (132). The existence of this metabolic switch in cancer cells has been substantiated in the following decades. Interestingly, some tumours have been found to contain two subpopulations of cancer cells that differ in their energy-generating pathways. One subpopulation consists of glucose-dependent (Warburg effect) cells that secrete lactate, whereas cells of the second subpopulation preferentially import and utilize the lactate produced by their neighbours as their main energy source, employing part

of the citric acid cycle to do so (136-138). These two populations evidently function symbiotically: the hypoxic cancer cells depend on glucose for fuel and secrete lactate as waste, which is imported and preferentially used as fuel by their better-oxygenated cognate cells (136-138). Additionally, it is becoming apparent that oxygenation, ranging from normoxia to hypoxia, is not necessarily static in tumours but instead fluctuates temporally and regionally (139), likely as a result of the instability and chaotic organization of the tumour-associated neovasculature (124).

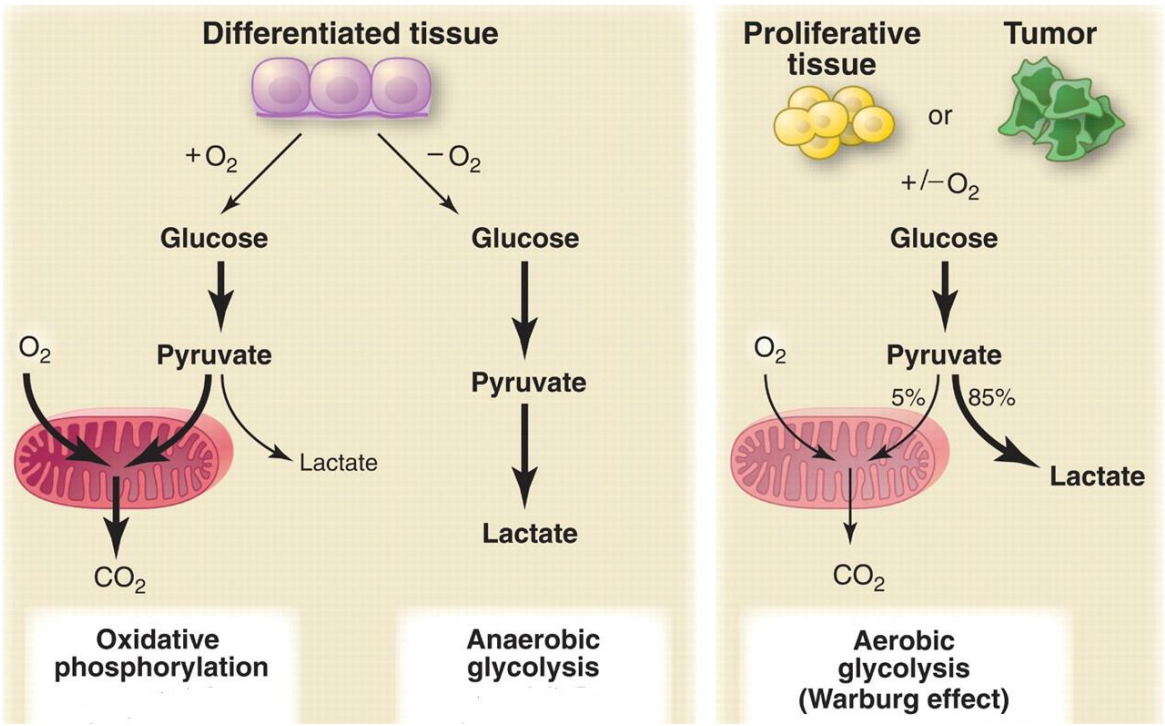

Figure 6: Schematic representation of the differences among oxidative phosphorylation, anaerobic glycolysis, and aerobic glycolysis (Warburg effect). In the presence of O_2, differentiated cells first metabolize glucose to pyruvate via glycolysis and then completely oxidize most of that pyruvate in the mitochondria by OXPHOS. When oxygen is limiting, cells metabolize by generating lactate (anaerobic glycolysis). Warburg observed that proliferating and cancer cells tend to convert most glucose to lactate regardless of whether oxygen is present (aerobic glycolysis). Mitochondria remain functional and some oxidative phosphorylation continues in both cancer cells and normal proliferating cells. In proliferating cells, ~10% of the glucose is diverted into biosynthetic pathways upstream of pyruvate production. Adapted from: Vander Heiden M.G., et al., Understanding the Warburg Effect: The Metabolic Requirements of Cell Proliferation. Science, 324(5930):1029-33, 2009.

While the changes in glycolytic pathway are almost well understood, the role of mitochondria in tumour metabolism is less known. It has been observed that mitochondrial function is essential in several tumours. For example the elimination of mtDNA from cancer cells (ρ° cells) reduces their growth rate and tumourigenicity in

vitro and *in vivo* (135). Moreover, disruption of mitochondrial function by loss of the TFAM gene reduced tumourigenesis in an oncogenic Kras-driven mouse model of lung cancer (130). Nevertheless, mtDNA and nDNA mutations that alter mitochondrial metabolism have been found in a wide variety of cancers (e.g. colon cancer, thyroid, breast and ovarian tumours, prostate and bladder cancer and neuroblastomas), and seem to enhance tumour formation and spread. Mutations in mtDNA involve electron transport chain proteins, thus inhibiting OXPHOS process (135); mutations in nDNA involve nuclear-encoded mitochondrial metabolic enzymes including fumarate hydratase (FH), succinate dehydrogenase (SDH) and isocitrate dehydrogenase 1 (IDH1) and IDH2, impairing mitochondrial metabolic functions (140).

The aberrant metabolism of cancer cells also leads to mitochondrial ROS production, and their effect on cell fate depends on the level at which ROS are present. Low levels of ROS provide a beneficial effect, supporting cell proliferation and survival pathways; conversely, high levels cause oxidative stress that can lead to cell death. Cancer cells are generally submitted to stressful environment and so they are prone to produce excessive quantities of ROS. To counteract oxidative damage, these cells need to enhance their antioxidant systems and degrade damaged proteins to prevent further damage (128).

In addition, the abnormal tumour microenvironment plays a major role in determining the metabolic phenotype of tumour cells. Heterogeneity in oxygenation, pH, and the concentrations of glucose and many other metabolites can contribute to cancer-specific changes in metabolism (127, 141). For instance, recent evidences indicate the importance of hypoxia and lack of nutrient (in particular glucose) in cell proliferation. These two factors can promote the process of malignant transformation. It is apparent that hypoxia can cause the progressive elevation in ROS production that can target mtDNA and maybe drive the malignant transformation process (31). In these conditions, the "Warburg effect" can become fundamental as the major source of ATP production and lead the adaptation of cancer cells to hostile environment.

Additionally, a glycolytic shift is also induced by impairment of the mitochondrial respiratory chain (142). This impairment of mitochondrial OXPHOS triggers glycolytic metabolism as a survival mechanism that often ends with cell collapse due to the inability of these damaged cells to reprogram their metabolism (143). Accordingly, the

glycolytic switch observed in cells lacking Lon may be an obligate consequence of their mitochondrial dysfunction, not being related to metabolic reprogramming of cancer cells. Conversely, the switch observed in cells overexpressing Lon is a mitochondria-controlled mechanism, which forms part of a generalized metabolic reprogramming that contributes to the development and progression of cancer (75).

Altogether, these findings indicate the presence of a strong link between mitochondria and cancer development, but the precise mechanisms at the basis of such link are still unknown. The understanding about the relationship between cancer metabolism and mitochondria is immature and further work still has to be done in order to elucidate these aspects.

1.3.2 Lon protease and cancer

In recent years, several groups, including us, have observed an up-regulation of mitochondrial Lon protease in different human cancer types, including (but not limited to) *ex vivo* malignant B-cell lymphoma from patients (59), mammary epithelial, cervical and non-small-cell lung cancer cell lines (144-146), oral squamous cell carcinoma, and colon cancer, either at RNA or protein level (66, 75). *In silico* analysis further expanded the spectra of tumor cells characterized by high levels of Lon expression, by including lung, colorectal, and head-and-neck cancer and metastatic prostate cancer. It has been observed that such up-regulation can significantly increase colony formation activity in some cancer cell lines compared with controls, probably leading to a higher proliferative rate (147).

At mitochondrial level, a higher expression of Lon determines deep changes in organelle architecture and functionality. Indeed, Lon up-regulation may also be critical for cancer cell survival by preventing toxicity in case of stress conditions like hypoxia, typical of tumour microenvironment. During hypoxia, often observed in solid tumours, Lon is up-regulated by the hypoxia inducible factor-1α (HIF1-α), and degrades the cytochrome c oxidase 4-1 subunit (COX4-1), thereby permitting the assembly of another subunit COX4-2, which confers optimized enzyme activity for low oxygen, thus adapting cancer cells to a hypoxic environment (figure 7) (76).

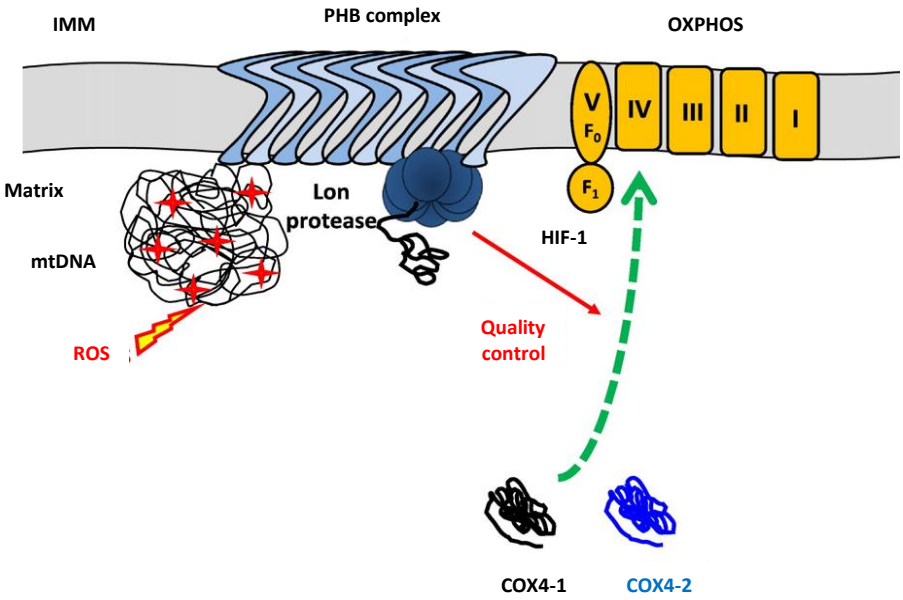

Figure 7: Implication of Lon protease and prohibitin in cancer. Prohibitin form a complex in the mitochondrial inner membrane. They may assist with protein folding and assembly. The association of prohibitin with mitochondrial nucleoid and Lon protease may assure protection and regulation of mt DNA. Under aerobic conditions, mammalian cells express COX4-1 subunits whereas under hypoxic conditions, they express COX4-2, respectively. The change in subunit composition provides a mechanism by which mitochondrial respiration is optimized according to O_2 concentration. Degradation of COX4-1 subunits via activation of the Lon protease provides a mechanism to maintain the efficiency of respiration in tumor cells. Adapted from: Bulteau A.L., Bayot A. Mitochondrial proteases and cancer. Biochim Biophys Acta, 1807(6):595–601, 2011.

Ectopic overexpression of Lon has been shown to induce a switch to glycolytic respiration, and to facilitate the proliferation and transformation of cells, as well as their capability to migrate and form metastasis in nude mice.

The overexpression of Lon has been shown to cause mitochondrial ROS generation, in different cell models (75, 146). In 293T, OEC-M1, and FADU cells, increased Lon interacts with NDUFS8 subunit of complex I and causes an increased level of this protein, which in turn determines an increase in mitochondrial ROS production, probably because of an impairment in the complex I assembly (146). Cheng *et al.* proposed that ROS, produced by Complex I, promote cell proliferation by activating MAPK (p38, JNK, and ERK1/2) and Ras-ERK signalling, pointing out the overexpression of Lon as the driving force to promote oncogenic transformation. Interestingly, Lon overexpression also promotes the expression of markers related with epithelial mesenchymal transition (EMT), such as E-cadherin, N-cadherin, Vimentin, and Snail,

and promotes cell migration via up-regulation of MMP-2, while Lon down-regulation impairs cell migration. Since EMT is inhibited by antioxidant molecules such as N-acetyl cysteine, Lon-induced EMT process is suggested to be dependent on ROS generation (146).

It has also been reported that Lon down-regulation by specific shRNA enhances cell death in cancer cell lines of lymphocytic and cervical origin (59, 146). The proteolytic defect causes accumulation of aggregated proteins inside mitochondria, while loss of chaperone function severely affects mitochondrial respiration and membrane potential, rendering cells extremely susceptible to apoptotic stimuli (31).

Reprogramming mitochondrial metabolism in cancer cells could also be obtained by post transcriptional and post translational mechanisms. We have recently shown that in colorectal cancer cells Lon is deacetylated by SIRT3. Indeed, SIRT3 interacts with Lon and its silencing causes an increase of Lon levels and acetylation (96). This protein is a mitochondrial specific sirtuin, which can regulate several metabolic pathways in mitochondria, and act both on pro- or anti- oncogenic targets (148, 149). The ability to regulate the activity of Lon likely represents one of the mechanisms used by SIRT3 to regulate and reprogram mitochondrial functions in cancer cells and to increase their resistance to stressors usually present in the tumour microenvironment.

The availability of a $Lon^{+/-}$ mouse model has shed some light on the role of Lon in malignant transformation in vivo. Quiròs *et al*. reported that Lon-haploinsufficient mice are protected against chemically induced colorectal cancer and melanoma, possibly because Lon regulates tumour bioenergetics by remodeling OXPHOS complexes and cellular glycolytic activity. Additionally, they found that LONP1-Knockdown induced a decrease in mitochondrial membrane potential and mtDNA content, increased mitochondrial fragmentation and ROS production, indicating a clear mitochondrial dysfunction. This results are in perfect agreement with the observation that, in xenograft model, growth of Lon-silenced cancer cells is significantly reduced if compared to control cells, while cells overexpressing Lon grow more rapidly. Finally, Lon higher expression is associated with short survival in patients with metastatic melanoma, and its overexpression in melanoma cells increases experimental metastasis formation, whereas knockdown of this protease decreases cell proliferation and lung metastasis (75). These results indicate that LONP1 is

essential for cell proliferation as well as for metastasis formation in vivo, and high levels of Lon are marker of poor prognosis in human melanoma and colorectal cancer. Thus, its overexpression is correlated with a more aggressive phenotype of cancer (75).

Nevertheless, data reported in literature about Lon expression and function in cancer cells are very different and sometimes contrasting. Thus far, it appears that interfering with Lon protease induces cytotoxic responses in some, but not all, cell types or cell lines probably due to the tissue specific differences between the experimental models, drawing attention to the lacking of knowledge about Lon relationship with cancer. Taken together, this data clearly indicate that Lon is a protein whose higher expression can favour tumour growth, while its down-regulation is related to slow proliferation rate, or even death, of cancer cells. Thus, Lon has a central role as regulator of mitochondrial activity in oncogenesis.

1.3.3 Inhibitors of Lon

Cancer depends on conserved defense mechanisms to survive oncogenic stress, which confer cellular survival, proliferation and chemoresistance. The identification of nononcogenic proteins participating in this cell stress response emerged as an important new class of viable targets for anticancer drug therapy. Since down-regulation of Lon leads to loss of mitochondrial function, reduced cell proliferation capacity, and apoptosis in cancer cells, Lon is gaining attention as a potential target in cancer therapy (59).

In *E. coli*, ADP acts as an inhibitor of the Lon protease indicating regulation in response to changes in energy charge (150). The bacterial Lon activity can be inhibited by T4 phage infection through the T4-encoded PinA protein a few minutes after infection (151).

To date, few inhibitors of mitochondrial Lon protease were identified. Not surprisingly, the serine protease inhibitor PMSF can inhibit Lon (59). Some proteasome inhibitors such as MG132 and *clasto*-lactacystinβ-lactone (cLβL) can diffuse into the mitochondria and inhibit the degradation of the steroidogenic acute regulatory protein (StAR), an endogenous substrate of mammalian Lon, suggesting that the

proteasome and Lon share some similarities in their proteolytic mechanism (69, 152). Moreover, peptydil boronate MG262-related bortezomib, the first therapeutic proteasome inhibitor to be tested in humans, still in use in the treatment of multiple myeloma and mantle cell lymphoma (153), was demonstrated to be a potent inhibitor of Lon protease activity by a competitive ATP-dependent mechanism (154).

These results gave rise to broad-spectrum screening for the identification of novel selective drugs, especially non-peptidic ones as they could have a better pharmacokinetics.

Coumarinic derivatives are natural compounds of a well-known family of non-peptidic, efficient low-molecular-weight and versatile protease inhibitors. Interestingly, they show no activity towards yeast proteasome, providing a better option to investigate the various biological roles of Lon protease without interference with the proteasome. However, further test are needed to determine their effects on others mitochondrial proteases, such as Clp (55).

Recently, considerable research interest has been focused on a novel category of anticancer compounds. 2-cyano-3, 12-dioxooleana-1,9(11)-dien-28-oic acid (CDDO), a synthetic oleanane triterpenoid, and its C-28 methyl ester derivative (CDDO-Me) have shown strong anti-inflammatory, antiangiogenic and anti-proliferative activity against a wide range of tumour cells, e.g. lymphocyte, breast, colon, pancreas, prostate, lung, ovary, skin, melanocyte, neurone (155, 156). Their proposed mechanism of action is by forming Michael adducts with reactive nucleophiles, such as free thiols, on target proteins. The wide spectrum CDDOs effects is explained, in part, by their concentration-dependent induction of oxidative stress, which alters various redox-sensitive proteins and signaling networks (59).

They exert a potent antiproliferative and proapoptotic activity through the mediator inhibition of different signaling pathways, such as mitogen activated protein kinase (MAPK), extracellular signal-regulated kinase 1 and 2 (Erk1/2), nuclear factor-kappa B (NF-kB), peroxisome proliferator-activated receptor (PPAR) and others (158-160).

Moreover, Lon has been shown to be directly and selectively inhibited by CDDO and its methyl ester derivative (CDDO-Me) *in vivo* and *in vitro*, and such an inhibition is associated with cell death in B cell lymphoma; both molecules have no effects on 20S proteasome (59). By using a biotinylated-CDDO as a probe, the mechanism of

inhibition was elucidated. CDDO forms a conjugate with Lon protease, which blocks the activity of Lon. Lymphoma B cells treated with CDDO exhibit the accumulation of electron-dense aggregates within mitochondria matrix and apoptotic cell death, in a way similar to that observed in Lon knockdown cells. Different cancer models show an analogue response in vitro and we have observed the same effects, in particular, on colon cancer and hepatocarcinoma cells (160, 168). These evidences give rise to ongoing preclinical and clinical trials (161).

Several studies demonstrated that induction of apoptosis in prostate cancer cells by CDDO-Me was inhibited by the use of mitochondrial complex I inhibitor, such as diphenyleneiodonium (DPI) or rotenone, indicating that CDDO-Me generates ROS by targeting the mitochondrial electron transport chain. The same outcome was observed in ovarian cancer cells, where pre-treatment with N-acetylecysteine (NAC) or the overexpression of antioxidant enzymes glutathione peroxidase (GPx) and superoxide dismutase1 (SOD1) prevent ROS generation and CDDO-Me induced apoptosis (162, 163). Together, these findings reveal that Lon protease activity inhibition plays a role in CDDO-induced cancer cell death, in a manner that seems depending on a ROS generation mechanism, supporting the concept that Lon could represent a novel anticancer drug target (162). In addition, the evidence that CDDO exhibits an additive effect on cell death when administered in combination with bortezomib, suggests that the inhibition of both mitochondrial and cytosolic proteolitic machineries could represents a chemotherapeutic strategy (164).

Finally, two small-molecule compounds, obtusilactone A (OA) and (-)-sesamin from *C. kotoense* (a small evergreen tree) were identified as potent Lon protease inhibitors through enzyme-based screening. *In vitro*, both molecules inhibit the activity of purified recombinant Lon. In cultured cells, OA causes a significant accumulation of aconitase, a specific substrate of Lon proteolytic activity, in a time- and dose-dependent manner. According to molecular docking analysis, OA and (-)-sesamin interact with Ser855 and Lys898 residues in the active site of the Lon protease, likely inhibiting the Lon activity (165, 168).

These results indicate that subjecting cancer cells to bimodal proteotoxic overload by inhibiting mitochondrial as well as cytosolic ATP-dependent proteases may provide a chemotherapeutic strategy for augmenting cancer cell death (59). Thus, taken

together, these observations indicate that Lon could be a novel promising anticancer drug target. However, some obstacles for developing an effective drug targeting Lon currently exist. First, it is quite difficult to target compounds to the mitochondrial matrix, as the IMM is highly impermeable. Second, Lon inhibitors available so far has a low grade of specificity. Indeed, a peroxisome-specific isoform of Lon protease (LONP2) exists (165-168), which displays a high degree of similarity with mitochondrial Lon, and whose enzymatic activity might be theoretically inhibited by drugs designed for Lon.

In addition, it must be noted that CDDO and CDDO-Me elicited a wide range of biological effects other than inhibiting Lon proteolytic activity. Given the importance of Lon in colon cancer, as well as in other types of cancer (31, 151, 154), the study and the validation of further inhibitors that selectively and specifically bind and block Lon activity are required and could be of interest to provide a new therapeutic option.

2. AIM OF THE WORK

The neoplastic transformation of normal cells into cancer cells is a multistep process, driven by several oncogenesis-associated cellular stresses such as DNA damage and mitotic stress, as well as to metabolic, proteotoxic, and oxidative stress. To survive in a microenvironment where nutrient are scarce and stressors are greater than those present in normal cells, cancer cells often have to activate adaptative mechanisms (59). Recent evidences suggest that Lon up-regulation is associated with tumour development, and its down-regulation causes profound alterations of mitochondrial proteome and function, and cell death. Thus, Lon can be considered a protein that does not initiate tumourigenesis *per se*, but it is important for cancer cell survival. Its inhibition could represent a possible new anticancer strategy.

Accordingly, the aim of this work was to clarify the role of Lon protease in cancer cells. Therefore, we analyzed the effects of Lon down-regulation in RKO colon cancer cells, in which Lon could be conditionally silenced by RNA interference. We studied the impact of Lon down-regulation on cellular apoptosis, mtDNA and mtRNAs levels, mitochondrial functionality and mitochondrial morphology. At the same time, we also analyzed the levels of Lon in tissue samples from colorectal cancer.

Furthermore, we wondered whether treating different human cancer cell lines, compared to normal fibroblast, with compounds that have a potential interest for cancer treatment, would provide the same effects found by shRNA knockdown of Lon. Thus, we evaluated the effects of pharmacological inhibition of Lon, using CDDO or CDDO-Me, on mitochondria of three different cancer cell lines (RKO human colon cancer cells, HepG2 hepatocarcinoma cells and MCF7 breast carcinoma cells). We paid a particular attention to parameters such as membrane potential, mass, morphology, dynamics and ROS content, and Lon proteolytic activity.

3. Materials and methods

3.1 Cell culture

RKO, HDLM-2, K562, PC3, DU145 were cultured in RPMI Glutamax medium supplemented with 10% foetal bovine serum (FBS) and gentamycin. SHSY5Y and MCF7 cells were maintained in Dulbecco's modified Eagle's medium (DMEM) Glutamax supplemented with 10% fetal bovine serum, and gentamycin. HepG2 cells were cultured in Minimun Essential Medium (MEM), supplemented with 10% FBS, 1% non essentials aminoacids, 1% vitamins, 1% L-glutamine, and gentamycin. Cells were maintained in 5% CO_2 atmosphere at 37°C. Human fibroblasts were obtained after informed and signed consent from 1 healthy subject (age 40 years) and used between 5^{th} and 7^{th} passages. Fibroblasts were isolated and established in culture according to standard methods (169). Fibroblasts were grown in 75 cm^2 flasks for 5 days in DMEM supplemented with 10% FBS, until confluence.

When required, cells were maintained in condition of glucose deprivation, by adding 2-Deoxy-D-glucose (2DG, 80 mM) to complete medium. When indicated, hydrogen peroxide (H_2O_2, 400 µM) was added to cell culture for four hours to induce oxidative stress. Cells were maintained in 5% CO_2 atmosphere at 37°C. The oleanane triterpenoid 2-cyano-3,12-dioxooleana-1,9,-dien-28-oic acid (CDDO) and its methylated derivative (CDDO-Me) were purchased from Cayman Chemical Company (Ann Arbor, Michigan, USA), were dissolved in DMSO and were used at concentrations up to 10 µM, while DMSO alone was added to control samples. For proliferation assay, $0.4x10^6$ cells were seeded and treated with CDDO, CDDO-Me or left untreated for control, and counted after 24, 48 and 72 hours.

Peripheral blood mononuclear cells (PBMC) were isolated by Ficoll-Hypaque density gradient according to standard procedures from twenty mL of venous blood collected into ethylenediaminetetraacetic acid (EDTA) tubes from each donor, who gave informed consent. Next, $10x10^6$ PBMC were incubated overnight in RPMI in the presence (then indicated as activated) or in the absence (then indicated as resting) of 2 µg/mL anti-CD3 anti-CD28. $90x10^6$ PBMC were used to separate CD14+ and CD19+ cells by using CD14+ and CD19+ magnetic beads, respectively. $18x10^6$ CD14+ cells

(then indicated as monocytes) and $5x10^6$ CD19+ (then indicated as B lymphocytes) were obtained and were then cultured in RPMI medium. Monocytes were incubated overnight in the presence (then indicated as activated monocytes) or in the absence (then indicated as resting monocytes) of 0.5 μg/mL lipopolisaccaride; whereas B lymphocytes were incubated in the presence (then indicated as activated B lymphocytes) or in the absence (then indicated as resting B lymphocytes) of 2 μM CpG oligonucleotides for 72 hours. At the end of the incubations the presence of activated cells was evaluated by flow cytometry. In particular, PBMC were stained with anti-CD4, anti-CD8, anti-HLA-DR, and anti-CD95, to analyse the amount of HLA-DR and CD95 double positive cells. Activated monocytes and B lymphocytes were evaluated on the basis of physical parameters. A minimum of 1 million cells per sample were acquired for the single cell analysis on Attune Acoustic Focusing Cytometer (Life Technologies, Carlsbad, CA, USA). The instrument is equipped with a blue laser (488 nm, 20 mW, for detection of FITC, PE, ECD and PE-Cy7 in this study) and a red laser (638 nm, 50 mW, for detection of APC and APC-H7), has four emission channels for the blue laser and two emission channels for the red laser, and allows up to six-color analysis in addition to forward (FSC) and side scatter (SSC) data collection. Data were acquired in list mode using Attune Cytometric 1.2.5 software, and then analyzed by FlowJo 9.8.4 (Tree Star Inc., Ashland, OR, USA) under Mac OSX. All culture media and culture reagents were from Life Technologies Corporation (Carlsbad, CA, USA).

3.2 Tissue samples and protein extraction

Formalin-fixed paraffin-embedded (FFPE) tissues were from patients who underwent surgical resection of colorectal cancer (CRC), and gave informed consent. Non-neoplastic (normal mucosa) colon tissues were excised from normal areas of surgical fragments placed distant to the tumour. FFPE microtome sections were deparaffinized according the protocol reported in Addis et al (170). Briefly, samples were deparaffinized by incubating at room temperature in xylene for 10 minutes, and then centrifuged at 12000x*g* for 3 minutes, and incubation/centrifugation steps were repeated twice more. The deparaffinized tissue pellets were then rehydrated with a

graded series of ethanol (100%, 95%, 90%, 70% and H_2O). All samples were then weighed, and matched amounts of tissues were each immersed at a 20% w/v ratio in a 20 mM Tris HCl, pH 8.8, 2% SDS, 200 mM dithiothreitol (DTT), extraction buffer. Samples were incubated at 100°C for 20 minutes, and then at 80°C for 2 hours with shaking. Extracts were centrifuged for 15 min at 12000x*g* at 4°C, quantified by the Bradford assay, and then loaded on acrylamide/bisacrylamide precast gels.

3.3 Constructs, retrovirus preparation, and infection

Experiments related to the inhibition of Lon, were performed on a clone of RKO colon cancer cell line, previously developed in our laboratory, in which Lon expression was silenced using a retroviral construct (RNAi-Ready-pSIREN-RetroQ-TetP-Lon and RNAi-Ready-pSIREN-RetroQZsGreen-Lon) for inducible and constitutive expression of Lon shRNA, respectively. To get these cells, the oligonucleotide 5'-GGGATCCGTTCGTCTCGCCCAGCCTTTTCAAGAGAAAGGCTGGGCGAGACGAACTTTTTGA ATTCCTT-3' was cloned into RNAi-Ready-pSIREN-RetroQ-TetP expression vector (Clontech, Germany) to express Lon shRNA under the control of the tetracycline repressor (tTS), and RNAi-Ready-pSIREN-RetroQZsGreen expression vector (Clontech, Mountain View, CA, USA) for constitutive expression of Lon shRNA. With regards to constitutive down-regulation, the retroviral constructs RNAi-Ready-pSIREN-RetroQ-ZsGreen-Lon and RNAi-Ready-pSIREN-RetroQ-ZsGreen-scramble were generated, and used to infect RKO cells. Cells with the highest ZsGreen fluorescence were sorted by using a MoFlo XDP flow cytometer (Beckman Coulter, Fullerton, CA, USA) and then maintained in culture. With regards to inducible down-regulation, the vector pQC-tTS-In was used to generate stable tTS-expressing cells that were selected for G418 resistance, and several resistant clones were isolated and screened with SIRENRetroQ-Tet-Luc luciferase vector to identify clones with low background and high shRNA induction. Stable tTS cells were infected with recombinant pSIREN-RetroQ-TetP-Lon virus, and selected with puromycin. In the end, it was obtained a cell clone in which a 71.0±8.5% reduction of Lon expression was observed after 72 hours of treatment with 4 μg/mL doxycycline; then, all the experiments were performed by culturing cells in control medium (Doxy-), which contained puromycin and G418 but not doxycycline,

and induction medium (Doxy+), which contained puromycin, G418 and doxycycline, for 72 hours.

For the experiments related to the overexpression of Lon the pMSCV-Puro empty vector and the pMSCV containing the cDNA encoding for Lon protease (pMSCV-Lon) were used to transiently transfect amphotrophic Phoenix (phxA) cells, and the retroviral transduction has been performed as follows. PhxA cells were seeded and transfected. Transient transfection was performed by using lipofectamine 2000 (Life Technologies Corporation) and 20 µg of pMSCV-Lon plus 0.9 µg of helper plasmid. PhxA cells were maintained in the presence of transfection mix for 16 hours, then switched to 20 mL of RKO medium and placed in the incubator for 24 hours. At the end of the incubation, the retroviral supernatant was collected, filtered with 0.45 µm filter and supplemented with 8 µg/mL hexadimethrine bromide, and used to stably transfect RKO cells. RKO cells were seeded in 6-well plates at density of $0.5x10^5$ cells/mL. Two mL of retroviral supernatants was added to RKO cells that were then centrifuged at 1,800 rpm at 32°C for 45 minutes. Cells were then placed in the 32°C incubator. After 2 hours, medium was replaced with fresh retroviral supernatants and centrifuged as indicated before. Cells were then placed in the 32°C incubator for 4 hours. At the end of incubation, normal medium was added to substitute retroviral supernatant, and cells incubated overnight. The day after, normal medium was removed and replaced with 4 mL of fresh retroviral supernatant, and cells were centrifuged at 1,800 rpm at 32°C for 45 minutes. Cells were then put at 32°C for 5 hours, and retroviral supernatants was replaced with normal medium. After 48 hours, 2 µg/mL puromycin was added to the cells. RKO cells which survived the selection were maintained in medium supplemented with 1 µg/mL puromycin.

3.4 Quantitative real time PCR

Quantification of mitochondrial transcripts

The quantification of mtRNA was performed on Doxy- and Doxy+ RKO cells, as previously described in (171). Total RNA was extracted from cells by using the RNeasy Mini Kit (Qiagen, Hilden, Germany) following the instructions supplied by the manufacturer. RNA was reverse transcribed with ImProm-II reverse transcriptase (Promega, WI, USA) following instructions of the manufacturer and using random hexamers as primers. RNA template was first mixed with 50 pmol random hexamers and incubated at 70°C for 5 min. Then a reverse transcription mix, containing ImProm-II Reaction Buffer 5x, 3 mM $MgCl_2$, 0.5 mM dNTPs mix (10 mM each dNTP) and 1u/µl RNasin Ribonuclease inhibitor (Promega), was added to the tubes which were incubated at 25°C for 5 minutes, 42°C for 60 minutes and 70°C for 15 minutes. The assay used four parallel PCR reactions to quantify three mitochondrial genes, NADH dehydrogenase 1 (ND1), NADH dehydrogenase 6 (ND6) and cytochrome B (cytB), and one nuclear gene, L13, using the same standard construct. The amplicons of interest (derived from ND1, CYTB, ND6 and L13 genes) were cloned together in a plasmid in order to obtain a single, reference DNA molecule to be used as the standard for the real-time PCR quantification of all four transcripts (patent PCT/NL03/00545). The use of a single, cleaved plasmid was preferred to guarantee the ratio among amplicons to be fixed at the value of 1:1:1:1. Each different transcript was quantified in a separate reaction to avoid non-specific amplifications and to ensure the maximal reliability of the study. Each reaction involved the following reagents: 2 µl of cDNA solution (sample), 12.5 µl SuperMix 2x (Invitrogen, California, USA), 0.4 µM direct and reverse primers for mitochondrial transcripts, 0.2 µM for L13, 0.2 µM Taqman probe (Operon, Huntsville, AL, USA) and water up to 25 µl. Primers and probes are listed in table 1.

Primer/Probe	Sequence
ND1 forward	5'-CCTTCGCTGACGCCATAAA –3'
ND1 reverse	5'-CGGTGATGTAGAGGGTGATG–3'
ND6 forward	5"-AACCCTGACCCCTCTCCTTC –3"
ND6 reverse	5"-TGGAGGTAGGATTGGTGCTG–3"
cytB forward	5"-AGTCCCACCCTCACACGATT–3"
cytB reverse	5"-TTGTTTGATCCCGTTTCGTG–3"
L13 forward	5"-GCTGGAAGTACCAGGCAGTGA–3"
L13 reverse	5"-ACCGGTAGTGGATCTTGGCTT–3"
ND1 Probe Fam490	5" – CCAAAGAGCCCCTAAAACCCGCC – 3"
ND6 Probe Fam490	5" – CCACCACCCCATCATACTCTTTCACCC – 3"
CYTB Probe Texas Red	5" – CAGCCCTAGCAGCACTCCACCTC – 3"
L13 Probe Texas Red	5" – TCTTTCCTCTTCTCCTCCAGGGTGGCT – 3"

Table 1: Names and sequences of primers and probes used for real time PCR quantification of mitochondrial transcripts.

The reactions were performed on an iQ5 Real Time PCR (Bio-rad Laboratories, Hercules, CA, USA) that was set as follows: 50°C for 2 min, 95°C for 6 min, followed by 45 cycles of amplification (95°C for 30 s, 60°C for 60 s). The reading wavelength depended on the probe in use: FAM490-labelled probes were detected at 520 nm, whereas those labelled with Texas Red were detected at 615 nm. All the experiments were performed in triplicate.

Quantification of mtDNA

The quantification of mtDNA was performed on Doxy- and Doxy+ RKO cells by an original method that has been developed by our group (172). The assay used two parallel PCR reactions to quantify mtDNA or nDNA using the same construct, known amounts of which were amplified as reference molecules. Previously, DNA was extracted using the QiaAmp DNA Mini Kit (Qiagen) according to manufacturer instructions. In the first reaction, mtDNA was measured using a mix containing 2 µL sample DNA, 12.5 µL SuperMix 2x (Invitrogen), 200 nM MT dir, 200 nM MT rev and 100 nM MT probe. The reactions were performed on a IQ5 Real Time PCR (Bio-rad

laboratories) that was set as follows: 50°C for 2 min, 95°C for 6 min, followed by 45 cycles of amplification (94°C for 30 s, 60°C for 60 s). The reading wavelengths were the same as described before in mt transcripts protocol. All the experiments were performed in triplicate. The same approach was used to quantify nDNA, which was required to obtain the number of copies of mtDNA per cell. In this case, primers GEN dir and GEN rev were used. The TaqMan probe Gen Probe was included in the reaction mixture throughout PCR as a real-time detector for the amplified product. The sequences of primers and probes are reported in table 2.

Primer/Probe	Sequence
GEN dir	5‟ – GGCTCTGTGAGGGATATAAAGACA – 3‟
GEN rev	5‟ – CAAACCACCCGAGCAACTAATCT - 3‟
MT dir	5‟ – CACAGAAGCTGCCATCAAGTA – 3‟
MT rev	5‟ – CCGGAGAGTATATTGTTGAAGAG – 3‟
Gen Probe Texas Red	5‟ – CTGTTCCGTTTCCTGCCGGTGC – 3‟
MT Probe Fam490	5‟ – CCTCACGCAAGCAACCGCATCC – 3‟

Table 2: Names and sequences of primers and probes used for real time PCR quantification of mtDNA.

To optimize the precision of the assay and express the results as absolute number of mtDNA copies per cell, the regions used as template for the two amplifications (i.e., those of mtDNA and nDNA) were cloned tail to tail in a vector (pGEM-11Z; Promega) to have a ratio of 1:1 of the molecules used as reference. Then, serial known dilutions of this vector, amplified in triplicate, were included in each PCR run to generate a standard curve from which the relative copy number of either mtDNA or nDNA present in the unknown samples was determined. The measured values for mtDNA and nDNA were always within the range of the standard curve and the correlation coefficient was always >0.995. Absolute values for the copies of mtDNA per cell were then simply obtained from the ratio between the relative values of mtDNA and nDNA (obtained versus the same vector), multiplied by 2 (as two copies of the nuclear gene are present in a cell).

3.5 SDS-PAGE and western blotting

Cells were lysed in RIPA buffer (50 mM Tris, pH 7.5, 0.1% Nonidet P-40, 0.1% deoxycholate, 150 mM NaCl, 4 mM EDTA, and protease inhibitors) to extract proteins and their concentration was determined by the Bradford assay. Total cellular proteins (10 to 60 µg) or isolated mitochondria (10 µg) were subjected to SDS-PAGE in 4-12% or 12% gels followed by transfer to the proteins onto a nitrocellulose membrane (Bio-Rad Laboratories, Hercules, CA, USA) and immunoblotting. The membrane was incubated in the presence of primary antibody, washed and incubated with a secondary antibody conjugated with horseradish peroxidase (HRP). HRP activity was detected using Immobilon Western Chemiluminescent HRP substrate (Millipore, Billerica, MA, USA). The blot was developed and images were captured by using a Chemidoc MP (Bio-Rad Laboratories). The densitometric analysis was performed using ImageLab 5.2.1 (Bio-Rad Laboratories) or ImageJ. The following antibodies were used: anti-TFAM (Abnova Corporation, Taipei, Taiwan), anti-VDAC1/Porin (Abcam Inc., Cambridge, MA), anti-β-actin (Abcam Inc.), MitoProfile Total OXPHOS Human WB antibody cocktail (Abcam), anti-GAPDH (Trevigen, Gaithersburg, MD, USA), anti-GRP75 (Thermo Scientific, Waltham, MA, USA), anti-MDHM (Thermo Scientific), anti-EFTu (Novus Biologicals, Littleton, CO, USA), anti-UCRI (Novus Biologicals), anti-cleaved Caspase-9 (Cell Signaling Technology, Danvers, MA, USA), anti-human mitochondrial protein (Millipore, Billerica, MA, USA), goat anti-mouse IgG (Fc):HRP (Serotec, Kidlington, UK), goat anti-rabbit IgG (Fc):HRP (Serotec, Kidlington, UK), goat anti-mouse F(ab')2 Alexa546 and a goat antirabbit F(ab')2 Alexa647 (Life Technologies Corporation). A custom anti-Lon polyclonal antibody (Primm, Milan, Italy) to the Histidine-Tag recombinant protein Lon (from aa 376 to aa 497; QQRLGREVEEKIKQTHRKYLLQEQLKIIKKELGLEKDDKDAIEKFRERLKELVVPKHVMDVVDEELSKLGLLDNHSSEFNVTRNYLDWLTSIPWGKYSNENLDLARAQAVLEEDHYGMEDV) was used to probe Lon.

3.6 Immunofluorescence analysis of mitochondrial morphology

Cells were grown on glass coverslips. After treatment, cells were washed with PBS, and fixed with 4% paraformaldehyde in PBS for 15 min. Fixed monolayer cells were permeabilized with 0.1% Triton X-100 in PBS for 5 minutes and blocked with 3% BSA in PBS for 30 minutes, at room temperature. Then, samples were incubated with primary antibodies in PBS containing 3% BSA, for 1 hour at RT. After washing in PBS containing 3% BSA, samples were incubated for 1 hour at RT with secondary antibodies. After washing in PBS samples were stained with 1 μg/mL DAPI in PBS for 1 minute, and then mounted with anti-fading medium (0.21 M DABCO and 90% glycerol in 0.02 M Tris, pH 8.0). Negative controls were samples not incubated with the primary antibody.

The following antibodies were used: anti-human mitochondrial protein (Millipore, Billerica, MA, USA) and custom anti-Lon polyclonal antibody (Primm, Milan, Italy) as primary antibodies; goat anti-mouse F(ab')2 Alexa647 and a goat anti-rabbit F(ab')2 Alexa488 (Life Technologies corporation) as secondary antibodies.

The multi-labelling immunofluorescence experiments were carried out avoiding cross-reactions between primary and secondary antibodies. Fluorescent samples were observed by a Nikon A1 confocal laser scanning microscope as described below. For multiple detection, the samples were sequentially excited with the respective laser wavelength: 405 nm lines of a diode laser for DAPI; 488 nm lines of the argon laser for ZsGreen; 543 nm line of a HeNe laser for Alexa 546 and 637 nm line of a diode laser for Alexa647. The excitation and the detection of the samples were carried out in sequential mode to avoid overlapping of the two signals.

Optical sections were obtained at increments of 0.5 μm in the z-axis and were digitized with a scanning mode format of 1024x1024 pixels and 4096 gray levels. Spectral analysis was carried out to exclude overlapping between multiple signals. The confocal serial sections were processed with ImageJ software to obtain three-dimensional projections and image rendering was performed by Adobe Photoshop Software.

Colocalization analysis was performed as previously described. Briefly, the 2-dimensional scatter plot diagram of each image was analyzed to evaluate the spatial colocalization of the signals and the Pearson's correlation was calculated. For each

scatter plot diagram, areas with the strongest colocalized signals, corresponding to pixels with intensity values greater than 2400 gray levels (on a scale from 0 to 4096) for both detectors, were selected to generate co-localization binary maps.
The experiment was performed in collaboration with Prof. Paolo Pinton (University of Ferrara) and Dott. Gianluca Carnevale (University of Modena e Reggio Emilia).

3.7 Transmission electron microscopy

Transmission electron microscopy experiments were performed to analyse mitochondrial ultrastructure in Doxy- and Doxy+ RKO cells. Scraped cells were centrifuged at 10,000 g at 6°C for 5 min. Pellets were fixed overnight with 2.5% glutaraldehyde in Tyrode's buffer, postfixed for 2 hours in 1% osmium tetroxide, dehydrated and embedded in Spurr resin. Semithin sections obtained through the whole thickness of the pellets were stained with toluidine blue and observed with a Zeiss Axiophot light microscope. Ultrathin sections were stained with uranyl acetate and lead citrate and observed with a JEM 2010 transmission electron microscope (Jeol, Tokyo). The images were obtained in collaboration with Prof. Daniela Quaglino (University of Modena and Reggio Emilia).

3.8 Two-dimensional gel electrophoresis (2-DE)

Sample preparation

The mitochondrial pellets, obtained as indicated above, were resuspended in 100 µL of 1% Triton X-100 and 2% SDS and solubilized by water-bath sonication. The mitochondrial pellets were subjected to sonication for 2 min in an ice-water bath by using a Branson LT9 sonifier (GIMA, Milan, Italy). The sonication was repeated three times after allowing the sample to cool down for 2 min in ice after each sonication. Then, the samples were incubated at 4°C for 30 minutes and treated with PlusOne 2-D Clean-Up Kit (GE Healthcare, Little Chalfont, United Kingdom). In the cleaning protocol, samples were leaved in wash buffer at -20°C for 24 hours. Mitochondrial protein pellets were then resuspended in rehydration solution containing 7 M Urea, 2

M Thiourea, 2% CHAPS, 65 mM DTT, 0.01% Bromophenol Blue, and protein concentration was determined by Bradford assay. 2DE was carried out using the Immobiline polyacrylamide system, as previously described on a preformed immobilized nonlinear pH gradient, from pH 3 to 10, 18 cm length, from GE Healthcare. Briefly, sample load was 60 µg per strip in analytical runs, and 800 µg per strip in preparative gels. Isoelectric focusing was performed on IPGphor system (GE Healthcare) at 16°C using two different protocols. For analytical gels: passive rehydratation for 16h, 500 V for 1h, 500-2000 V for 1h, 3500V for 3h, from 3500 to 8000 V in 30 min and 8000 V for 12h. For preparative gels a preliminary step at 200 V constant for 12h was added. Thereafter, immobilized pH gradient strips were reduced (2% dithioerythritol) and alkylated (2.5% iodoacetamide) in equilibration buffer (6M urea, 50mM Tris-HCl, pH 6.8, 30% glycerol, 2% SDS). When the equilibration phase was finished, strips were loaded onto 12% acrylamide vertical gels using an Ettan DALTsix electrophoresis unit (GE Healthcare). Analytical gels were stained with silver-stain whereas preparative gels for mass spectrometric analysis were stained with colloidal Coomassie. Analytical and preparative gel images stained by silver nitrate or Coomassie Blu were digitized using a Imagescanner (GE Healthcare). For each condition, two biological and three analytical replicates were performed and only the spots present in all the replicates were taken into consideration for subsequent analysis.

Protein identification by MALDI-ToF/ToF-MS

Protein identification was carried out by Peptide Mass Fingerprinting (PMF) on 4800 Plus MALDI TOF/TOF instrument (Applied Biosystems). Electrophoretic spots from Coomassie stained gels were excised and destained in 2.5 mM ammonium bicarbonate and 50% acetonitrile (ACN), and dehydrated in acetonitrile. They were then rehydrated in trypsin solution and digested overnight at 37 C. 1 µL of each digested protein was spotted onto the MALDI target and allowed to dry. Then 1 µL of matrix solution (saturated solution of CHCA in 50% v/v ACN and 0.1% v/v TFA) was applied to the dried sample, which was dried again. After acquiring the mass of the peptides, a mass fingerprinting search was carried out in Swiss-Prot/TrEMBL database using MASCOT (Matrix Science Ltd., London, UK, http://www.matrixscience.com).

Taxonomy was limited to Homo Sapiens, mass tolerance was 40 ppm, and the acceptable number of missed cleavage sites was set at one. Alkylation of cysteine by carbamidomethylation was assumed and oxidation of methionine was considered as a possible modification. The criteria used to accept identifications included the extent of sequence coverage (at least 10%), the number of matched peptides (at least 4) and a probabilistic score at $p<0.05$.

Protein identification by LC–MS/MS analysis

Trypsin digests that did not produce unambiguous MALDI-ToF/ToF identifications subsequently underwent peptide sequencing on a nano CHIP-ESI/QTOF. The mass spectrometer was a 6520 Accurate Mass Q-TOF LC/MS (Agilent Technologies). After injection (3 µL), the peptides were trapped on the enrichment column (4 mm and 40 nL) of a Prot ID-Chip-43(II) using 100% solvent A (97% HPLC grade water + 0.1% v/v formic acid + 3% v/v ACN) at a flow rate of 3µL/min. After the enrichment phase, separation was performed on the analytical column of the chip (43 mm x 75 µm) using a linear gradient from 3% to 25% solvent B (5% HPLC grade water + 95% v/v ACN + 0.1% v/v formic acid) for 17 min and flow rate of 450 nL/min. A high voltage of 1825V was applied for stable spray operation. Both MS and MS/MS spectra were acquired using autoMS/MS mode (Agilent MassHunter Workstation acquisition B.02.00). MS spectra were acquired in the 350-1700m/z range and a maximum of six precursors per cycle (2+ and 3+) were selected for MS/MS experiments (50-1700 m/z range). The MS/MS ion search was carried out in Swiss-Prot/UniprotKB databases using MASCOT. Taxonomy was limited to Homo sapiens, peptide precursor charge was set at 2+ or 3+, mass tolerance at ± 20 ppm for precursor peptide and ± 0.1 Da for fragment peptides and the acceptable number of missed cleavage sites was set at one. Alkylation of cysteine by carbamidomethylation was taken as a fixed modification, while oxidation was considered as a possible modification. We considered significant peptides with individual ion scores ($-10\text{Log}[P]$, where P is the probability that the observed match is a random event) that indicated identity ($p<0.05$).

3.9 Isolation of mitochondria

In some experiments, mitochondria were isolated from cells according to the following protocol. Cells were washed with PBS and twice with ice-cold homogenization buffer (0.25 M sucrose, 0.25 mM EGTA, 5 mM HEPES, 1 mM DTT and protease inhibitor cocktail, pH 7.4). Cells were then trypsinized, suspended in 5 mL of homogenization buffer, and disrupted by 10 strokes of a Teflon pestle in a glass homogenizer. The homogenization and subsequent steps were performed on ice. The homogenates were centrifuged at 1000xg for 10 minutes. The pellet was rehomogenized and centrifuged at 1000xg. The combined supernatants were centrifuged at 17000xg for 15 minutes. The pellet was resuspended in iodixanol (Optiprep, Sigma Aldrich) diluted in homogenization buffer to obtain 36% iodixanol concentration. This fraction was layered with 30% and 10% iodixanol-containing homogenization buffer, and the gradient was centrifuged at 50,000xg for 4 hours (SW41 Titanium swing-out rotor L-70 Ultracentrifuge, Beckman Coulter, Fullerton, CA). Mitochondria were banded above the 10-30% interface, and were collected by aspiration. The mitochondrial fraction was diluted 1:1 in ice-cold PBS and centrifuged at 14,000 rpm for 15 minutes in a bench-top centrifuge. The mitochondria pellet were washed again with 1 mL of PBS, centrifuged, frozen in liquid nitrogen and stored at -80°C. All chemical reagents were from Sigma Aldrich (St. Louis, MO, USA).

3.10 Flow cytometry

Apoptosis, mitochondrial O_2^-, cellular H_2O_2, mitochondrial membrane potential (MMP), mitochondrial mass were assayed by polychromatic flow cytometry according to protocols reported below. All the experiments were performed using a 16-parameters CyFlow ML flow cytometer (Partec GmbH, Munster, Germany), equipped with a 488-nm blue solid-state laser, a 635-nm red diode laser, a UV mercury lamp HBO, a 532-nm green solid state laser, a 405-nm violet laser, and a CCD camera. Data were acquired in list mode by using FloMax (Partec) software, and analyzed by FlowJo 9.5.2 (Treestar Inc., Ashland, OR, USA) under MacOS X. A minimum of 20,000 cells per sample were acquired, and each experiment was repeated at least four times.

Apoptosis and mitochondrial O_2^-

To measure apoptosis, cells were stained with Annexin-V (ANXV) Alexa Fluor 488 conjugate (absorption wavelength 488 nm and emission wavelength 519 nm, Invitrogen) in Annexin-V binding buffer (10 mM HEPES, 140 mM NaCl, 2.5 mM CaCl2, pH 7.4), to detect phosphatidylserine exposure on the cell surface, and TO-PRO-3 iodide (TOPRO, absorption wavelength 642 nm and emission wavelength 661 nm, Invitrogen), to detect loss of plasma membrane integrity. To measure mitochondrial O_2^-, before assaying for apoptosis, adherent cells were stained with 5 µM MitoSOX Red (absorption wavelength 510 nm and emission wavelength 580 nm, Invitrogen) that is able to selectively enter into mitochondria where is oxidized by SOD in presence of O_2^-, emitting red fluorescence. This staining enables to measure mitochondrial O_2^- only in living cells. When required, we used mitochondria Peroxy Yellow 1 (mitoPY1, Sigma Aldrich, St. Louis, MO, USA) which specifically detects mitochondrial hydrogen peroxide (mtH_2O_2). For this experiment cells were first loaded with 10 µM mitochondria peroxy yellow 1 (mitoPY1) mitoPY1 in complete medium for 60 minutes, and then treated with CDDO or CDDO-Me for up to 24 hours. As a positive control, cells were treated with 1mM H_2O_2 for 1 hour. Supernatants were collected and cells stained with MitoSOX red superoxide indicator (MitoSOX), and with annexin-V (AnxV), and TO-PRO-3 iodide (TOPRO).

For each experiment, $0.4x10^6$ cells were seeded and treated with Doxyand Doxy+, CDDO, CDDO-Me or left untreated for control. Supernatant from cultures was collected in a facs tube together with trypisinized cells (either stained or unstained with MitoSOX Red). Cells were centrifuged at 1200 rpm for 5 minutes, stained with ANXV Alexa Fluor 488 conjugate (3 µl of ANXV conjugate and 197 µl of ANXV binding buffer) and then incubated for 10 minutes in dark. Cells were resuspended in 1 mLof ANX-V binding buffer and stained with 0.1 µM TOPRO before acquisition.

Samples were analyzed by flow cytometry. In particular, cells were first gated on the basis of physical parameters. Then, in living cells (AnxV-/TOPRO- cells) the median fluorescence intensity (MFI) of mitoPY1 and MitoSOX was analysed. The MFI of the unstained sample was subtracted to the MFI of the stained sample to avoid any influence related to the eventual autofluorescence. Then, the net MFI value obtained

for control sample was set to 100 and other samples calculated according the following formula: Relative MFI level = (treated sample net MFI / untreated sample net MFI)x100.

Cellular H_2O_2

To measure cellular H_2O_2, cells were stained with 2 µM 2',7'-dichlorodihydrofluorescein diacetate (H_2DCF-DA, Life Technologies corporation), a lipid soluble substance that penetrates into the cells where it is oxidized into the fluorescent molecule 2,7-dichlorofluorescein (DCF) which emits at 520 nm when excited at 488 nm. For each experiment, $0.4x10^6$ cells were seeded and treated with Doxyand Doxy+. Adherent cells were incubated with 2 µM H_2DCF-DA for 30 min at 37°C and washed with PBS. Cells were then trypsinized, resuspended in 1 mL of PBS and then analyzed by flow cytometry.

The MFI of the unstained sample was subtracted to the MFI of the stained sample to avoid any influence related to the eventual autofluorescence. Then, the net MFI value obtained for control sample was set to 100 and other samples calculated according the following formula: Relative MFI level = (treated sample net MFI / untreated sample net MFI)x100.

Mitochondrial membrane potential (MMP)

Mitochondrial membrane potential was analysed by staining cells with 5,5',6,6'-tetra-chloro-1,1',3,3'-tetraethylbenzimidazolyl-carbocyanine iodide (JC-1, Life Technologies Corporation) (173), a lipophilic cationic molecule that forms aggregates inside mitochondria when mitochondrial membrane is normal, whereas stays in the cytosol as a monomer when MMP is depolarized. After excitation at 488 nm, JC-1 monomers emit in the green region of the spectrum (with a maximum at 527 nm) and aggregates display an orange/red fluorescence (maximum at 590 nm with a tail of fluorescence 462 nm).

Considering JC-1 fluorescence, we identified two populations of cells with different MMP: cells with high (H) MMP, and cells with intermediate/low (I/L) MMP. Such a metachromatic property allows a relatively simple identification of cells with a high or

a low MMP (174). Briefly, for each experiment, $0.4x10^6$ cells were seeded and treated with Doxyand Doxy+, CDDO, CDDO-Me or left untreated for control. Trypsinized cells were stained with (2.5 µM) 1,25 mg/mL JC-1 for 10 minutes at 37° C in the dark, resuspended in 1 mL of complete medium and then analyzed by flow cytometry. Valinomycin (10 µM, Sigma Aldrich, St. Louis, MO, USA) was used as positive control, as it permeabilizes mitochondrial membrane (175).

MitoTracker

In order to measure mitochondrial mass, cells were stained with MitoTracker Green FM (Life Technologies corporation) (176), which appears to localize to mitochondria regardless of mitochondrial membrane potential. After excitation at 490 nm, the fluorophore emits at 516 nm in the green region of the spectrum. Briefly, for each experiment, $0.4x10^6$ cells were seeded and treated with Doxyand Doxy+, CDDO, CDDO-Me or left untreated for control. Adherent cells were incubated with 200 nM MitoTracker Green in culture media for 30 minutes at 37° C and washed with PBS. Cells were then trypsinized, resuspended in 1 mL of PBS and then analyzed by flow cytometry.

Caspase-3 activation

The activation of caspase-3 was evaluated by using the CellEvent Caspase-3/7 Green Detection Reagent (CellEvent, Life Technologies Corporation), which consists of a four amino acid peptide, which is intrinsically non-fluorescent and emits fluorescence when cleaved by caspase-3/7 in apoptotic cells. Briefly, cells were treated with CDDO or CDDO-Me. Then, supernatants were collected, cells were trypsinized, and stained with 5 µM CellEvent for 30 minutes, and then analyzed by flow cytometry.

3.11 ATP quantification

Cellular ATP was measured by CellTiter-Glo Luminescent Cell Viability Assay (Promega Corporation). Luminescence was measured with an Askent Luminometer (Agilent, Santa Clara, CA, USA). Each experiment was repeated three times, and each measurement was performed in duplicate. Data were normalized to protein

concentration that was determined by the Bradford assay.

3.12 Glutathione quantification

Total glutathione was measured by Glutathione Assay Kit (Cayman chemical company, Ann Arbor, MI, USA), following manufacturer instructions. Absorbance was measured with a MR-96A microplate reader (Mindray, Shenzhen, China). Each experiment was repeated at least three times, and data were normalized according to protein concentration that was determined by the Bradford assay.

3.13 Oxygen consumption rate (OCR)

To measure OCR cells were first seeded into petri dish and then moved to XF24 cell culture microplates. Cells where seeded into petri dish on day 1. The following day doxycycline was added to cell culture and incubated for 48 hours. On day 4, cells were trypsinized and seeded at $0{,}5x10^5$/well in XF24 cell culture microplates, and then incubated at 37°C in 5% CO_2. On day 5, cells where assayed for oxygen consumption rate (OCR) with a XF24 Extracellular Flux Analyzer (Seahorse Bioscience, Billerica, MA, USA). After an OCR baseline measurement, oligomycin, carbonyl cyanide 4-(trifluoromethoxy) phenylhydrazone (FCCP), rotenone and antimycin A were sequentially added to each well to reach final concentrations of 1 µM oligomycin, 0.4 µM (Doxy-) and 0.2 µM (Doxy+) for FCCP, and 1 µM rotenone and antimycin A. Data are expressed as pmol of O_2 per minute. O_2 calculation method was (LEVEL) Direct (AKOS). The experiment was performed in collaboration with Prof. Paolo Bernardi (University of Padova).

3.14 Immunohistochemical analysis

The specimens were obtained from patients who were treated surgically for primary sporadic colorectal carcinoma and selected from Pathological Anatomy Unit of Modena Hospital.

The surgical specimens were fixed in 10% buffered neutral formalin for 24 hours. Tissue samples were embedded in paraffin, cut and stained with Hematoxylin and Eosin for histological diagnosis. For each case, a representative paraffin-embedded

block containing tumour tissue and normal mucosa was sectioned at 4 µm. Immunoperoxidase staining was performed with the Benchmark XT Automatic Staining System using diaminobenzidine (DAB) as chromogen (Ventana, Strasbourg, France) and using the View DAB Detection Kit (Ventana, Strasbourg, France). At the end of the reaction, slides were counterstained with Hematoxylin. Rabbit polyclonal antibody anti-human Lon was used at a dilution of 1:500 for 1 hour at 37°C.

3.15 Statistical analysis

Two-dimensional image analysis was carried out using ImageMaster 2D Platinum software version 6.0 (GE Healthcare). Relative spot volumes, calculated as %V (V single spot/V total spots on a gel, where V is the integration of the OD over the spot area), were used for quantitative analyses in order to decrease experimental errors. The normalized spot volume was averaged and standard deviation was calculated. A fold change of 2.0 as then chosen as threshold of expression variation. Statistical data were obtained using Prism software (Graph Pad, La Jolla, CA, USA). Protein spot variation was considered significant when showing a p-value <0.05 and at least a 2-fold change in relative volume %V. For real time quantitative PCR, and for functional assays, experiments were repeated up to nine times, significance was determined by Kruskal-Wallis or Mann Whitney tests, and p values <0.05 were considered significant.

For cytofluorimetric analysis, data obtained after staining with fluorescent probes represent the median of the net fluorescence value ± standard deviation (SD). The net fluorescence value was obtained, linearising the fluorescence values from the logarithmic scale and subtracting the linearised median value of the blank (i.e. the sample containing cells treated in the same manner, but without any staining) from the median fluorescence value of the stained sample to eliminate any autofluorescence background.

Statistical analysis were performed by using GraphPad Prism software (San Diego, CA, USA). For functional assays experiments were repeated at least three times, differences have been analyzed by Student's t-test, and values of p less than 0.05 were considered as statistically significant.

4. RESULTS

4.1 Lon expression is modulated in human cancer cell lines

In silico analysis of publicly available data has shown that Lon is up-regulated in many solid tumours, including colon carcinoma (see: http://www.ebi.ac.uk/gxa/experiment/ E-MT AB-62), and often down-regulated in blood tumours (including acute lymphoblastic leukaemia, acute myeloid leukaemia, and acute promyelocytic leukaemia). To confirm these data, we analyzed Lon expression, both at the mRNA and protein level, in cancer cell lines of different origin in comparison with normal nonproliferating or proliferating cells; relative mRNA levels are reported in Figure 1A. We found that Lon mRNA was highly expressed in cells like K562 (human erythromyeloblastoid leukaemia), DU145 (prostate carcinoma), PC3 (prostatic adenocarcinoma, grade IV), SHSY5Y (neuroblastoma), MCF7 (breast carcinoma), and RKO (colon carcinoma), if compared to normal resting PBMCs (Peripheral Blood Mononuclear Cells). In particular, Lon relative expression was 0.68±0.38 in resting PBMCs, 1.17±0.33 in PBMCs activated with anti-CD3 plus anti-CD28 monoclonal antibodies, 1.99±1.14 in resting purified B lymphocytes, 2.62 ± 0.48 in CpG DNA-activated B cells, 6.16±3.74 in resting purified monocytes, 4.41±0.25 in lipopolysaccharide-activated monocytes, 30.54±24.93 in K562 cells, 9.46±8.7 in HDLM2, 15.35±14.29 in DU145 cells, 10.19±1.8 in PC3 cells, 14.43±3.8 in RKO cells, 22.79±12.40 in SHSY5Y cells, 7.08±3.9 in HepG2 cells, and 7.94±0.62 in MCF7 cells. Consistent with mRNA data, Lon protein levels were increased in cell lines from solid tumours (Figure 1B and Figure 1C), including DU145 cells (3-fold increase), PC3 cells (20-fold increase), RKO cells (15-fold increase), SHSY5Y cells (14-fold increase), and MCF7 cells (10-fold increase), if compared to normal cells (i.e. resting monocytes). Lon protein was actually expressed at extremely low levels in in resting PBMCs from healthy donors, as well as in purified B cells and monocytes, regardless of their activation status.

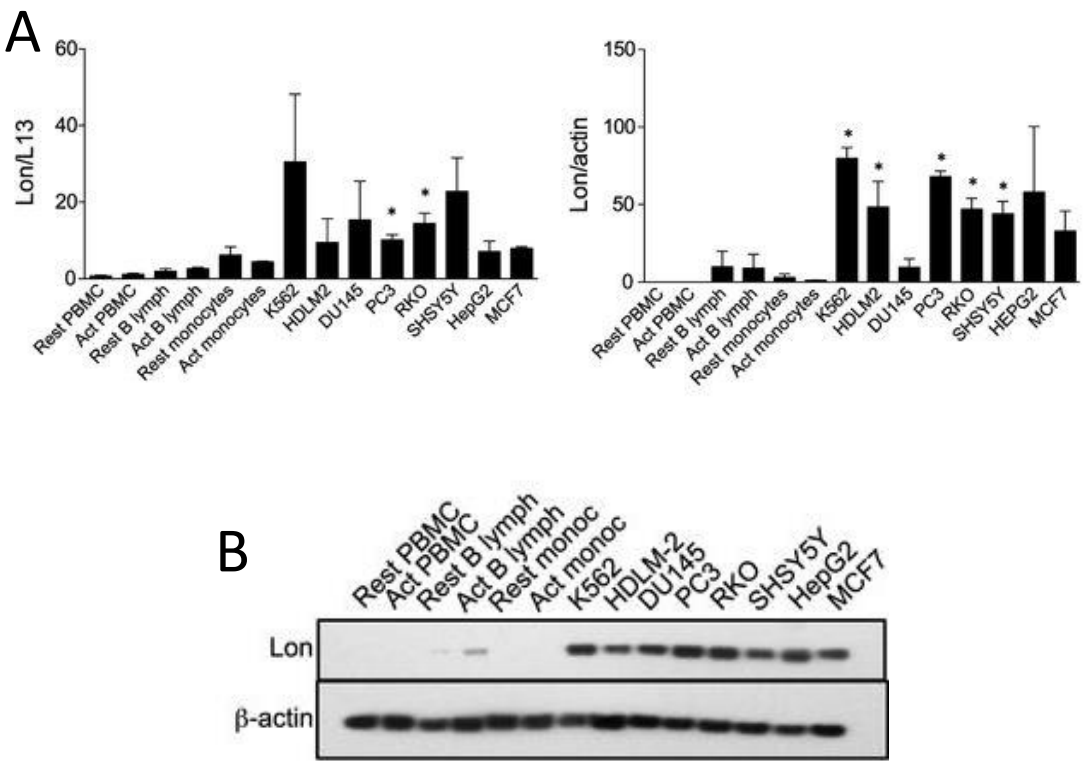

Figure 1: Lon is up-regulated in cancer cells. **A.** mRNA transcript (left panel) and protein levels (right panel) of Lon in cells from different origins. Lon mRNA levels were normalized to L13 mRNA; Lon protein levels were normalized to β-actin. Values represent means ± SD of 3 independent experiments, each in triplicate. **B.** A representative immunoblot of Lon and β-actin is shown. **P* < 0.05 vs. resting PBMCs.

4.2 Lon down-regulation increases cell susceptibility to apoptosis

RKO colon cancer cells were selected as a model to assess the effects of Lon down-regulation in cells deriving from solid tumors. These cells have been used for a long time and well characterized in our laboratory, and they showed remarkably high levels of Lon protease. First, it has been ascertained that Lon was actually localized in mitochondrial matrix in these cells. For this purpose, we performed an immunocytochemical staining using a custom polyclonal antibody able to identify specifically Lon and an antibody able to detect human mitochondria, along with a DAPI staining to evidence the nucleus. Figure 2 shows respectively the single signals for Lon, mitochondria (hMit) and DAPI, and the merged signal indicating the actual colocalization of Lon and mitochondria. No signal outside mitochondria could be

detected.

Then, we targeted Lon mRNA by RNA interference, using the retroviral vector RNAi-Ready-pSIRENRetroQ-ZsGreen, which allows a constitutive silencing of the target gene in stably transfected cells. Cells were selected on the basis of ZsGreen expression, and those with the highest ZsGreen fluorescence were sorted and seeded. As shown in Figure 3 (left panel), Lon protein was significantly reduced in shLon cells compared with shCTRL cells. However, culture of shLon cells for a long time resulted in a progressive decrease of ZsGreen+ cells, which represented about one third of cells after 20 days of culture and much less thereafter (not shown); the percentage of ZsGreen+ cells remained stable (>95%) in shCTRL (Figure 3, middle panel). Indeed, in living, ZsGreen- cells a concomitant re-expression of Lon protease, whose levels returned similar to that present in shCTRL, was observed (Figure 3, right panel).

Because constitutive down-regulation of Lon resulted in massive cell death, a doxycycline-inducible model has been generated. Among all clones, the RKO Tr2 was chosen to perform the experiments due to its 71.0±8.5% reduction of Lon expression after 72 hours of treatment with doxycycline Figure 4A**.** On these cells, the analysis of apoptosis was performed by flow cytometry by staining with ANXV and TOPRO. ANXV binds to phosphatidylserine, which is exposed on the cell surface during the first stages of apoptosis, whereas TOPRO detects loss of plasma membrane integrity. With this staining, it is possible to distinguish four different subpopulations: early apoptotic (ANXV+ TOPRO-), late apoptotic (ANXV+ TOPRO+), necrotic (ANXV- TOPRO+) and living (ANXV-TOPRO-) cells. Down-regulation of Lon increased spontaneous tendency to undergo apoptosis after such culture period. After 72 hours of Lon silencing, early apoptotic cells lightly increased from 5.44±0.89 to 7.8±1.52, late apoptotic cells from 1.01±0.33 to 8.62±3.59, and necrotic cells from 1.31±0.27 to 6.49±5.27. After 96 hours, early apoptotic cells increased from 5.99±0.56 to 19.7±3.1, late apoptotic cells from 2.49±0.04 to 22.8±0.28, and necrotic cells from 5.28±1.88 to 6.99±2.37. A more pronounced increase of cell death could be observed after 168 hours (Figure 4B).

Then, we analyzed mitochondrial and cytosolic levels of cytochrome c (cyt c), cleaved caspase-9, and PARP in order to understand if the increased apoptotic cell death is mediated by intrinsic pathway. As shown in figure 4C, cells where Lon was down-regulated showed a massive release of cyt c in the cytosol (left panel), which led to

activation of caspase-9 and PARP (right panel). Thus, silencing of Lon determines apoptosis through cyt c release from mitochondria, which led to intrinsic apoptosis.

We decided to perform all the experiments at the conditions of minor cell death, i.e. culturing cells in control medium (Doxy-), which contains puromycin and G418 but not doxycycline, and induction medium (Doxy+), which contains puromycin, G418 and doxycycline, for 72 hours.

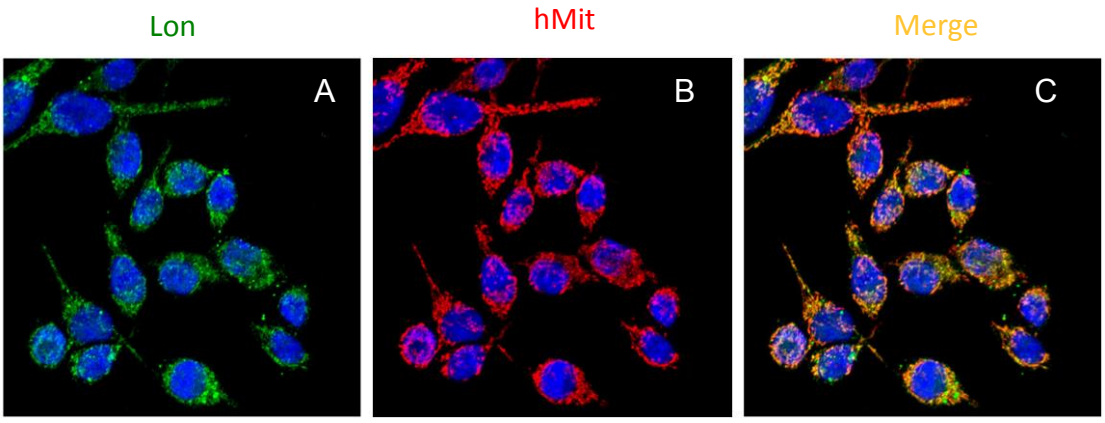

Figure 2: Lon localized in mitochondrial matrix. Representative image of localization of Lon protease in mitochondria in RKO cells obtained by confocal microscopy. It is shown: in panel A Lon staining, in panel B mitochondria staining (hMit), in panel C the merge of all staining indicating Lon and mitochondria colocalization.

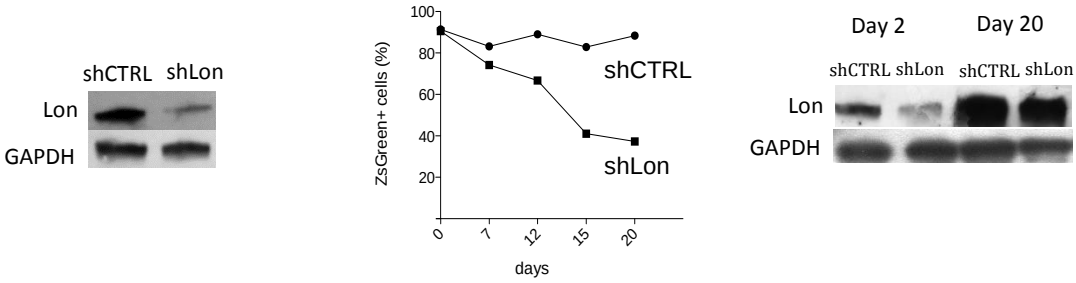

Figure 3: Immunoblot analysis of total lysates from shCTRL and shLon cells (left panel); quantification of the percentage of ZsGreen positive cells among shCTRL and shLon cells (middle panel); immunoblot analysis of Lon from total lysates obtained from shLon and shCTRL cells after 2 and 20 days of culture (right panel).

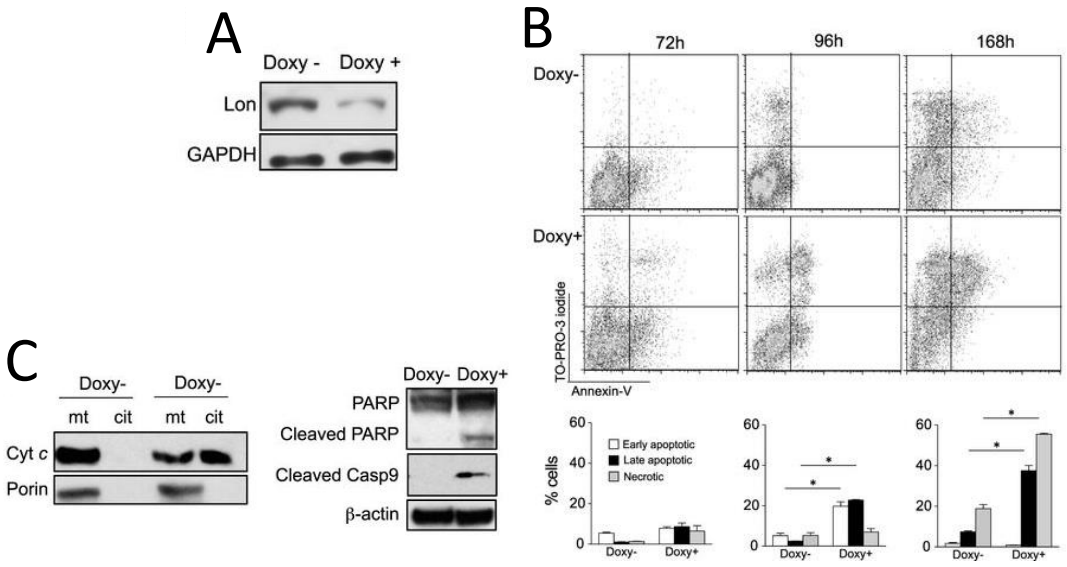

Figure 4: **Analysis of RKO cells where Lon was down-regulated by doxycycline. A.** Immunoblot analysis showing the down-regulation of Lon by doxy. **B.** Cytofluorimetric quantification of early and late apoptotic cells and of necrotic cells after 72, 96 and 168 hours of culture in RKO cells where Lon was down-regulated by doxy. Representative dot plots reporting annexin-V staining vs. TO-PRO-3 iodide staining are reported. Values represent the mean ± SD of five independent experiments; *P<0.05. **C.** Left panel: immunoblot analysis of cytochrome c (cyt c) in mitochondrial fraction obtained from RKO cells where Lon was down-regulated by doxy. Right panel: immunoblot analysis of PARP and cleaved caspase 9 in total lysates from RKO cells where Lon was down-regulated by doxy.

4.3 Lon down-regulation strongly affects mitochondrial proteome

In order to identify changes in mitochondrial proteome caused by Lon silencing, we performed two dimensional gel electrophoresis (2-DE) on proteins isolated from highly purified mitochondria of RKO cells where Lon was down-regulated. Figure 5A shows a representative image of 2-DE from Doxy- and Doxy+ cells. Sixty-two spots that appeared different in samples from Doxy- and Doxy+ cells were excised from 2-DE gels and submitted for mass spectrometry analysis; 56 were clearly identified as 39 individual proteins. Two spots detected in silver stained gels were not clearly resolved in preparative gels and 4 spots, present in very low amounts in analytical gels, were not visible after colloidal Coomassie staining of preparative gels. The identified spots are listed in Table 1. More than 83.0% of identified proteins were mitochondrial; among them, 26.0% were related to stress response, 14.8% to ribosome assembly, 12.7% to oxidative phosphorylation (OXPHOS), 8.5% to Krebs cycle, 6.3% to fatty acid β-oxidation, and the remaining 14.7% to mitochondrial cristae integrity, ketone body

catabolism, mtDNA transcription and maintenance. If classified on the basis of submitochondrial localization, 29.0% of proteins were identified as matrix proteins, 53% as membrane proteins and 18.0% as unknown compartment. Seventeen protein spots, which correspond to 9 individual proteins, namely ATP5J, ATPA, CH60, GRP75, HSPB1, PDIA3, S10AB, UCRI, VDAC1, were more abundant in mitochondria from Lon-deficient cells. Conversely, 39 protein spots, which correspond to 24 individual proteins, were decreased in mitochondria from Lon-deficient cells (Figure 5B). To further confirm these results, we selected 4 representative proteins (EFTu, UCRI, GRP75, MDHM) and re-analysed their expression in the same cells by western blot. As expected, Lon down-regulation caused an increase of GRP75 and a reduction of EFTu, UCRI, MDHM (Figure 5C).

Spot No	Short name	Protein name	UniProt ID[a]	Matched sequences/ searched sequences	Score [b]	Seq. coverage %[c]	Therotical MW (Da)
1	ACADS	Short-chain specific acyl-CoA dehydrogenase	P16219	12/14	535	40	44611
2	ANXA2	Annexin A2	P07355	4/6	98	24	38808
3	ATIF1	ATPase inhibitor	Q9UII2	4/4	184	16	12241
4	ATP5J	ATP synthase-coupling factor 6	P18859	7/7	671	53	12580
5	ATPA	ATP synthase subunit alpha	P25705	20/36	1664	67	59828
6	ATPD	ATP synthase subunit delta	P30049	6/8	946	46	17479
7	C1QBP	Complement component 1 Q subcomponent-binding protein	Q07021	5/5	132	41	31742
8	CALU	Calumenin	O43852	17/24	836	72	37198
9	CH10	10 kDa heat shock protein	P61604	7/8	356	54	10925
10	CH-60	60 kDa heat shock protein	P10809	12/24	1339	47	61187
11	CH-60	60 kDa heat shock protein	P10809	11/14	499	28	61187
12	CH-60	60 kDa heat shock protein	P10809	11/11	796	25	61187
13	CH-60	60 kDa heat shock protein	P10809	14/16	829	33	61187
14	CHCH3	Coiled-coil-helix-coiled-coil-helix domain-containing protein 3	Q9NX63	16/19	837	52	26421
15	COX5A	Cytochrome c oxidase subunit 5A	P20674	9/9	882	38	16923
16	DHE3	Glutamate dehydrogenase 1	P00367	10/14	334	26	61701
17	DLDH	Dihydrolipoyl dehydrogenase	P09622	20/25	1126	56	54713
18	ECI1	Enoyl-CoA delta isomerase 1	P42126	13/13	1080	56	33080
19	EFTU	Elongation factor Tu	P49411	8/23	623	55	49852
20	EFTU	Elongation factor Tu	P49411	4/13	160	32	49852
21	EFTU	Elongation factor Tu	P49411	11/11	533	31	49852
22	EFTU	Elongation factor Tu	P49411	12/12	767	33	49852
23	EFTU	Elongation factor Tu	P49411	15/15	591	43	49852

24	EFTU	Elongation factor Tu	P49411	28/33	3646	77	49852
25	ETFB	Electron transfer flavoprotein subunit beta	P38117	18/19	987	65	28054
26	GRP75	Stress-70 protein, mitochondrial	P38646	15/16	848	28	73920
27	GRP75	Stress-70 protein, mitochondrial	P38646	14/15	862	26	73920
28	GRP75	Stress-70 protein, mitochondrial	P38646	10/10	510	19	73920
29	H2B1C	Histone H2B type 1-C/E/F/G/I	P62807	5/12	616	63	13898
30	HSPB1	Heat shock protein beta-1	P04792	4/5	80	29	22826
31	IDH3A	Isocitrate dehydrogenase [NAD] subunit alpha	P50213	5/7	217	22	40022
32	IMMT	Mitochondrial inner membrane protein	Q16891	24/50	1029	55	84026
33	IMMT	Mitochondrial inner membrane protein	Q16891	29/51	1376	50	84026
34	MDHM	Malate dehydrogenase	P40926	13/14	477	45	35937
35	MDHM	Malate dehydrogenase	P40926	17/21	1709	67	35937
36	PDIA1	Protein disulfide-isomerase	P07237	29/47	2073	80	57480
37	PDIA3	Protein disulfide-isomerase A3	P30101	25/35	1413	61	57146
38	PDIA3	Protein disulfide-isomerase A3	P30101	28/41	3061	65	57146
39	PDIA3	Protein disulfide-isomerase A3	P30101	13/13	522	28	57146
40	PGAM1	Phosphoglycerate mutase 1	P18669	10/18	355	77	28900
41	PROF1	Profilin-1	P07737	9/13	866	75	15216
42	ROA2	Heterogeneous nuclear ribonucleoproteins A2/B1	P22626	5/7	144	22	37464
43	RT22	28S ribosomal protein S22	P82650	7/8	281	27	41425
44	S10AB	Protein S100-A11	P31949	4/5	193	49	11847
45	SCOT1	Succinyl-CoA:3-ketoacid coenzyme A transferase 1	P55809	19/25	1088	64	56578
46	SCOT1	Succinyl-CoA:3-ketoacid coenzyme A transferase 1	P55809	5/5	160	15	56578
47	SCOT1	Succinyl-CoA:3-ketoacid coenzyme A transferase 1	P55809	10/10	425	27	56578
48	SODM	Superoxide dismutase [Mn]	P04179	7/8	316	27	24878
49	SSBP	Single-stranded DNA-binding protein	Q04837	5/7	200	40	17249
50	THIL	Acetyl-CoA acetyltransferase	P24752	12/33	820	83	45456
51	TPM3	Tropomyosin alpha-3 chain	P06753	10/17	198	40	32856
52	TRAP1	Heat shock protein 75 kDa	Q12931	21/46	857	68	80345
53	UCRI	Cytochrome b-c1 complex subunit Rieske,	P47985	8/10	579	34	29934
54	VDAC1	Voltage-dependent anion-selective channel protein 1	P21796	9/9	271	46	30868
55	VDAC1	Voltage-dependent anion-selective channel protein 1	P21796	15/23	2014	77	30868
56	VDAC2	Voltage-dependent anion-selective channel protein 2	P45880	12/16	1601	65	32060

Table 1: Qualitative and quantitative data and associated statistics from two-dimensional analysis. a) Swiss-Prot/TrEMBL accession number; b) Percentage of amino acid sequence coverage of matched peptides in the identified proteins; c) MASCOT score (Matrix Science, London, UK; http://www.matrixscience.com).

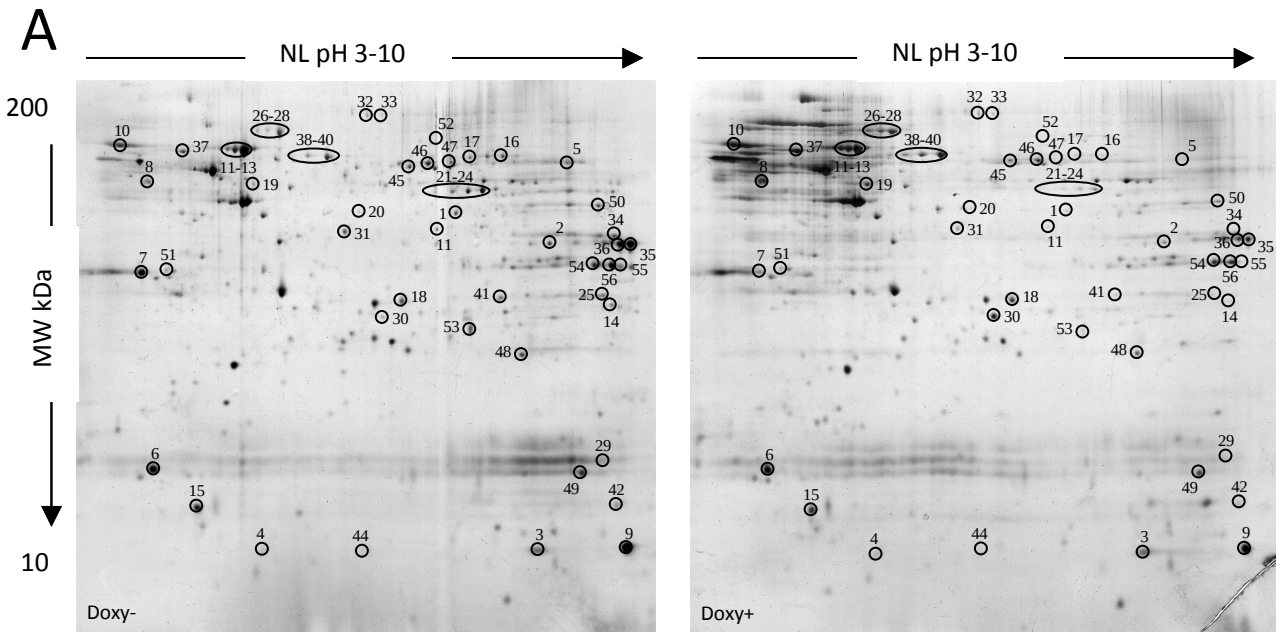
A
NL pH 3-10
NL pH 3-10
200
MW kDa
10
Doxy-
Doxy+

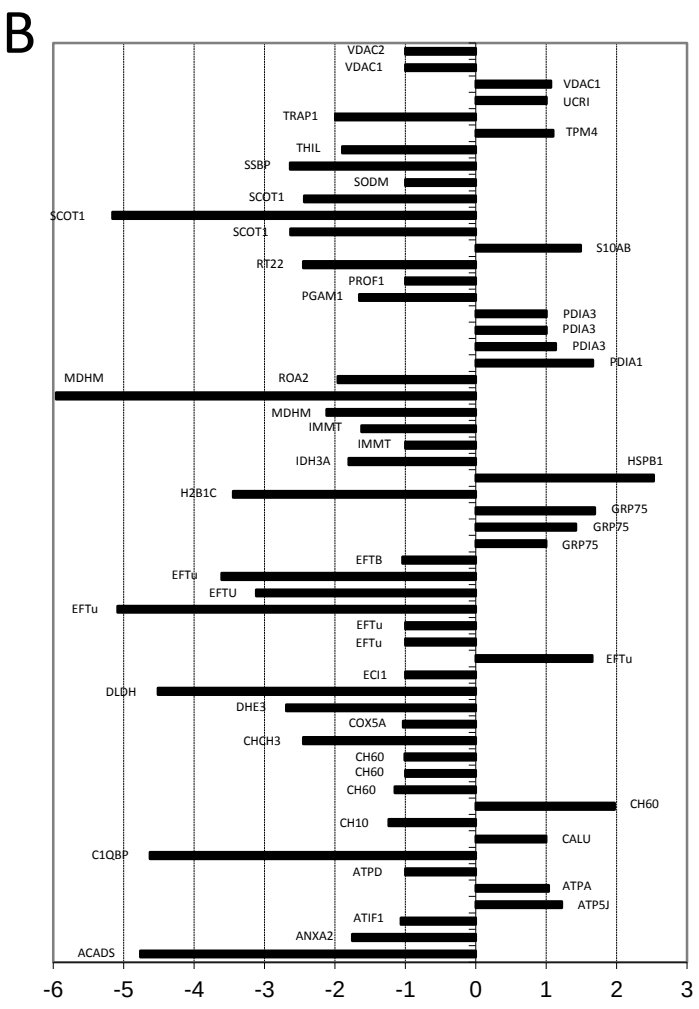
B
VDAC2
VDAC1
VDAC1
UCRI
TRAP1
TPM4
THIL
SSBP
SODM
SCOT1
SCOT1
SCOT1
S10AB
RT22
PROF1
PGAM1
PDIA3
PDIA3
PDIA3
PDIA1
MDHM
ROA2
MDHM
IMMT
IMMT
IDH3A
HSPB1
H2B1C
GRP75
GRP75
GRP75
EFTB
EFTu
EFTU
EFTu
EFTu
EFTu
EFTu
ECI1
DLDH
DHE3
COX5A
CHCH3
CH60
CH60
CH60
CH60
CH10
CALU
C1QBP
ATPD
ATPA
ATP5J
ATIF1
ANXA2
ACADS
-6
-5
-4
-3
-2
-1
0
1
2
3

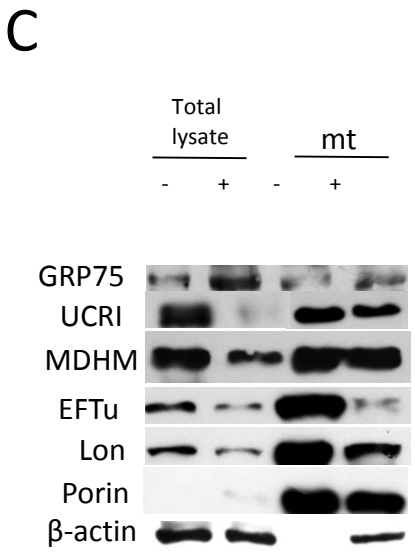
C
Total lysate
mt
-
+
-
+
GRP75
UCRI
MDHM
EFTu
Lon
Porin
β-actin

Figure 5: Lon down-regulation affects mitochondrial proteome. **A.** Representative two dimensional gels (2-DE) images of mitochondrial proteins obtained from doxycyclineregulated RKO cells. Numbers indicate spots that are significantly different (P<0.05) between Doxy- and Doxy+ cells according to Student's t-test. **B.** Quantitative analysis of spots identified by mass spectrometry. Spot quantification (percentage volume of each spot) was performed on 2-DE using ImageMaster 2D Platinum version 7.0 software. **C.** Immunoblot analysis of total lysates and mitochondrial fractions from Doxy- (-) and Doxy+ (+) cells for the following proteins: GRP75, UCRI, MDHM, EFTu, Lon, β-actin, porin.

4.4 Lon down-regulation impairs mtDNA transcription and steady state levels of OXPHOS complexes

Because Lon is known to bind mtDNA (63) and to be involved in its maintenance and transcription through the regulation of TFAM, the main factor driving mtDNA transcription (71), we decided to measure the levels of mtDNA, mtRNAs and TFAM in control and silenced cells by real time PCR and immunoblotting. We chose to quantify three different mitochondrial transcripts: ND1, encoding for subunit 1 of the NADH dehydrogenase complex and lying at the 5' end of the H strand; cytB, encoding for cytochrome B and lying at 3' end of the H strand; and ND6, encoding for subunit 6 of the NADH-dehydrogenase complex, and being the only mRNA encoded by the L strand (5' end). While mtDNA levels were almost unchanged (Figure 6A), mitochondrial transcripts for ND1, ND6 and cytB showed a 57.0%, 35.7%, 29.9% reduction in Doxy+ cells, respectively (Figure 6B). We also observed a concomitant reduction of TFAM protein (51.0±4.8%) (Figure 6C). As levels of mtRNAs encoding components of the respiratory chain appeared severely reduced, we analysed the steady-state levels of OXPHOS complex by immunoblotting using 5 mAbs, one each against Complex I subunit NDUFB8, Complex II subunit 30kDa (30 kDa IP), Complex III subunit Core 2 (core 2), Complex IV subunit II (COXII), and ATP synthase subunit alpha (F1a). 30kDa Ip, COXII, and NDUFB8 were markedly reduced (Figure 6D), meaning that complex I, complex II, and complex IV were severely affected by Lon down-regulation; complex I was the most altered, with a >90% reduction in silenced cells. Complex II and Complex IV had a 70% and a 61% decrease, respectively. Treatment with H_2O_2 increased Lon level, as expected; such increase was also observed in Doxy+ cells, where upregulation of Lon by H_2O_2 counteracted, even if not completely, silencing by shRNA. However, the partial recovery of Lon induced by H_2O_2 was not sufficient to re-establish the normal levels of OXPHOS proteins (Figure 6D).

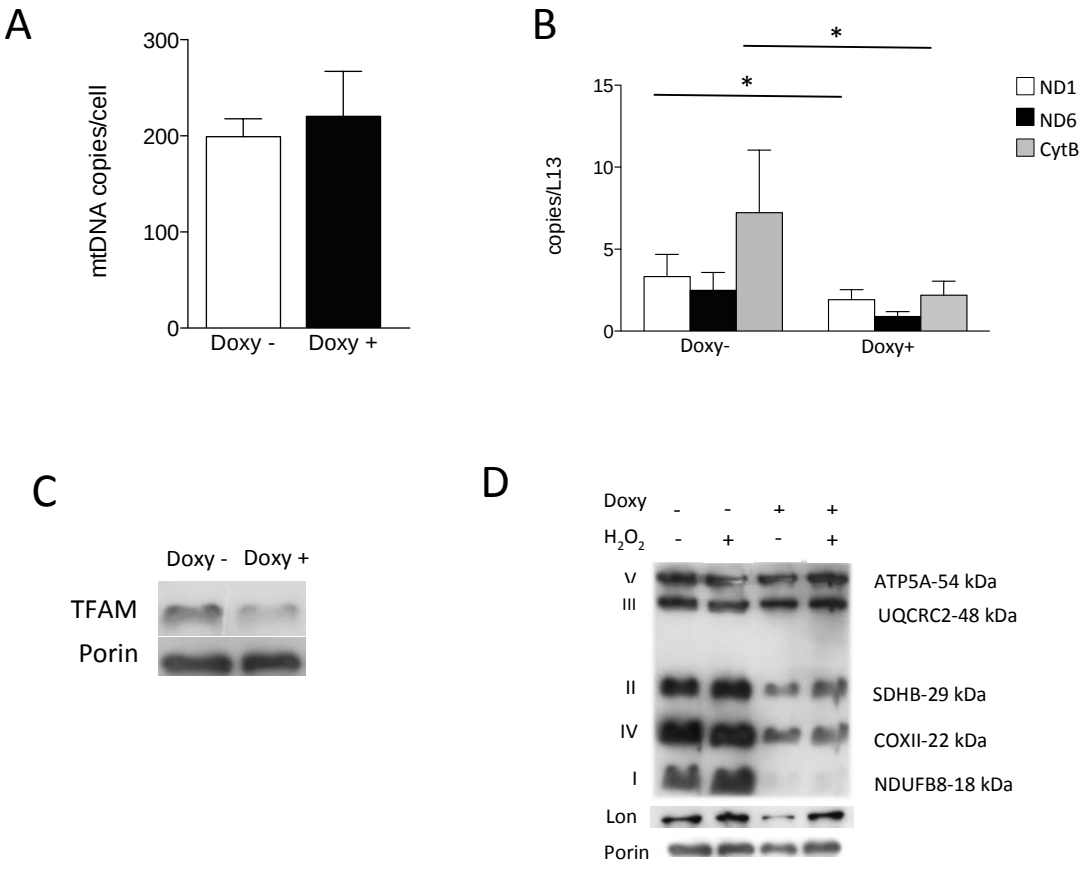

Figura 6: **Lon down-regulation impairs mtDNA transcription and steady state levels of OXPHOS complexes.** **A.** Analysis of mitochondrial DNA (mtDNA) content in cells with doxycycline-regulated Lon down-regulation and controls. Values represent the mean ± SD of six experiments. **B.** Analysis of mitochondrial transcript ND1, ND6 and cytB in cells with doxycycline-regulated Lon down-regulation and controls. Values represent the mean ± SD of six experiments; *P <0.05. **C.** Immunoblot analysis of TFAM protein levels. **D.** Immunoblot analysis of electron transport chain proteins in cells with doxycycline-regulated Lon decrease at the steady state level.

4.5 Lon down-regulation impairs ATP synthesis and mitochondrial respiration

Considering the reduction of electron transport chain complexes, we next asked whether these changes could significantly alter mitochondrial functionality. For this purpose, we measured ATP levels in control and silenced cells by luminescence assay, to ascertain the actual impairment of OXPHOS process. Since after Lon down-regulation there was no significant reduction of ATP levels at basal conditions (Figure 7A), we decided to submit cells to a stress stimulus, i.e. 2DG (20, 40, 80 nM), a glucose analogue that inhibits glycolysis forcing cell to undergo mitochondrial respiration. Only in presence of the highest concentration of 2DG (80 mM), Lon down-regulation

caused a reduction of ATP levels, which dropped from 0.25±0.04 to 0.03±0.001 nmol/mg proteins (Figure 7A). Moreover, we decided to measure oxygen consumption rate (OCR) in control and silenced cells by XF24 Extracellular Flux Analyser that permits to analyse oxygen levels produced by monolayered cells. It is possible to measure several key parameters to understand mitochondrial status: basal respiration without any stimulation, ATP turnover and proton leak by adding oligomycin, maximal respiration by adding FCCP and non-mitochondrial respiration by adding antimycin A and rotenone. Figure 7B shows that control cells display a normal respiration profile whereas Lon silencing caused a marked decrease in mitochondrial respiration, and abolished both basal and FCCP stimulated OCR.

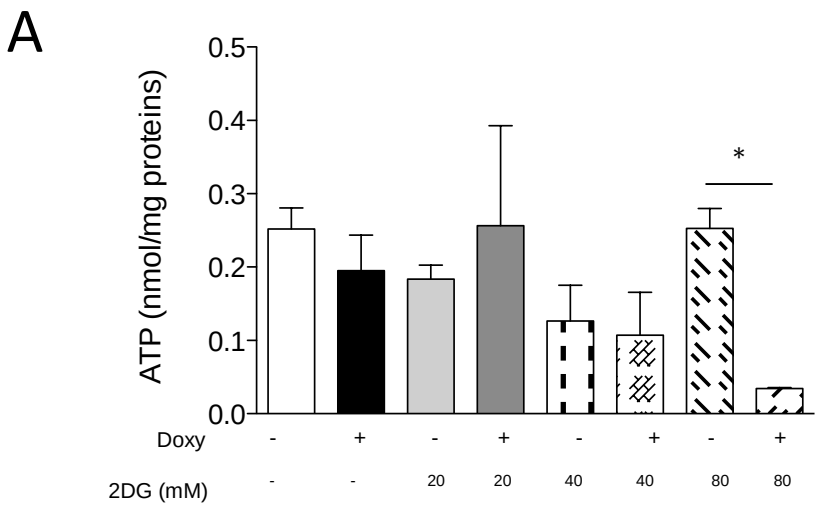

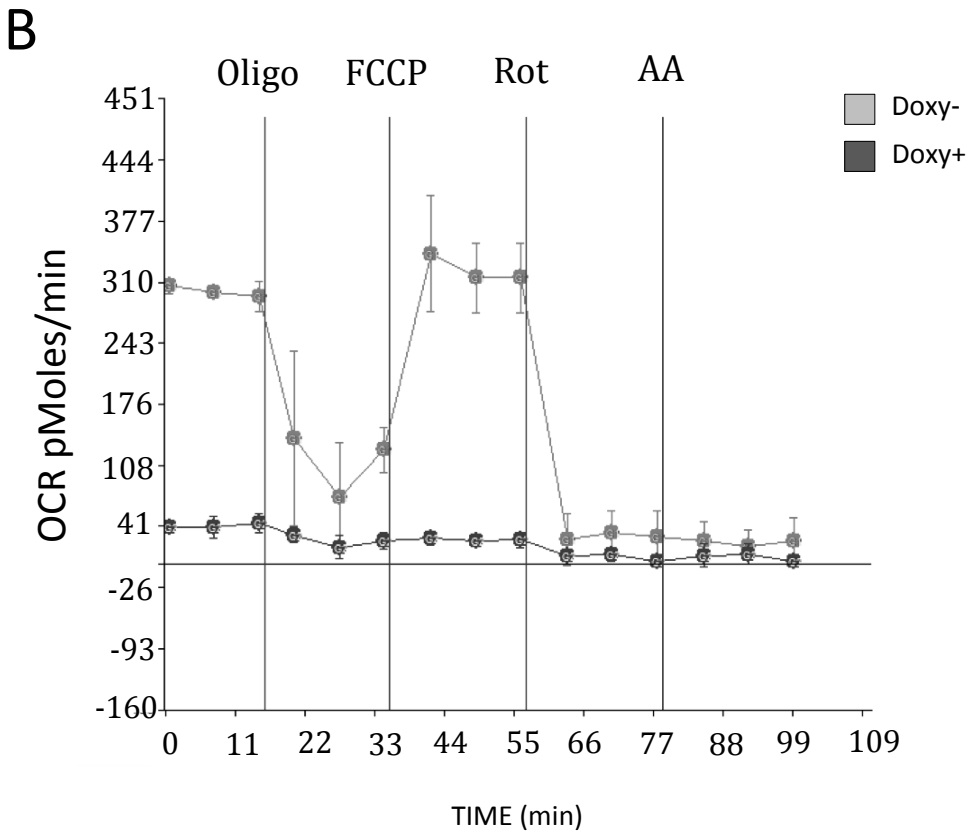

Figure 7: Lon down-regulation affects ATP synthesis and mitochondrial respiration A. Quantification of ATP levels in cells with doxycycline-regulated Lon down-regulation and controls after treatment with 2DG at the indicated doses. Values represent the mean ± SD of nine independent experiments; **P*<0.05. **B.** Representative traces of OCR experiments performed on monolayers of viable RKO cells with doxycycline-regulated Lon down-regulation and controls. A, B, C and D indicate progressive additions of oligomycin (1 μM), FCCP (0.2 μM in Doxy- cells and 0.4 μM in Doxy+ cells), rotenone (1 μM), and antimycin (1 μM), respectively.

4.6 Lon down-regulation alters redox status of RKO cells

To evaluate the redox status of Lon-deficient cells, reactive oxygen species and total glutathione were measured. We observed a 3-fold increase of relative levels of cellular H_2O_2 (Figure 8A) and a 1.3-fold increase of mitochondrial O_2^- (Figure 8B) in cells where Lon was down-regulated. There changes in ROS levels were associated with a 1.5 fold reduction of total glutathione (Figure 8C).

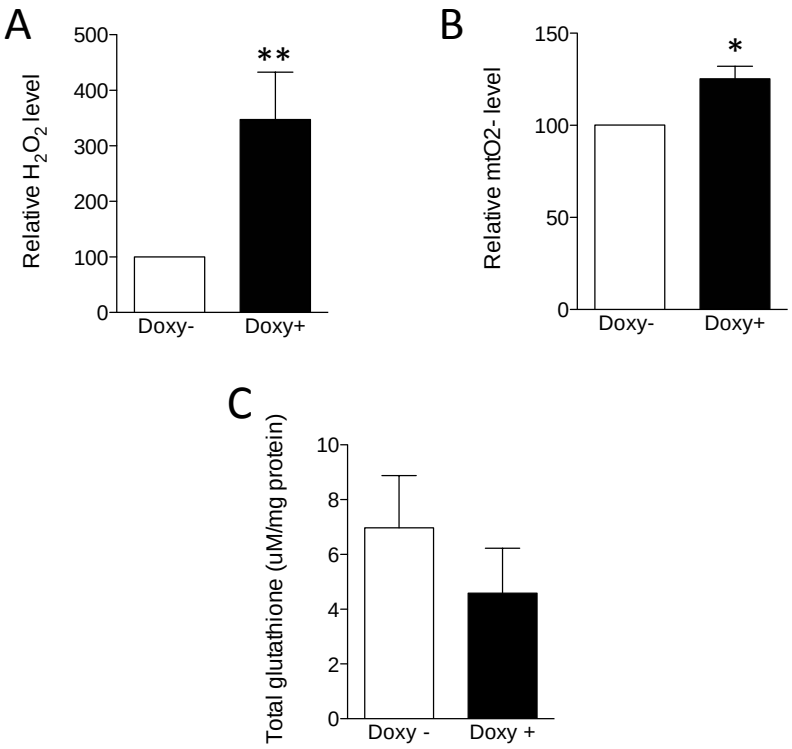

Figure 8: **Lon down-regulation alters redox status of RKO cells.** Detection of hydrogen peroxide (H_2O_2) in cells with doxycycline-regulated Lon expression, as revealed by flow cytometry. **A.** Data are expressed as percentage of change with respect to control samples, set to 100%, and represent the mean ± SD of four experiments; ***P* <0.01. **B.** Detection of mitochondrial anion superoxide (mtO_2^-) in cells with doxycycline-regulated Lon expression, as revealed by flow cytometry. Data are expressed as percentage of change with respect to control samples, set to 100% and represent the mean ± SD of four experiments; **P* <0.05. **C.** Detection of total glutathione (GSH) in cells with doxycycline-regulated Lon expression. Values represent the mean ± SD of six experiments.

4.7 Lon down-regulation alters mitochondrial morphology

We wondered whether impaired electron transport chain caused alterations of mitochondria morphology. To analyse mitochondrial ultrastructure in detail, electron microscopy images have been acquired of both doxy- and doxy+ cells. As reported in figure 9A and 9B, silenced cells were characterized by an increase in the number of dying cells, some exhibiting superficial blebs, a typical sign of apoptosis. Control cells showed typical elongated mitochondria characterized by cristae running parallel one to the other within an electrondense matrix (Figure 9C and 9E). By contrast, in Lon-deficient cells numerous mitochondria were very heterogeneous in size and shape (Figure 9D, F), and were characterized by dilated cristae, vacuoles and heavily electrondense deforming inclusions (Figure 9G and 9H). The variety of mitochondrial

morphological alterations may reflect the extent of impaired OXPHOS function and perhaps a different response of the cells depending on their metabolism. To confirm this observation, three-dimensional images of mitochondrial network were obtained by confocal microscopy with mtDsRed labelling.

We observed a different shape of mitochondrial network in Lon silenced cells and control cells. In particular, figure 10A shows a typical largely interconnected and continuous “tubular”network in control cells (left panel), while Lon down-regulation revealed an evident fragmentation leading to network disruption (right panel). Analysis of microscopy images shows that these changes did not impact the total number of mitochondria, as well as the mitochondrial network volume (Figure 10B, middle and left panels), which were similar in silenced and control cells; the mean volume a single mitochondrion was increased by 1.5-fold (Figure 10B, right panel).

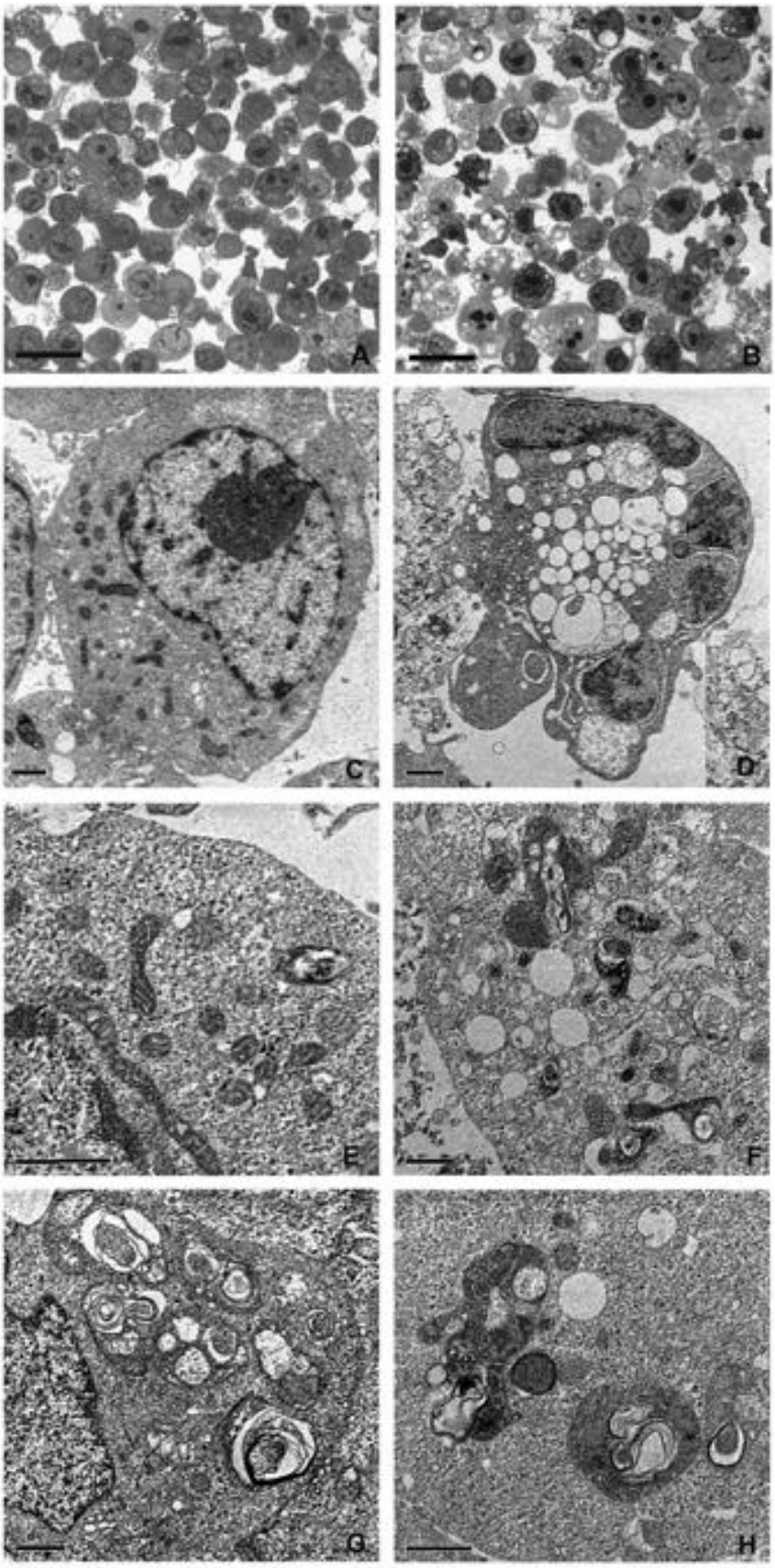

Figure 9: **Lon down-regulation alters mitochondrial morphology.** Representative images obtained by transmission electron microscopy of Doxy- (A, C, E) and Doxy+ (B, D, F-H) cells showing that Lon down-regulation affects mitochondrial architecture. Scale bars = 1 μm.

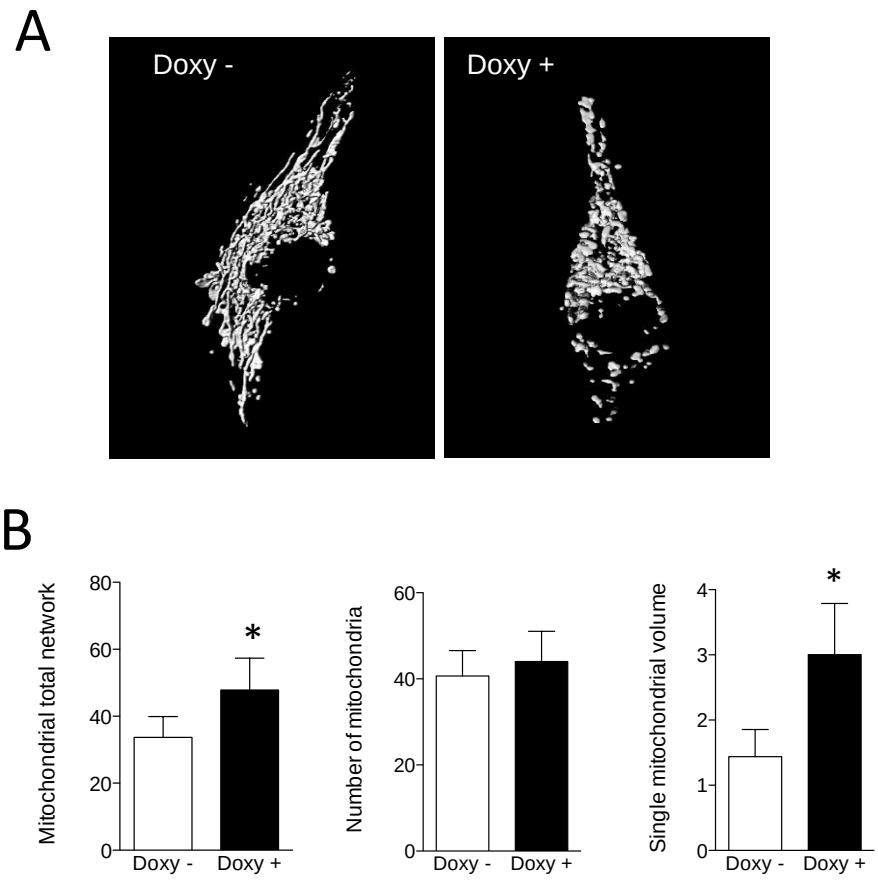

Figure 10: **Lon down-regulation alters mitochondrial morphology.** Representative fluorescence images of mtDsRed-labeled mitochondria in cells with doxycycline-regulated Lon down-regulation and controls. Quantitative analysis of changes in mitochondrial morphology expressed as total number of mitochondria (middle), single mitochondrial volume (right), and mitochondrial network (left). Values represent the mean ± SD of twenty experiments; *P <0.05.

4.8 Lon is overexpressed in CRC ex-vivo cells

Considering that Lon is up-regulated in RKO cancer cells, we asked if Lon could be up-regulated also in colorectal cancer (CRC) samples obtained from patients.

In collaboration with Dr. Lorena Losi (University of Modena and Reggio Emilia), Lon protein expression was analysed by immunohistochemical staining in a set of human CRC samples. Samples were from normal and cancer mucosa of patients that underwent surgical resection of the colorectal cancer. The patient set contained 18 men and 15 women (age 46-85, median age 67.15). Primary tumors were localized in the colon and the stages at diagnosis were I (8), II (8), III (9), IV (8) according to the TNM and WHO classification. The percentage of Lon+ cells was >75% in 11 CRC

samples, 30-75% in 15 CRC samples and <30% in 6 CRC samples; a representative image is reported in figure 11A.

In the same samples, staining for β-catenin, E-cadherin, Ki-67 and p53 were also performed; data of 13 samples are summarized in the representative figure 11B, and representative images of immunohistochemical staining are reported in Figure 11A. E-cadherin was expressed at the membrane level (indicated with +) in all samples. Interestingly, seven samples with β-catenin at the nuclear level (N), rather than at the membrane level (M), showed a strong up-regulation of Lon. The percentage of Ki-67+ cells was 59.6±14.28 in samples where Lon was up-regulated, and 48.57±15.73 in samples where Lon was down-regulated or unchanged. Regarding p53, immunohistochemistry showed nuclear staining (indicated with +) in 19 out of 33 CRC samples. Thus, in the majority of colon cancer samples of stage I-IV that we tested, Lon was up-regulated relative to normal mucosa, and this up-regulation was paralleled by the nuclear localization of β-catenin and p53, and higher proliferation levels as estimated by Ki-67.

Lon up-regulation was also confirmed by western blot analysis on the same samples. We obtained protein lysates from formalin fixed, paraffin-embedded samples, provided by Prof. Lorena Losi. After deparaffinisation and rehydration, samples were immersed in extraction buffer to obtain protein lysates. We analyzed Lon protein expression by western blot in 22 out of 33 human colorectal cancer (CRC) samples and compared it with that measured in the surrounding nontransformed mucosa for each patient. The representative figure 11C suggests that Lon is up-regulated in cancer cells, compared to the normal mucosal counterparts. Lon levels were normalized to β-actin levels and the ratio was considered for statistical analysis. In particular, we observed a 2-fold increase of Lon protein levels in CRC samples (figure 11B).

A

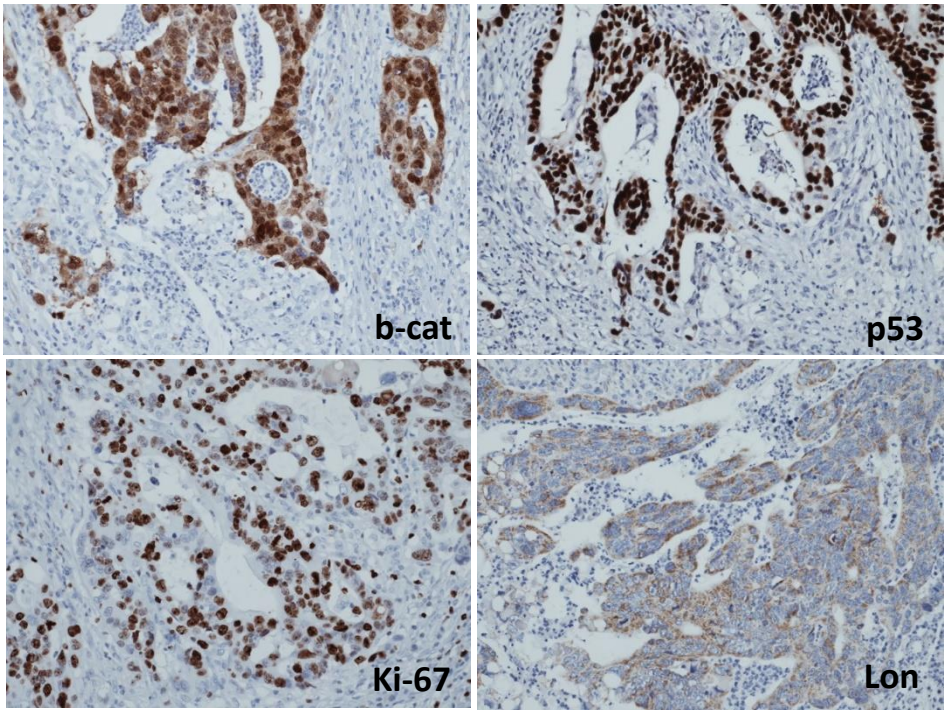

B

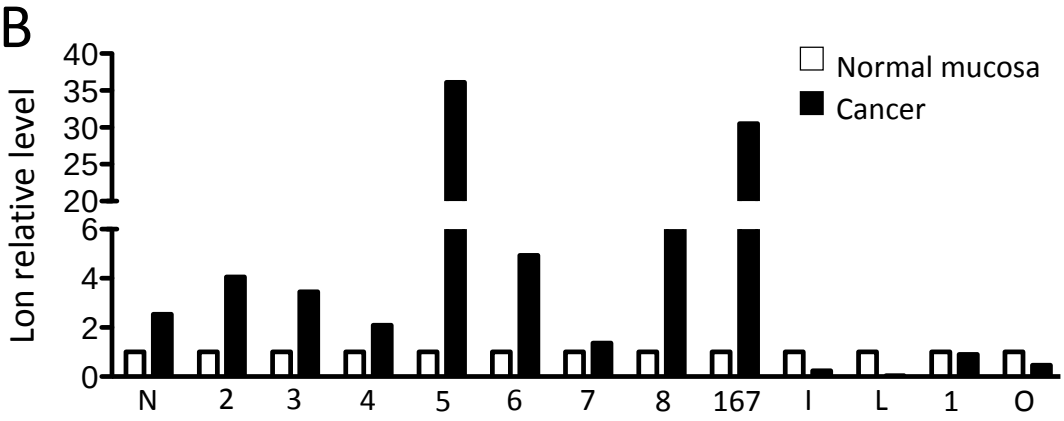

	N	2	3	4	5	6	7	8	167	I	L	1	O
E-cad	+	+	+	+	+	+	+	+	+	+	+	+	+
b-cat	M	N	N	M	N	M	M	N	M	M	M	M	M
p53	-	+	+	+	+	+	-	+	+	+	-	+	+
Ki67	50	60	60	50	40	60	60	80	70	30	30	90	30
Stage	III	II	I	III	II	III	III	II	III	II	III	III	III

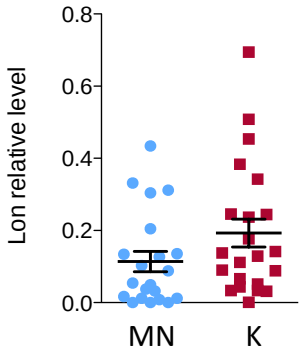

C

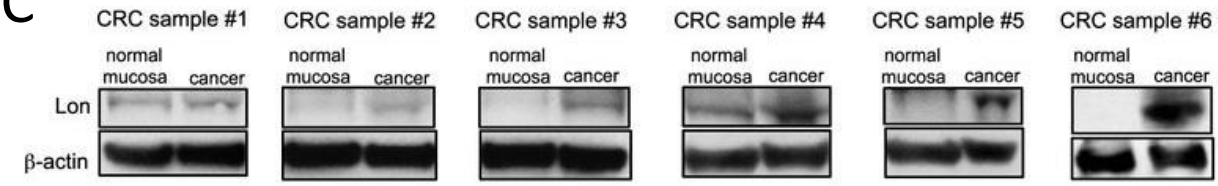

Figure 11: Lon is overexpressed in CRC ex-vivo cells. A. Representative immunoistochemical stainings. **B**. Lon levels in CRC samples compared to paired normal mucosa. Results of immunohistochemical analysis for E-cadherin (E-cad), β-catenin (β-cat), p53, Ki-67 in the same samples are also reported together with tumour stage. Concerning E-cad, + indicates its presence on the membrane; concerning β-cat, M and N indicates its presence an the membrane or in the nucleus respectively; regarding p53, + indicates that p53 is mutated and accumulates in the nucleus whereas – indicates that p53 is wild-type; concerning Ki-67, the percentage of positive cells is reported. Lon relative expression as a whole is also reported in the histogram on the right. **C.** Representative immunoblots reporting Lon quantification in tissues from CRC and normal mucosa.

4.9 CDDO and CDDO-Me decrease proliferation, induce apoptosis in cancer cells, and increase mitochondrial hydrogen peroxide and mitochondrial superoxide anion

Because RNA interference down-regulation of Lon induces profound alterations of mitochondrial functionality and morphology, we wondered whether pharmacological inhibition of Lon could have the same effects. The triterpenoid 2-cyano-3,12-dioxooleana-1,9,-dien-28-oic acid CDDO and its methylated form CDDO-Me are able to inhibit Lon in a dose-dependent manner, and recently several studies reported their anticancer and anti-proliferative effects (60). Therefore, we chose three cell lines in use for a long time and well characterized in our laboratory to investigate the effect of such inhibition. In particular, we opted for RKO colon carcinoma line, HepG2 liver hepatocellular carcinoma line and MCF7 breast adenocarcinoma line.

We first analyzed the effects of CDDO or CDDO-Me on cell growth by culturing the three cell lines with increasing concentrations (0.1, 1, 2.5, 5 and 10 μM) of these molecules for up to 72 hours. As shown in Figure 12A and 12B, counting adherent cells revealed that inhibition of Lon induced a time- and concentration- dependent inhibition of cell proliferation. Indeed, we observed a pronounced reduction of cells in culture after treatment with both inhibitors (figure 12B). However, CDDO-Me was much stronger than CDDO in inhibiting cell growth in all cell lines.

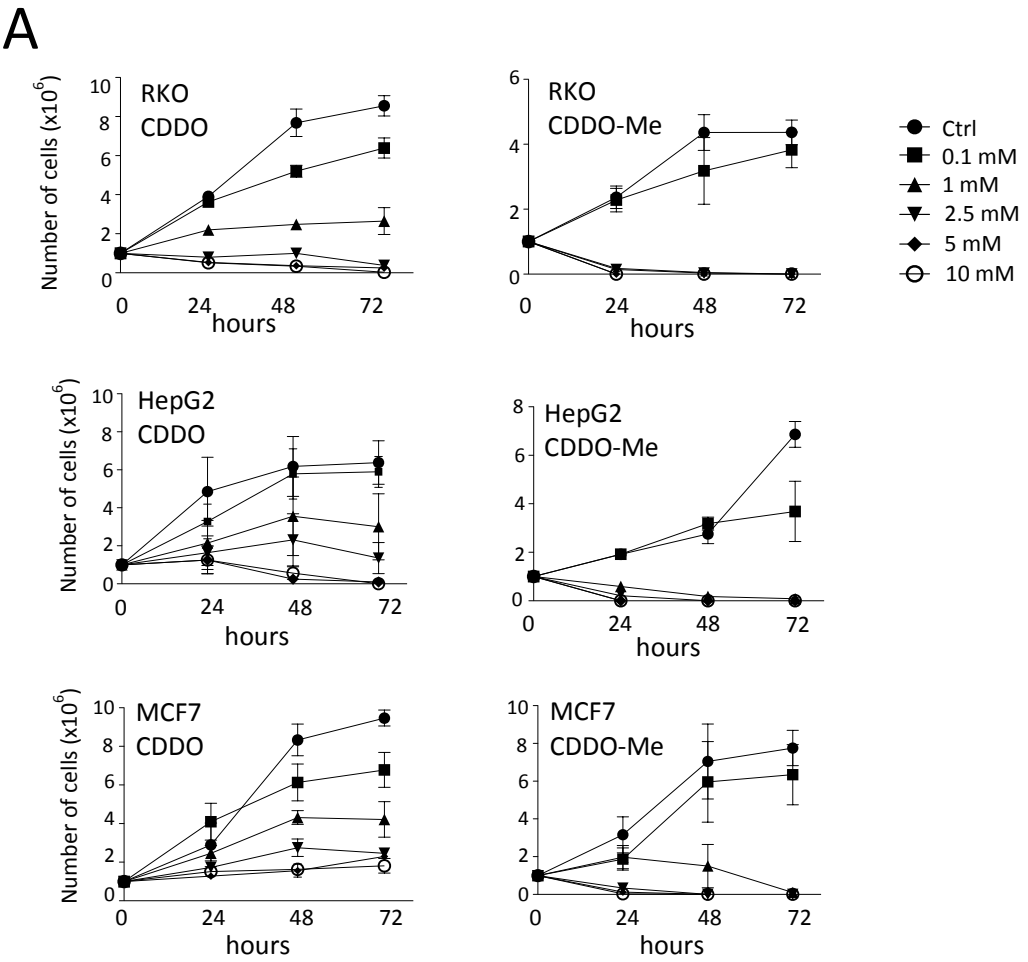

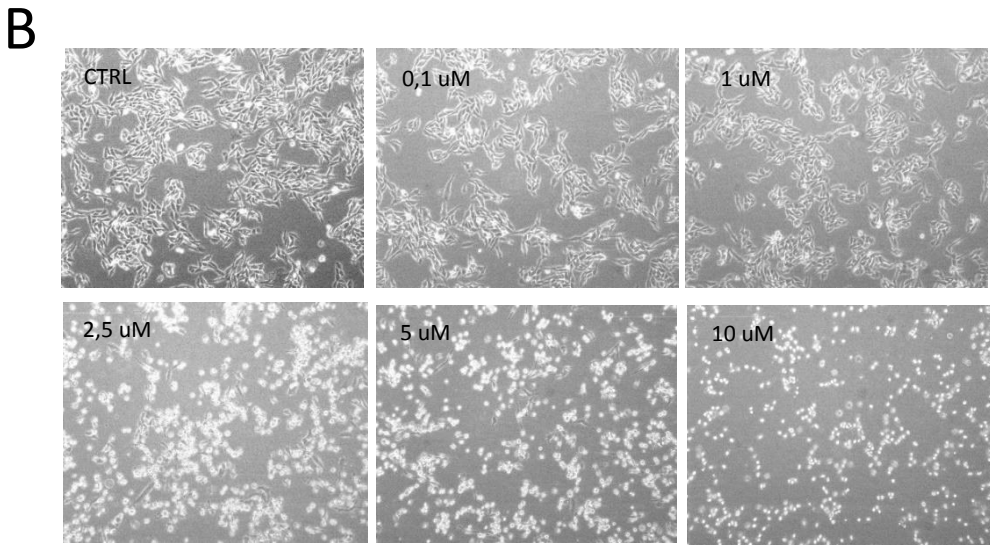

Figure 12. CDDO and CDDO-Me decrease proliferation in cancer cells. **A.** Growth curve of RKO, HepG2 and MCF7 cells incubated with the indicated concentrations of CDDO (left panel) or CDDO-Me (right panel) for up to 72 hours; DMSO-treated cells were considered as controls (Ctrl). **B.** Representative image of RKO cell culture after treatment with CDDO 0.1, 1, 2.5, 5 and 10 µM or left untreated for control.

Next, we wondered if the observed decrease in cellular proliferation was associated with an increase in cell death. Thus, to investigate the inhibitory mechanisms induced by these drugs, we analysed their effects on apoptosis, and on mitochondrial functionality and morphology. First, we performed a cytofluorimetric analysis to investigate simultaneously apoptosis and production of reactive oxygen species (ROS) at the single cell level. In particular, cells were first loaded with mitochondria peroxy yelow 1 (mitoPY1), which specifically detects mitochondrial hydrogen peroxide (mtH_2O_2), and then treated for up to 24 hours with CDDO or CDDO-Me. Then, supernatans were collected and cells stained with MitoSOX red superoxide indicator (MitoSOX), with annexin-V (AnxV), which binds to phosphatidylserine, a molecule exposed on cell surface during the first stages of apoptosis, and TOPRO-3 iodide (TOPRO), which detects loss of plasma membrane integrity. As shown in figure 13A, early apoptotic cells were those positive for AnxV and negative for TOPRO, whereas late apoptotic/necrotic cells were positive for TOPRO, independently on AnxV. Also in this case, CDDO-Me was more potent than CDDO in inducing cell death for RKO, HepG2 and MCF7 cells (Figure 13B and 13C, and Figure 13D, 13E and 13F): a slight increase in cell death was observed after 6 hour incubation with CDDO and 1-2.5 µM CDDO-Me. In particular, in RKO cells, we observed a strong increase in the percentage of early apoptotic cells after 16 and 24 hours of incubation, both CDDO and CDDO-Me led to a strong increase in the percentage of early apoptotic cells (Figure 13B and 13C, left panels). Regarding HepG2 cells, higher concentrations of CDDO and CDDO-Me were needed to induce apoptosis (Figure 13D and 13E). In addition, we investigated whether the viability of normal cell could also be affected by triterpenoids. For this purpose, we obtained primary cultures of human fibroblasts and we treated these cells with increasing concentrations of CDDO and CDDO-Me for 6, 16 and 24 hours. The results showed that CDDO and CDDO-Me did not induce apoptosis in human fibroblasts, except for the highest tested concentration of CDDO-Me, and only after 16 and 24 hours of incubation (Figure 14A and 14B).

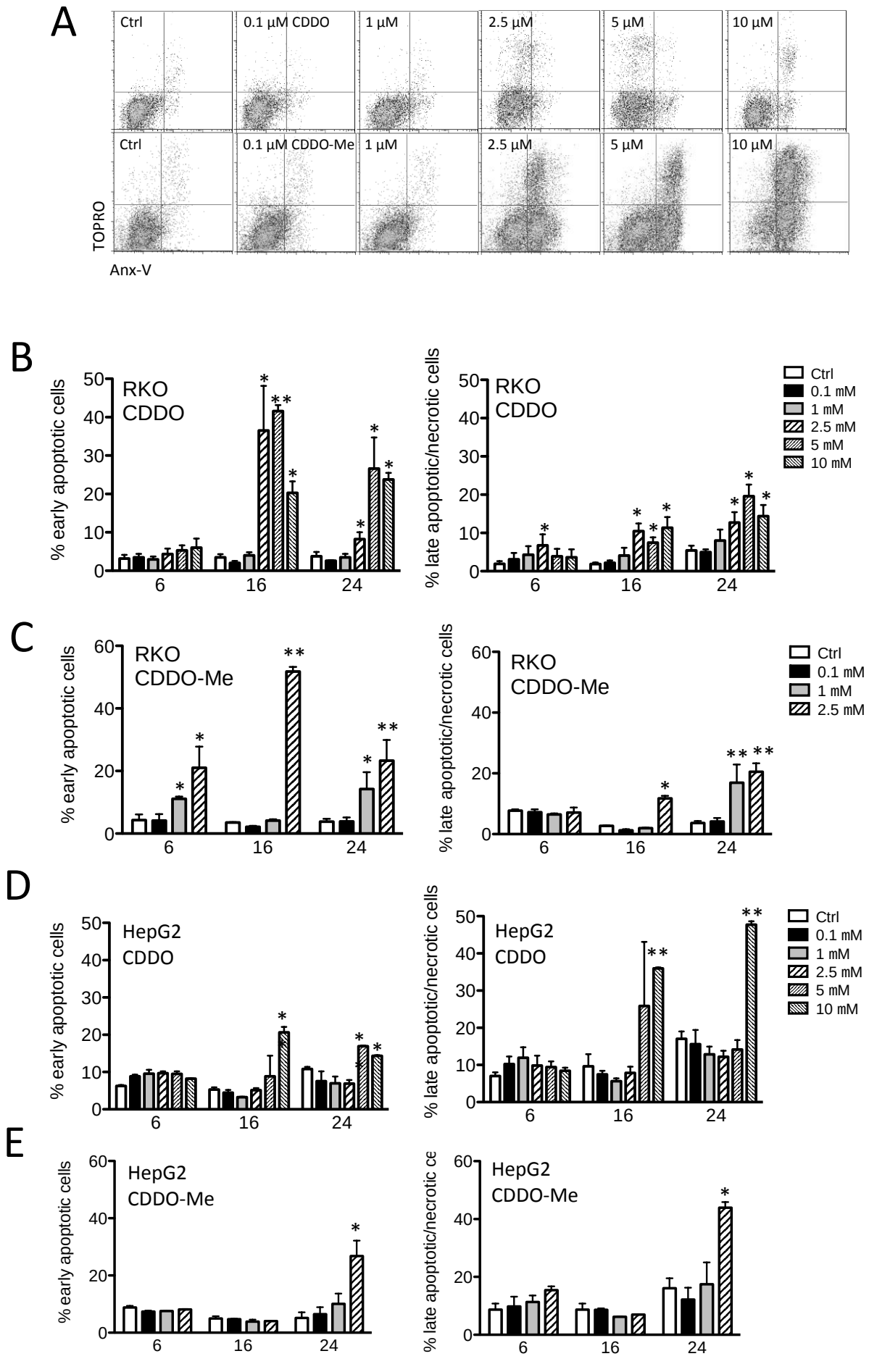
A
Ctrl
0.1 μM CDDO
1 μM
2.5 μM
5 μM
10 μM
Ctrl
0.1 μM CDDO-Me
1 μM
2.5 μM
5 μM
10 μM
TOPRO
Anx-V
B
RKO
CDDO
% early apoptotic cells
% late apoptotic/necrotic cells
Ctrl
0.1 mM
1 mM
2.5 mM
5 mM
10 mM
C
RKO
CDDO-Me
% early apoptotic cells
% late apoptotic/necrotic cells
Ctrl
0.1 mM
1 mM
2.5 mM
D
HepG2
CDDO
% early apoptotic cells
% late apoptotic/necrotic cells
Ctrl
0.1 mM
1 mM
2.5 mM
5 mM
10 mM
E
HepG2
CDDO-Me
% early apoptotic cells
% late apoptotic/necrotic ce
6
16
24

F

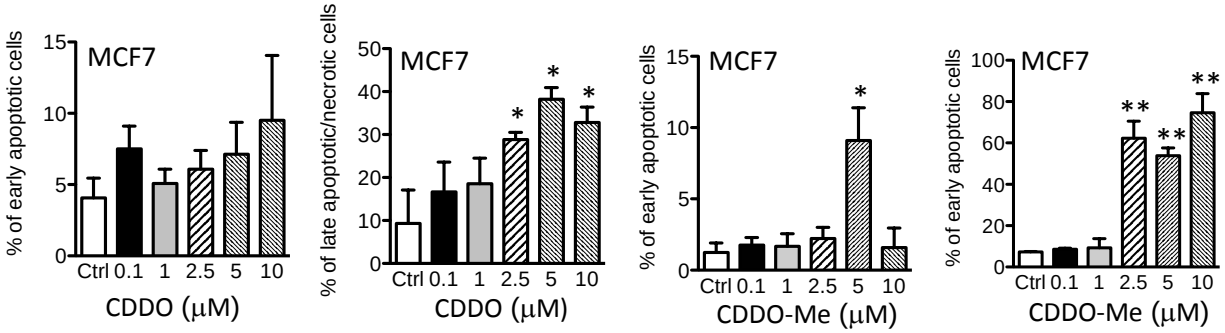

Figure 13: CDDO and CDDO-Me are anti-proliferative and induce apoptosis in cancer cells. A. Representative flow cytometric dot plots combining Annexin-V (AnxV) Alexa Fluor Pacific Blue and TO-PRO-3 iodide (TOPRO) staining in RKO cells treated with DMSO (Ctrl), or with increasing concentrations of CDDO or CDDO-Me for 24 hours. **B.** Percentage of early apoptotic cells (AnxV+/TOPRO- cells) and late apoptotic/necrotic cells (AnxV-/TOPRO+ and AnxV+/TOPRO+ cells) in RKO cells treated with CDDO 0.1, 1, 2.5, 5 and 10 μM or left untreated for control for up to 24 hours. Values represent the mean ± SD of five independent experiments, **P*<0.05 and ***P* <0.01 *vs.* Ctrl. **C.** Percentage of early apoptotic cells and late apoptotic/necrotic cells in RKO cells treated with CDDO-Me 0.1, 1, 2.5, 5 and 10 μM or left untreated for control for up to 24 hours. Values represent the mean ± SD of five independent experiments, **P* <0.05 and ***P* <0.01 *vs.* Ctrl. **D.** Percentage of early apoptotic cells and late apoptotic/necrotic cells in HepG2 cells treated with CDDO 0.1, 1, 2.5, 5 and 10 μM or left untreated for control for up to 24 hours. Values represent the mean ± SD of three independent experiments, **P* <0.05 *vs.* Ctrl and ***P* <0.01 *vs.* Ctrl. **E.** Percentage of early apoptotic cells and late apoptotic/necrotic cells in HepG2 cells treated with CDDO-Me 0.1, 1, 2.5, 5 and 10 μM or left untreated for control for up to 24 hours. Values represent the mean ± SD of three independent experiments, **P* <0.05 *vs.* Ctrl and ***P* <0.01 *vs.* Ctrl.
F. Percentage of early apoptotic cells and late apoptotic/necrotic cells in MCF7 cells after treatment with the indicated concentrations of CDDO or CDDO-Me for 24 hours. Values represent the mean ± SD of three independent experiments, **P* <0.05 *vs.* Ctrl and ***P* <0.01 *vs.* Ctrl.

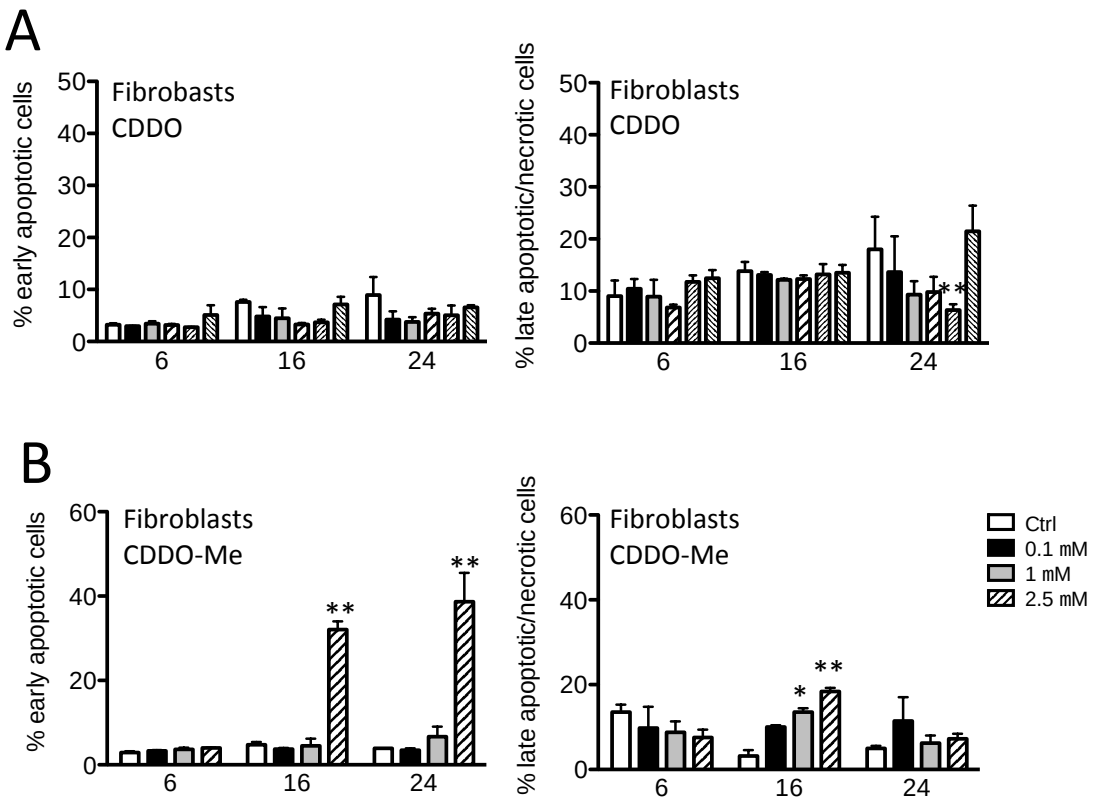

Figure 14: CDDO and CDDO-Me do not induce apoptosis in primary fibroblasts. A. Percentage of early apoptotic cells and late apoptotic/necrotic cells after treatment with CDDO for up to 24 hours. Values represent the mean ± SD of three independent experiments. ***P* <0.01 *vs.* Ctrl. **B.** Percentage of early apoptotic cells and late apoptotic/necrotic cells after treatment with CDDO-Me for up to 24 hours. Values represent the mean ± SD of three independent experiments, **P* <0.05 *vs.* Ctrl and ***P* <0.01 *vs.* Ctrl.

We next examined the effects of CDDO and CDDO-Me on the activation of caspase-9 and caspase-3, in order to understand if apoptotic cell death was mediated by the intrinsic pathway. As shown in figure 15A, we were able to detect both the activation of caspase-9, evidenced by the presence of the band at 39 kDa, and the decreased expression of the full length protein (47 kDa), at least after 24 hours of treatment with CDDO-Me. The concentration of 2.5 µM CDDO or CDDO-Me lead to the activation of caspase-9, which occurred after 6-hours treatment in RKO cells. As reported in Figure 15B, activated caspase-3/7 was detected by flow cytometry and showed a major increase after 16 and 24 hours of treatment, both for CDDO and CDDO-Me (Figure 15C).

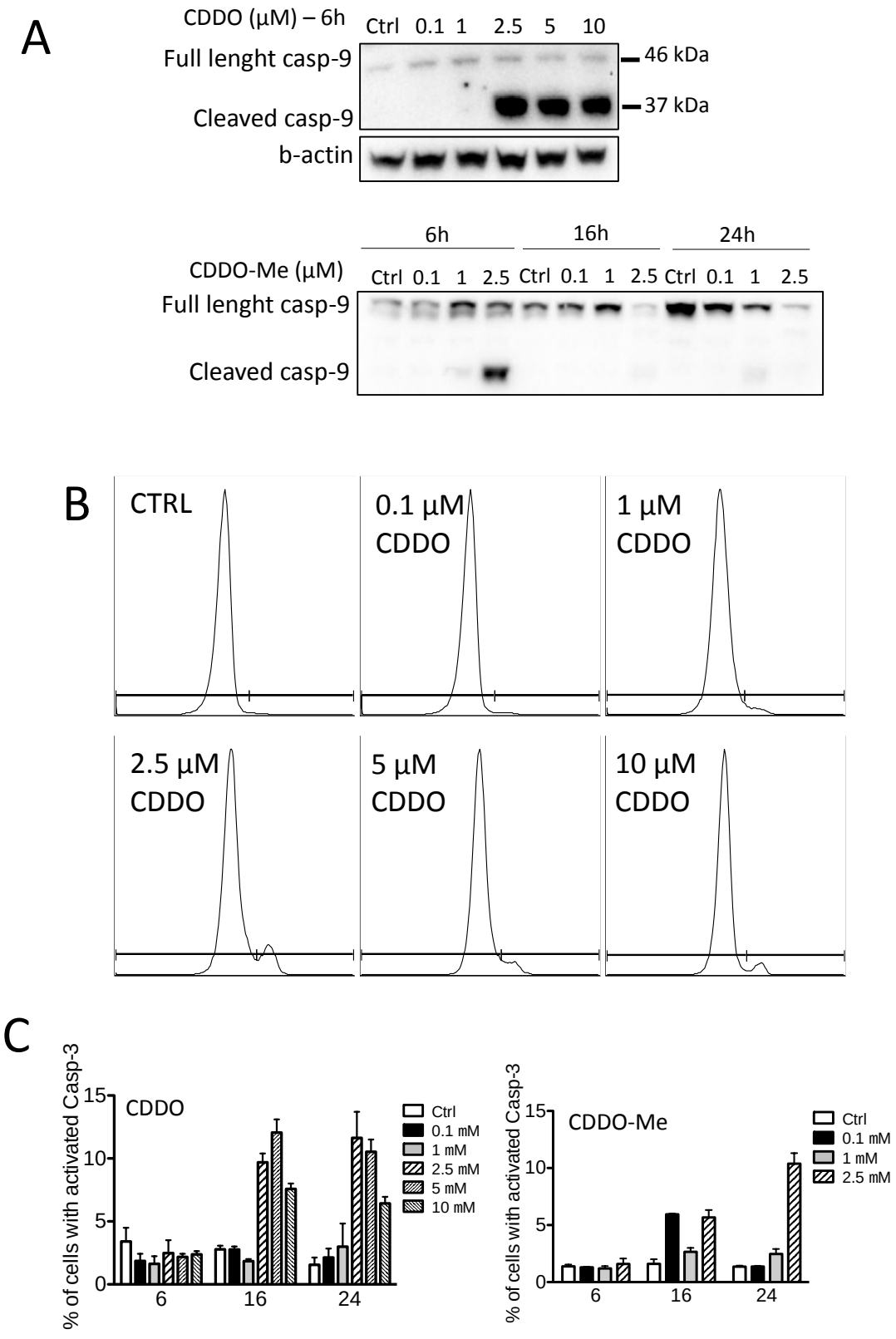

Figure 15: CDDO and CDDO-Me lead to activation of caspase-9 and caspase-3/7. A. Western blot analyses showing caspase-9 activation in RKO cells after treatment with CDDO and CDDO-Me at the indicated concentrations. Cells treated with 1 µM staurosporine (STS) for 4 hours were used as positive controls for caspase-9 activation. **B.** Representative histograms showing CellEvent Caspase-3/7 Green Detection Reagent in RKO cells treated with increasing concentrations of CDDO, as revealed by flow cytometry. **C.** Quantification of cells with activated caspase-3/7 after treatment with CDDO or CDDO-Me or up to 24 hours. Data represent the mean ± SD of four independent experiments; **P* <0.05 and ** *P* <0.01 *vs.* Ctrl.

In addition, we know that Lon is an important regulator of adaptive mechanism of cells to oxidative stress. Concerning ROS, the gating strategy is reported in Figure 16A**.** Here, we reported a representative dot plot showing AnxV and TOPRO fluorescences to discriminate viable and dead cells, together with the histograms showing mitoPY1 and mitoSOX fluorescences in AnxV-/TOPRO- cells indicating the content of mtH_2O_2 and mtO_2^- in living cells. In this figure, RKO were treated with H_2O_2, a molecule known to induce oxidative stress. In particular, is to note the shift of fluorescence between untreated control cells and those treated with H_2O_2. Thus, we analysed oxidative status of cells after treatment with CDDO or CDDO-Me. The quantification of mitoPY1 and mitoSOX is reported in Figure 16B and 16C for RKO cells, and in Figure 16D and 16E for HepG2 cells. In RKO cells, when CDDO was used, an increase in mtH_2O_2 and mtO_2^- was in part observed at 6 hours, but especially after 16 hours of incubation (Figure 16B); when CDDO-Me was used, mtH_2O_2 and mtO_2^- increased at 2.5 µM after 16 hours of incubation (Figure 16C). A slight increase after 24 hours of incubation was also observed. In HepG2 cells, CDDO led to a two to five-fold increase in mtH_2O_2 after 6, 16 and 24 hours of treatment. A parallel increase in mtO_2^- levels was observed after 6 and 16 hours of incubation (Figure 16D). When RKO cells were treated with CDDO-Me, the increase of mtH_2O_2 and mtO_2^- was not observed after 6 hours of treatment but only after 16 hours in the presence of 2.5 µM CDDO-Me (Figure 16B). No change of mtH_2O_2 and mtO_2^- was observed in HepG2 cells treated with CDDO-Me (Figure 16E). We also investigated whether triterpenoids could increase mitochondrial ROS (mtROS) in non-transformed cells, *i.e.* primary fibroblasts, and we found that CDDO and CDDO-Me induced ROS generation but at lower levels compared to RKO and HepG2 cells (Figure 16F and 16G). While in RKO and HepG2 cells after CDDO treatment, mtH_2O_2 had a 3- to 5-fold increase, in primary fibroblasts 10 µM CDDO was the only concentration able to induce a 1.5-fold increase of mtH_2O_2 (Figure 16E, left panel). A similar, or even lower, increase was observed for mtO_2^- (Figure 16F, right panel).

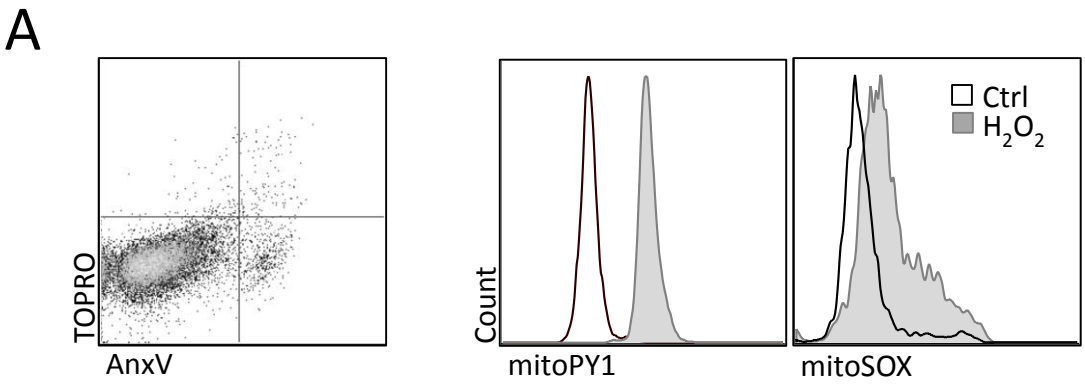
A
TOPRO
AnxV
Count
mitoPY1
mitoSOX
Ctrl
H2O2

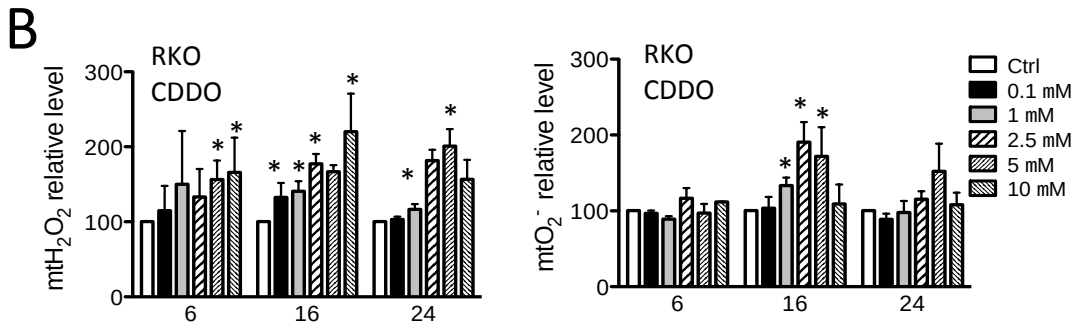
B
RKO
CDDO
mtH2O2 relative level
mtO2- relative level
Ctrl
0.1 mM
1 mM
2.5 mM
5 mM
10 mM
6
16
24

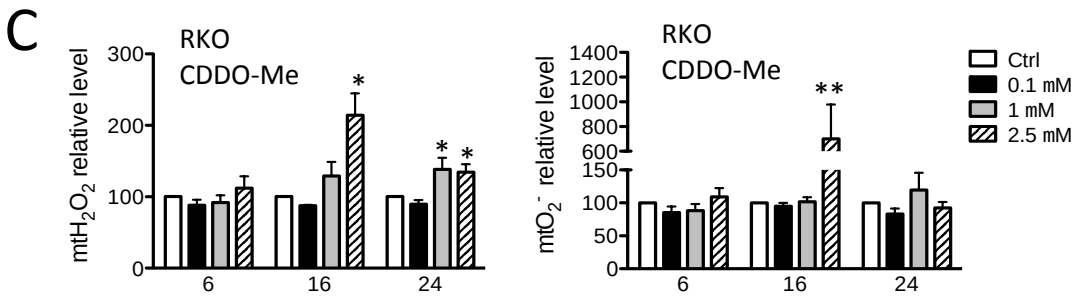
C
RKO
CDDO-Me
mtH2O2 relative level
mtO2- relative level
Ctrl
0.1 mM
1 mM
2.5 mM
6
16
24

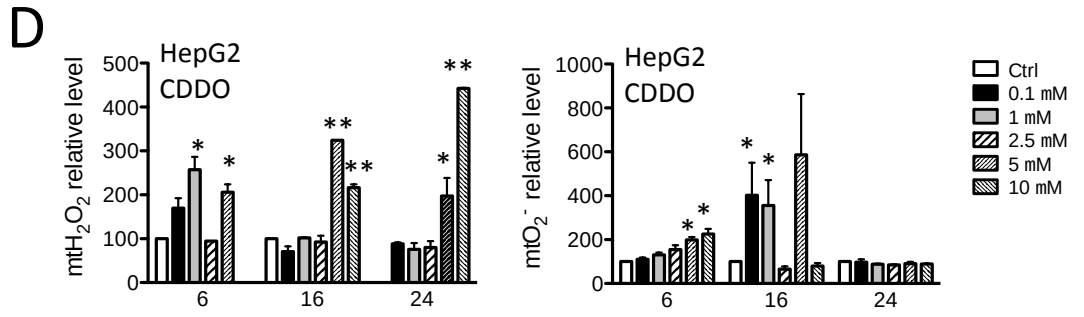
D
HepG2
CDDO
mtH2O2 relative level
mtO2- relative level
Ctrl
0.1 mM
1 mM
2.5 mM
5 mM
10 mM
6
16
24

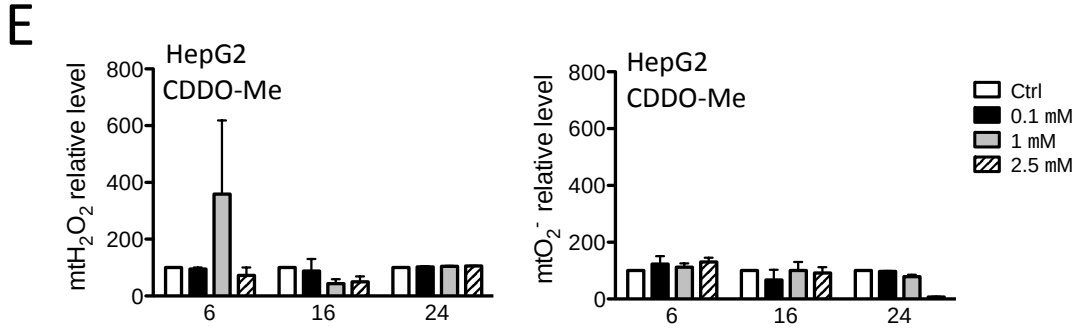
E
HepG2
CDDO-Me
mtH2O2 relative level
mtO2- relative level
Ctrl
0.1 mM
1 mM
2.5 mM
6
16
24

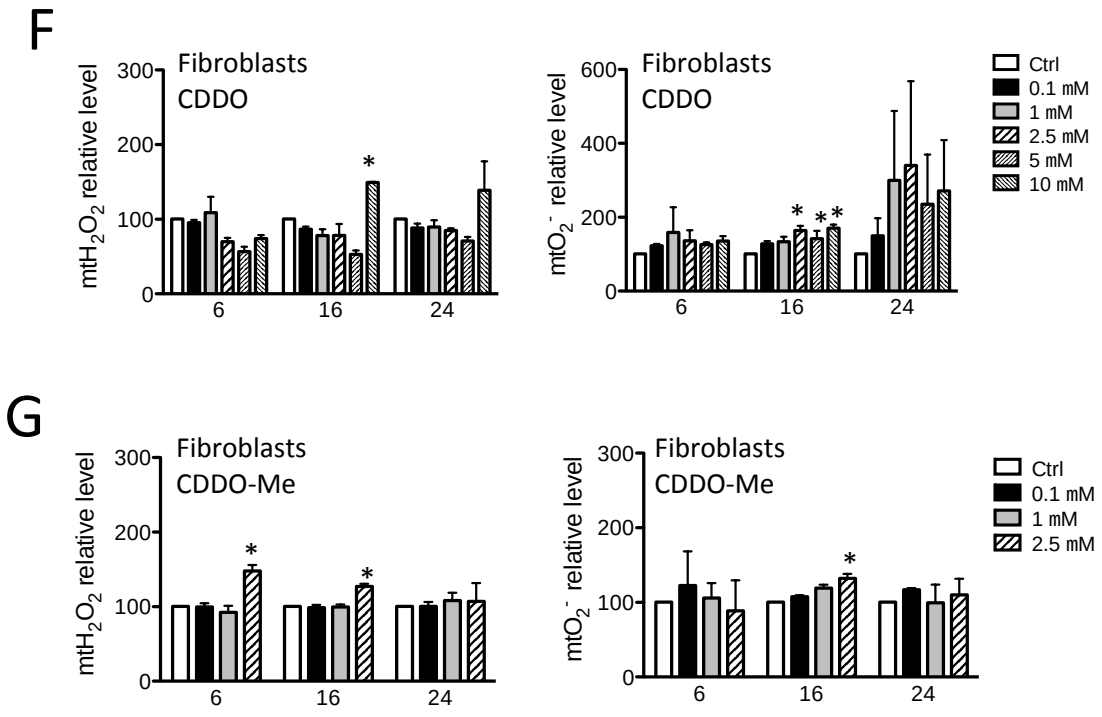

Figure 16: CDDO and CCDO-Me increase mitochondrial ROS production. A. Representative dot plot showing AnxV and TOPRO fluorescences to discriminate viable and dead cells, together with the histograms showing MitoSOX Red Superoxide Indicator (mitoSOX) and Mitochondria Peroxy Yellow 1 (mitoPY1) to detect mitochondrial anion superoxide and mitochondrial hydrogen peroxide in living cells (*i.e.*, those that were AnxV-/TOPRO- cells, indicated by the square). H_2O_2 was used as positive control. **B.** Quantification of mitochondrial hydrogen peroxide (mtH_2O_2) and mitochondrial anion superoxide (mtO_2^-) in RKO cells treated with CDDO up to 24 hours. Data are expressed as percentage of increase in median fluorescence intensity (MFI) and represent the mean ± SD of four independent experiments; **P* <0.05 and ***P* <0.01 *vs.* Ctrl. **C.** Quantification of mtH_2O_2 and mtO_2^- in RKO cells treated with CDDO-Me for up to 24 hours. Data are expressed as percentage of increase in MFI and represent the mean ± SD of four independent experiments; **P* <0.05 and ***P* <0.01 *vs.* Ctrl. **D.** Quantification of mitochondrial hydrogen peroxide (mtH_2O_2) and mitochondrial anion superoxide ($mtO_2^{\cdot-}$) in HepG2 cells treated with CDDO for up to 24 hours. Data are expressed as percentage of increase in mean fluorescence intensity (MFI) and represent the mean ± SD of three independent experiments; **P* <0.05 and ***P* <0.01 *vs.* Ctrl. **E.** Quantification of mtH_2O_2 and mtO_2^- in HepG2 cells treated with CDDO-Me for 6, 16 and 24 hours. Data are expressed as percentage of increase in mean fluorescence intensity (MFI) and represent the mean ± SD of three independent experiments; **P* <0.05 *vs.* Ctrl. **F.** Quantification of mtH_2O_2 and mtO_2^- in primary cultures of fibroblasts treated with CDDO for up to 24 hours. Data are expressed as percentage of increase in mean fluorescence intensity (MFI) and represent the mean ± SD of three independent experiments; **P* <0.05 *vs.* Ctrl. **G.** Quantification of mtH_2O_2 and mtO_2^- in primary cultures of fibroblasts treated with CDDO-Me for 6, 16 and 24 hours. Data are expressed as percentage of increase in mean fluorescence intensity (MFI) and represent the mean ± SD of three independent experiments; **P* <0.05 *vs.* Ctrl.

4.10 CDDO and CDDO-Me induce mitochondrial depolaritation

We wondered which mitochondrial alterations lead to cell death. Thus, we analyzed the effects of triterpenoids on mitochondrial membrane potential (MMP) after 24 hours of culture in the presence of CDDO or CDDO-Me (0.1, 1, 2.5, 5 and 10 μM) by using the MMP sensitive fluorescent probe JC-1. In Figure 17 representative dot plots of green fluorescent JC-1 monomers vs orange/red JC-1 aggregates are shown, whereas in Figure 17B, 17C and 17D the quantification of cells with depolarized mitochondria is reported for RKO, HepG2 and MCF7 cells, respectively. Increasing concentrations of triterpenoids determine a parallel increase in the percentage of cells with depolarized mitochondria. When CDDO was used, the concentration of 2.5 μM was sufficient to observe the presence of RKO cells with depolarized mitochondria, but higher concentrations were required to obtain a similar effectin HepG2 cells. Also in this case, CDDO-Me was much more potent, since the concentration of 1 μM was sufficient to cause a significant increase of cells with depolarized mitochondria both in RKO and in HepG2 cells. It is to note that concentrations higher than 2.5 μM induced massive cell death, so that the measure of membrane potential had little meaning.

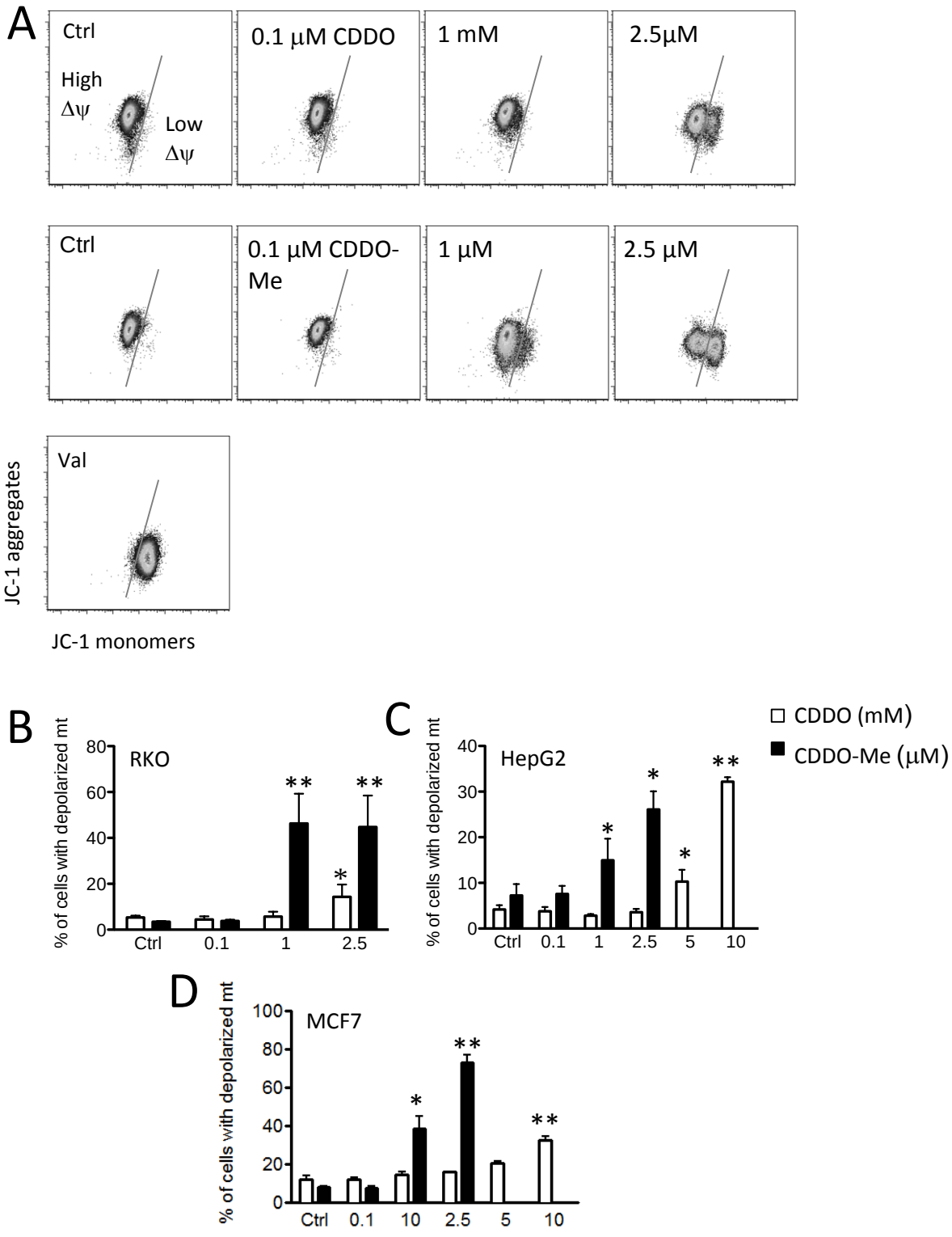

Figure 17: CDDO and CDDO-Me alter mitochondrial membrane potential (MMP). A. Representative dot plots showing JC-1 monomers and aggregates in cells treated with DMSO (Ctrl) and increasing concentrations of CDDO or CDDO-Me. Valinomycin (Val) was used a positive control for mitochondrial depolarization. **B.** Quantification of RKO cells with depolarized mitochondria. Values represent the mean ± SD of five independent experiments, **P* <0.05 and ***P* <0.01 *vs.* Ctrl. **C**. Quantification of HepG2 cells with depolarized mitochondria. Values represent the mean ± SD of three independent experiments, *P < 0.05 *vs.* Ctrl and **P <0.01 *vs.* Ctrl. **D.** Quantification of MCF7 cells with depolarized mitochondria. Values represent the mean ± SD of three independent experiments, *P <0.05 *vs.* Ctrl and **P <0.01 *vs.* Ctrl.

4.11 Lon inhibition results in altered morphology of mitochondria

We wondered whether changes in ROS production and MMP were accompanied by alteration of mitochondrial morphology and mitochondrial mass.

Therefore, we stained mitochondria by means of a red fluorescent antibody and nucleus with blue fluorescent DAPI, and observed cells by confocal microscopy. Cells from the three lines were treated with CDDO or CDDO-Me, either at 1 and 2.5 μM, or left untreated for controls. Untreated control cells showed a well organized mitochondria network that perfectly delineates the cell shape. As shown in the representative figure 18, cells treated with CDDO and CDDO-Me contained fragmented mitochondria, that were present also at 1 μM concentration in all cell lines. In particular, CDDO treated cells showed a clear fragmentation of the network that was directly correlated with the dose of CDDO used. In agreement with previous analysis, CDDO-Me exerted a stronger action upon mitochondrial morphology, as network dissolution is even more pronounced and the signal undefined, being almost vanished after the treatment with the highest dose (Figure 18).

We next investigated if the impairment of mitochondrial morphology is associated with changes of mitochondrial mass. Thus, the three lines (RKO, MCF7 and HepG2 cell lines) had been treated with increasing concentrations of CDDO (0.1, 1, 2.5, 5 and 10 μM), and CDDO-Me (0.1, 1 and 2.5 μM), and mitochondria were stained with MitoTracker Green FM and analysed by flow cytometry. Both drugs altered mitochondrial mass, in particular after 16 and 24 hours of treatment with CDDO both in RKO and in HepG2 cells (Figure 19A and 19B). Slight modifications in mitochondrial mass were observed with CDDO-Me.

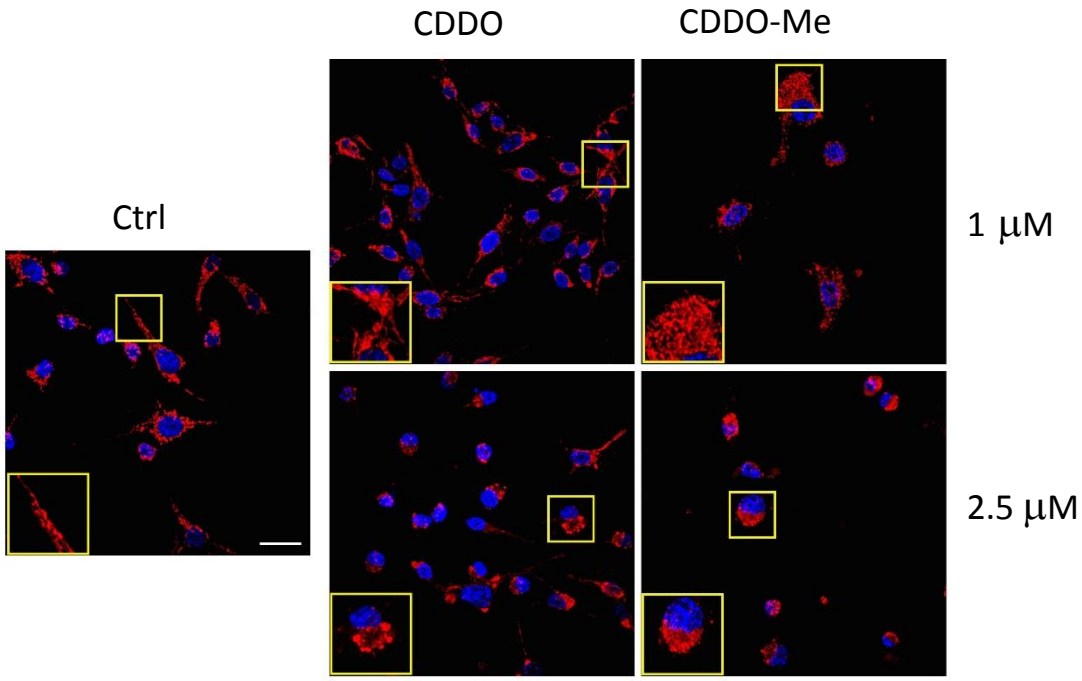

Figure 18: CDDO and CDDO-Me affect mitochondrial morphology. Representative immunofluorescence_images showing mitochondria in RKO cells treated with 1 µM and 2.5 µM CDDO and CDDO-Me. Red fluorescence represents mitochondria labelled with anti-human mitochondrial protein and with goat anti-rabbit F(ab')2 Alexa 647. Nuclei were counterstained with DAPI.

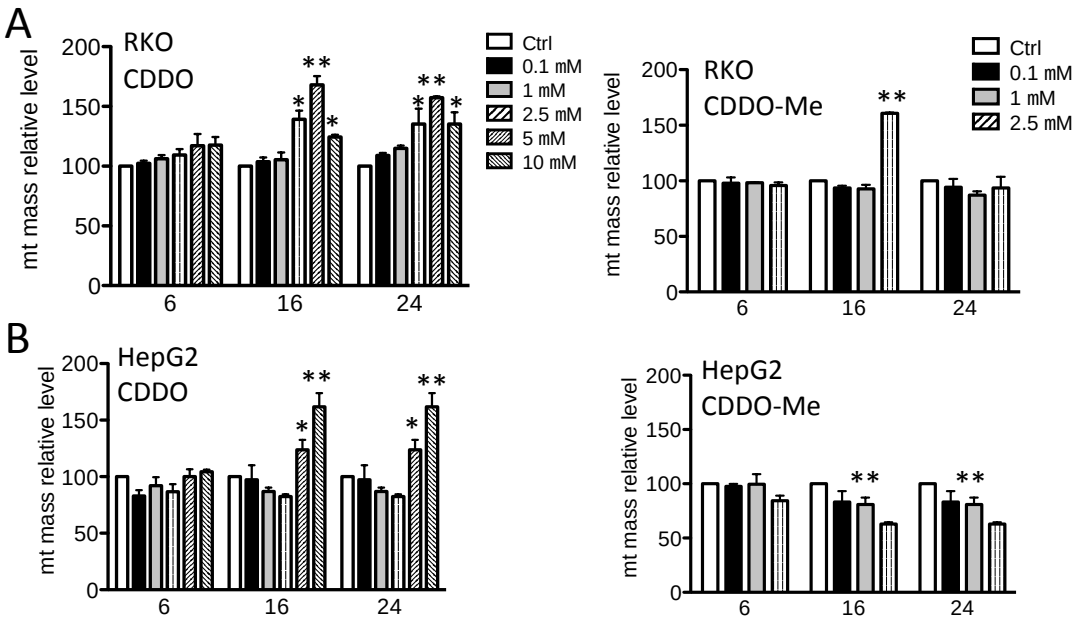

Figure 19: CDDO and CDDO-Me alter mitochondrial mass. **A.** Detection of mitochondrial mass in RKO treated with DMSO (Ctrl) and increasing concentrations of CDDO and CDDO-Me for up to 24 hours, as revealed by flow cytometry. Data are expressed as percentae of increase in median fluorescence intensity (MFI) in comparison to Ctrl, set to 100%, and represent the mean ± SD of four indipendent experiments; ***P* <0.01 *vs*. Ctrl). **B.** Detection of mitochondrial mass in HepG2 cells treated with DMSO (Ctrl) and increasing concentrations of CDDO and CDDO-Me for up to 24 hours, as revealed by flow cytometry. Data are expressed as percentage of increase in MFI in comparison to Ctrl, set to 100%, and represent the mean ± SD of four independent experiments; * P <0.05, ** P <0.01 *vs.* Ctrl.

4.12 Lon overexpression protect cells from apoptosis induced by CDDo and CDDO-Me

Considering that Lon is a stress protein that is induced by multiple stressors, and that the main effects of triterpenoids are exerted when Lon levels are very low, we wondered whether Lon overexpression could protect RKO cells from CDDO-induced cell death. Thus Lon was overexpressed by using a retroviral vector (pMSCV-Lon, containing cDNA encoding for Lon protease) to stably transduce RKO cells. We firstly confirmed that Lon was correctly localized to mitochondria in these cells (Figure 20B) and that cells transduced with pMSCV-Lon had increased levels of Lon mRNA and Lon protein. In pMSCV-Lon cells, a 3-fold increase and a 2-fold increase was observed for Lon mRNA and Lon protein, respectively (Figure 20A). Cells overexpressing Lon were less prone to undergo apoptosis than control cells after treatment with CDDO and CDDO-Me (Figure 20C). Interestingly, also in this case CDDO-Me was more potent than CDDO in inducing cell death.

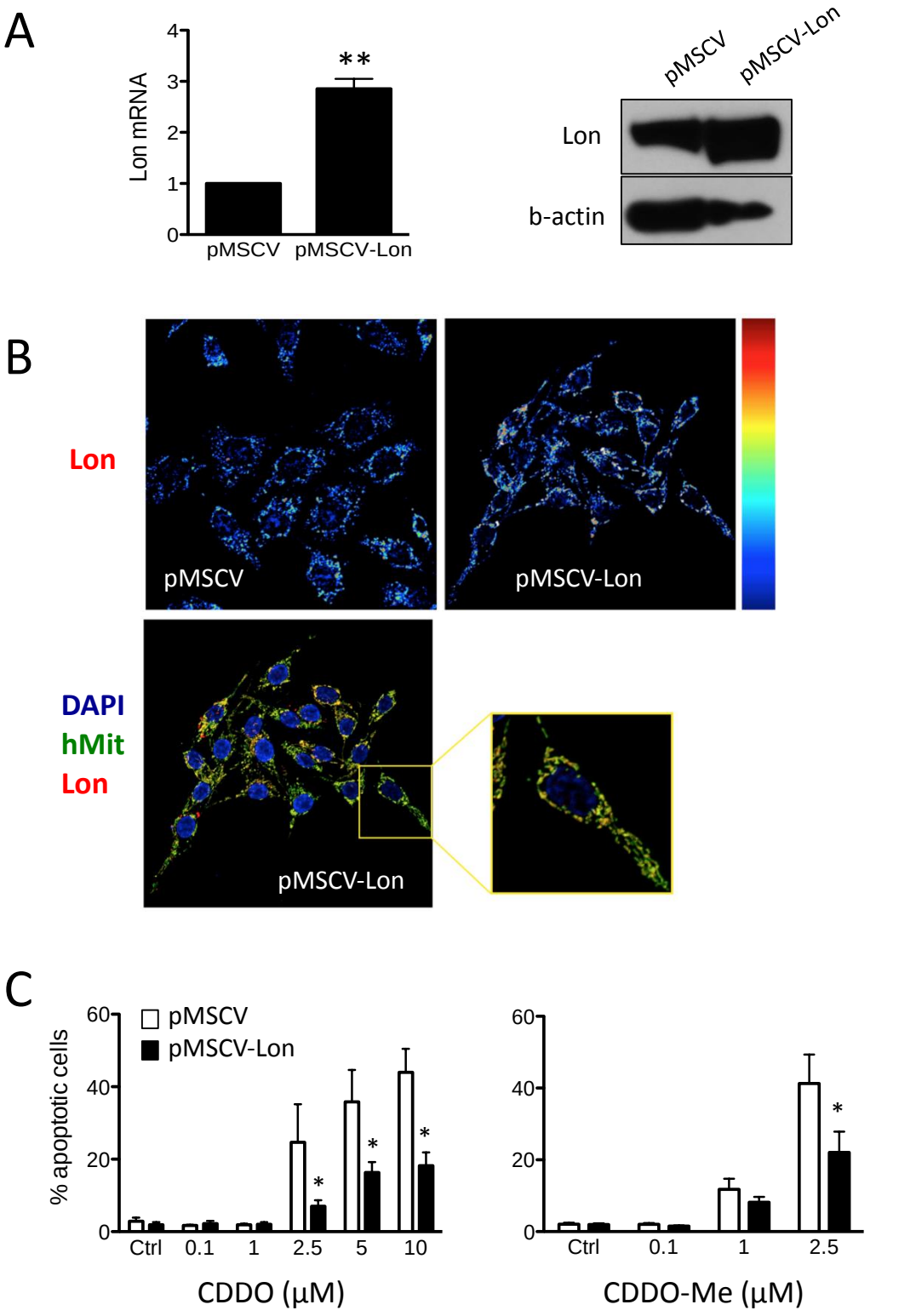

Figure 20: Overexpression of Lon protects cells from apoptotic cell death induced by CDDO and CDDO-Me. **A.** Expression of Lon mRNA and Lon protein in control cells (pMSCV) and cells overexpressing Lon (pMSCV-Lon). Values represent the mean ± SD of five indipendent experiments, $^{**}P < 0.01$ *vs*. Ctrl. **B.** Representative pseudocolour maps (upper panels; red indicates maximal expression) obtained by confocal microscopy after immunostaining cells with anti-Lon antibody. In lower panels, representative confocal microscopy images show that Lon is localized to mitochondria in pMSCV-Lon cells. Cells were immunostained with anti-Lon (red) and anti-human mitochondria (hMit, green). Nuclei were counterstained with DAPI. **C.** Percentage of apoptotic cells after treatment with CDDO up to 10 µM, and CDDO-Me up to 2.5 µM. Values represent the mean ± SD of five indipendent experiments $^{*}P < 0.05$ *vs*. Ctrl.

5. DISCUSSION

The neoplastic transformation of normal cells into cancer cells is driven by diverse oncogenesis-associated cellular stressors such as DNA damage and mitotic stress, as well as to metabolic, proteotoxic, and oxidative stress. To promote this 'poor of nutrient, in which cancer cells grow is extremely hostile, tumour cells have to activate several anti-stress pathways and defense mechanisms. Such of these pathways are mediated by nononcogenic proteins that are essential for the survival and proliferation of cancer cells. Among these proteins, a crucial role is played by Lon protease. It does not initiate tumourigenesis *per se,* but is essential for cancer development. Thus, Lon can be considered as potential target for anticancer drug therapy (59).

The role of Lon in human cells has not been well clarified yet, although its activities and the effects of its silencing have been described in bacteria and yeast. In particular, the disruption of a functional PIM1 gene, encoding for the yeast Lon protease, determines the accumulation of electron-dense inclusions in the mitochondrial matrix and the alteration of mtDNA, thus leading to mitochondrial functionality impairment (46, 47).

Several studies and our results show that Lon protease is up-regulated in several human cancer cells, but not in normal or highly proliferating, non-transformed cells. On the contrary, Lon down-regulation induces cell death in lymphoma cells (59), as well as in our cancer cell model, RKO cells. In these cells, apoptotic cell death occurred by the intrinsic pathway, with release of cytochrome c in the cytosol, and activation of caspase-9 and PARP. Thus, Lon is essential for maintaining mitochondrial functionality and morphology in RKO colon carcinoma cells, and for their survival.

The strong conservation of Lon protease during evolution suggests that human Lon should also have several substrates. We found that Lon down-regulation causes profound alterations of mitochondrial proteome, inducing an increase or decrease of proteins involved in mitochondrial functionality, such as energetic metabolism, mitochondrial architecture, ribosome assembly, mtDNA metabolism and stress response. Two Lon functions appear involved in this phenomenon: the absence of Lon proteolytic activity, and loss of Lonp1 chaperone function (94). Indeed, Lon degrades

oxidized or damaged proteins preventing their accumulation and assists folding and assembly of proteins involved in mitochondrial respiration.

The increased level of proteins like UCRI, ATPA, ATP5J, among others, suggest that such proteins could be possible targets of Lon proteolytic activity. The upregulation of GRP75 and PDIA3, two proteins associated with the response to protein misfolding and aggregation, supports this observation. In particular, PDIA3 catalyzes isomerization, reduction and oxidation of disulfides, and provides a link between protein misfolding and apoptotic cell death (177). Thus, the marked reduction of some electron transport chain subunits, such as NDUFB8, COXII, and SDHB is probably due to their misfolding.

We also analyzed whether changes in mitochondrial proteome affect mitochondrial functionality and morphology. Concerning mitochondrial functionality, we first observed a significant reduction in mtRNA transcripts. This indicates that Lon plays a crucial role for the expression of OXPHOS subunit deriving from mtDNA, and for the stability of the transcription machinery. As observed in other species, Lon controls directly the levels of TFAM, the main factor driving mtDNA replication and transcription (86). We also know that Lon binds mtDNA in a sequence specific manner and that its binding protects the molecules from oxidative damage (84). The lack of significant changes in mtDNA content, that has been measured in Lon-silenced cells after 72 hours of culture, can be explained taking into account the short period of culture, when a reasonable number of viable cells is likely still present.

Second, along with alterations in mitochondrial transcripts levels, Lon silencing causes a reduction of several subunits of mitochondrial inner membrane complexes, being Complex I the most affected. It is known that some complexes are entirely encoded by mtDNA, whereas others are partially encodes by the nucleus, and that Lon displays also chaperone properties participating to the assembly and folding of mitochondrial polypeptides (63). For this reason, the reduction of levels of proteins encoded by mtDNA can be a direct consequence of reduced mitochondrial transcripts, while the reduction of the other proteins can be due as a consequence of misfolding or increased turnover of nuclear encoded subunits. These alterations in respiratory chain assembly deeply affect cellular respiration, which is severely impaired at basal conditions and did not increase even in presence of FCCP. Similarly, impairment in

OCR and in extracellular acidification rate has been observed in HeLa cells where Lon was down-regulated by shRNA (145).

Apparently, this impairment is not mirrored in a parallel reduction of ATP synthesis at basal conditions. However, the alteration of the capability to synthetize ATP is probably masked by the high rate of glycolysis that provides the ATP necessary for cell functions. When 2DG is added to cell culture, ATP synthesis by glycolysis is inhibited and the impairment of respiration emerges.

Third, we observed that Lon silencing causes profound alterations of mitochondrial architecture and morphology. It is well known that Lon degrades preferentially proteins that are oxidized or damaged. The presence of electron-dense inclusion bodies inside mitochondria confirms that unfolded proteins accumulate in Lon-deficient cells.

Moreover, one of the major sources of ROS is the mitochondrial electron transport chain, particularly when it is impaired and the electron flux is disrupted (19). Our data show the increase of ROS and decrease of GSH in Lon-silenced cells, confirming the increase of oxidized proteins that cannot be degrade by Lon, thus causing their accumulation observed by microscopy. Confocal microscopy further strengthens these date and shows a higher fragmentation of cell mitochondrial network. These results suggest that the modifications that we observed in mitochondrial morphology can be ascribed not only to functional modifications described above, but also to the reduction of some proteins clearly essential for mitochondrial architecture maintenance.

In concordance with results obteined in RKO colon cancer cells, we observed that the large part of CRC ex-vivo samples showed a higher Lon expression in cancer mucosa samples if compared to normal mucosa counterpart. In addition, in the majority of colon cancer samples of stage I-IV that we tested, we observed that Lon up-regulation was paralleled by the nuclear localization of β-catenin and p53, and higher proliferation levels as estimated by Ki-67. Ki-67 is a nuclear protein associated with cellular proliferation and high level of this protein is a poor marker prognosis for patients with breast cancer (178). Also E-cadherin and p53 play a crucial role in coordinating the response of cells to oncogenic activation (179). Thus, their

dysregulation is implicated in tumour progression. These results underline the essential role of Lon protease in cancer development.

Because RNAi down-regulation of Lon induces changes in mitochondrial proteome, and has a deep impact on mitochondrial functionality and morphology, we evaluated whether pharmacological inhibition of Lon could have the same effects. Indeed, the possibility to use molecules able to inhibit Lon activity, alone or in combination, could pay new way to control tumour cells proliferation and thus, to develop new anticancer strategies. For these reason, we aimed to study the effects of two inhibitors of Lon proteolytic activity, the triterpenoids CDDO and CDDO-Me, in different cancer cells. In recent years several studies reported the antiproliferative and anticancer effects of these two molecules (60). Our results confirmed that triterpenoids are able to inhibit cell growth in a concentration-dependent manner and to induce apoptosis in RKO, HepG2 and MCF7 cells. In particular, CDDO-mediated apoptosis was identified by an increase in phosphatidylserine exposure, and by the activation of caspase-3, together with the activation of caspase-9, indicating that triterpenoids are able to exert toxic effects on mitochondria.

As previous studies demonstrated that the mechanism by which triterpenoids induce apoptosis depends on an excessive oxidative stress, we analysed mitochondrial redox state and MMP. We found that CDDO leads to increased mtH_2O_2 and mtO_2^- production, particularly after 16 hours of treatment. Accordingly, the higher levels of ROS found in CDDO and CDDO-Me treated cells, support the hypothesis that oxidative stress can lead to cell death in cells where Lon has been inhibited. Indeed, the capability of these two agents to induce apoptosis and to increase oxidative stress can be due to their direct interaction with electron transport chain complexes, which induce ROS production and damages on mitochondrial proteins, and to the inhibition of Lon that reduces the removal of cytotoxic proteins aggregated within the mitochondria.

Complexes I and III of the mitochondrial electron transport chain are major sites where superoxide is generated, either in the matrix (Complex I and III), or in the intermembrane space (Complex III) (180). The inhibition of ROS generation protects cells from growth inhibition and induction of apoptosis. Indeed, the treatment with inhibitors of complex I of respiratory chain, either by overexpression of antioxidant

enzymes (glutathione peroxidase and superoxide dismutase), prevented apoptosis induced by triterpenoids in prostate, pancreatic and ovarian cancer cells (154, 161).

It is to note that cancer cells produce higher levels of ROS than normal cells (25). So, these ROS play an important role in cancer progression by stimulating cell growth and genetic instability, but also they generate an intrinsic oxidative stress which renders cells highly dependent on antioxidant systems and/or highly sensitive to agents that dysregulate redox status. For instance, the association of 2-methoxyestradiol (2-ME), which inhibits superoxide dismutase, to arsenic trioxide, which causes ROS increase, has a strong cytotoxic activity in leukemia cells (181). Similarly, hydrogen peroxide and 2-ME can induce oxidative stress that leads to apoptotic and autophagic cell death in transformed cells but not in normal, non-transformed cells (182). Interestingly, our results indicate that CDDO and CDDO-Me act in a similar way, as they increase mitochondrial oxidative stress, which contributes to apoptotic cell death in cancer cells, but fail to induce mtROS increase and apoptosis in normal fibroblasts.

Changes in MMP have been postulated to be early obligate events in apoptotic signaling pathway. Accordingly, our results show that triterpenoids determine a concentration-dependent increase in percentage of cells with depolarized mitochindria.

Oxidative stress generated by CDDO and CDDO-Me led also to an increase in mitochondria with fragmented appearance, and an increase in mitochondrial mass, at least for CDDO. Indeed, we observed an altereted morphology in mitochondria of cells treated with both molecules. The reasons at the basis of the increase in mitochondrial mass are not clear, but it is plausible that it could represent a response to stress in order to enhance energy supply. Indeed, several studies reported that mitochondrial mass increases in the presence of oxidative stress and that such increase depends on MMP and protein synthesis in the cytoplasm (183). A similar increase has also been observed in different cell types undergoing apoptotic cell death, including HepG2, MCF7 and HeLa cells (184).

In conclusion, we found that triterpenoids are potent stressors for mitochondria. In particular, their capability to induce apoptotis in cancer cells through a mitochondria-specific generation of oxidative stress, suggest that these molecules could be good candidates for anticancer therapy. In addition, overexpression of Lon can reduce

apoptotic cell death induce by these agents, indicating that Lon is essential for mantaining mitochondrial shape and functions and for survival of cancer cells. So, the study and validation of further molecules that specifically bind and block Lon activity are required and could pave new way to develop innovative therapeutic option.

Finally, these data suggest that Lon can be considered as a novel anticancer drug target.

6. REFERENCES

1. De Pauw A, Tejerina S, Raes M, Keijer J and Arnould T. Mitochondrial (dys)function in adipocyte (de)differentiation and systemic metabolic alterations. Am J Pathol, 175(3):927–39, 2009.
2. Duchen MR. Mitochondria in health and disease: perspectives on new mitochonbdrial biology. Mol Aspects Med, 25(4):365–451, 2004.
3. Mokranjac D and Neupert W. Protein import into mitochondria. Biochem Soc Trans, 33(Pt 5): p. 1019-23, 2005.
4. Rutter GA and Rizzuto R. Regulation of mitochondrial metabolism by ER Ca2+ release: an intimate connection. Trends Biochem Sci, 25(5):215–21, 2000.
5. Leblanc C, Richard O, Kloareg B, Viehmann S, Zetsche K, Boyen C. Origin and evolution of mitochondria: what have we learnt from red algae?, 31(3):193-207, 1997.
6. D Yang, Y Oyaizu, H Oyaizu, G J Olsen, and C R Woese. Mitochondrial origins Proc Natl Acad Sci U.S.A., 82(13): 4443–7, 1985.
7. Andersson SG, Zomorodipour A, Andersson JO, Sicheritz-Pontén T, Alsmark UC, Podowski RM, Näslund AK, Eriksson AS, Winkler HH, Kurland CG. The genome sequence of Rickettsia prowazekii and the origin of mitochondria. Nature, 396(6707):133–40, 1998.
8. Chinneryn PF, Hudson G. Mitochondrial genetics. Br Med Bull, 106:135–59, 2013.
9. Falkenberg M, Larsson NG, Gustafsson CM. DNA replication and transcription in mammalian mitochondria. Annu Rev Biochem, 76:679–99, 2007.
10. Lim SE, Longley MJ, Copeland WC. The mitochondrial p55 accessory subunit of human DNA polymerase gamma enhances DNA binding, promotes processive DNA synthesis, and confers N-ethylmaleimide resistance. J Biol Chem, 274(53): p. 38197-203, 1999.
11. Gray H, Wong TW. Purification and identification of subunit structure of the human mitochondrial DNA polymerase. J Biol Chem, 267(9): p. 5835-41, 1992.
12. Longley MJ, Nguyen D, Kunkel TA, Copeland WC. The fidelity of human DNA polymerase gamma with and without exonucleolytic proofreading and the p55 accessory subunit. J Biol Chem, 276(42): p. 38555-62, 2001.
13. Brown TA, Cecconi C, Tkachuk AN, Bustamante C, Clayton DA. Replication of mitochondrial DNA occurs by strand displacement with alternative light-strand origins, not via a strand-coupled mechanism. Genes Dev, 19(20): p. 2466-76, 2005.
14. Bowmaker M, Yang MY, Yasukawa T, Reyes A, Jacobs HT, Huberman JA, Holt IJ. Mammalian mitochondrial DNA replicates bidirectionally from an initiation zone. J Biol Chem, 278(51): p. 50961-9, 2003.
15. Asin-Cayuela J, Gustafsson CM. Mitochondrial transcription and its regulation in mammalian cells. Trends Biochem Sci, 32(3): p. 111-7, 2007.
16. Clayton DA. Replication and transcription of vertebrate mitochondrial DNA. Annu Rev Cell Biol,. 7: p. 453-78, 1991

17. Enriquez JA, Fernández-Silva P, Garrido-Pérez N, López-Pérez MJ, Pérez-Martos A, Montoya J. Direct regulation of mitochondrial RNA synthesis by thyroid hormone. Mol Cell Biol, 19(1): p. 657-70, 1999.

18. Lin YW, Lien LM, Yeh TS, Wu HM, Liu YL, Hsieh RH. 9-cis retinoic acid induces retinoid X receptor localized to then mitochondria for mediation of mitochondrial transcription. Biochem Biophys Res Commun, 377(2): p. 351-4, 2008.

19. Galluzzi L, Kepp O, Trojel-Hansen C, Kroemer G. Mitochondrial control of cellular life, stress, and death. Circ Res, 111(9):1198–207, 2012.

20. Andreu AL, DiMauro S. Current classification of mitochondrial disorders. J Neurol, 250(12): p. 1403-6, 2003.

21. Schägger H, Pfeiffer K. Supercomplexes in the respiratory chains of yeast and mammalian mitochondria. EMBO J, 19(8):1777–83, 2000.

22. Lenaz G, Genova ML. Structural and functional organization of the mitochondrial respiratory chain: a dynamic super-assembly. Int J Biochem Cell Biol, 41(10):1750–1772, 2009.

23. Carew JS, Huang P. Mitochondrial defects in cancer. Mol Cancer, 1: p. 9, 2002.

24. Penta JS, Johnson FM, Wachsman JT, Copeland WC. Mitochondrial DNA in human malignancy. Mutat Res, 488(2): p. 119-33, 2001.

25. Pelicano H, Carney D, Huang P. ROS stress in cancer cells and therapeutic implications. Drug Resist Updat, 7(2): p. 97-110, 2004.

26. Xu RH, Pelicano H, Zhou Y, Carew JS, Feng L, Bhalla KN, Keating MJ, Huang P. Inhibition of glycolysis in cancer cells: a novel strategy to overcome drug resistance associated with mitochondrial respiratory defect and hypoxia. Cancer Res, 65(2): p. 613-21, 2005.

27. Venditti P, Di Stefano L, Di Meo S. Mitochondrial metabolism of reactive oxygen species. Mitochondrion, 13(2):71–82, 2013.

28. Nyström T. Role of oxidative carbonylation in protein quality control and senescence. EMBO J., 24(7):1311–7, 2005.

29. Poyton RO, Ball KA, Castello PR. Mitochondrial generation of free radicals and hypoxic signaling. Trends Endocrinol. Metab., 20(7):332–40, 2009.

30. Shringarpure R, Grune T, Davies KJ. Protein oxidation and 20S proteasome-dependent proteolysis in mammalian cells. Cell Mol Life Sci, 58(10):1442–50, 2001.

31. Bulteau AL, Bayot A. Mitochondrial proteases and cancer. Biochim Biophys Acta, 1807(6):595–601, 2011.

32. Indo HP, Davidson M, Yen HC, Suenaga S, Tomita K, Nishii T, Higuchi M, Koga Y, Ozawa T, Majima HJ. Evidence of ROS generation by mitochondria in cells with impaired electron transport chain and mitochondrial DNA damage. Mitochondrion, 7(1-2):106–18, 2006.

33. Lenaz G, Bovina C, D'Aurelio M, Fato R, Formiggini G, Genova ML, Giuliano G, Merlo Pich M, Paolucci U, Parenti Castelli G, Ventura B. Role of mitochondria in oxidative stress and aging. Ann NY Acad Sci, 959:199–213, 2002.

34. Kwong JQ, Beal MF, Manfredi G. The role of mitochondria in inherited neurodegenerative diseases. J Neurochem, 97(6):1659–75, 2006.

35. Quiros PM, Langer T, Lopez-Otin C. New roles for mitochondrial proteases in health, ageing and disease. Nat Rev Mol Cell Biol, 16(6):345-59, 2015.

36. Stiburek L, Cesnekova J, Kostkova O, Fornuskova D, Vinsova K, Wenchich L, Houstek J, Zeman J.YME1L controls the accumulation of respiratory chain subunits and is required for apoptotic resistance, cristae morphogenesis, and cell proliferation. Mol Biol Cell, 23, 1010–1023, 2012.

37. Haynes CM, Petrova K, Benedetti C, Yang Y, Ron D. ClpP mediates activation of a mitochondrial unfolded protein response in C. elegans. Dev Cell, 13, 467–480, 2007.

38. 35 Sundararajan Venkatesh, Jae Lee, Kamalendra Singh, Irene Lee, and Carolyn K Suzuki. Multitasking in the mitochondrion by the ATP-dependent Lon protease. Biochim Biophys Acta, 1823(1):56–66, 2012.

39. Rotanova TV, Botos I, Melnikov EE, Rasulova F, Gustchina A, Maurizi MR, and Wlodawer A. Slicing a protease: structural features of the ATP-dependent Lon proteases gleaned from investigations of isolated domains. Protein Sci, 15(8):1815–28, 2006.

40. Bin Lu, Tong Liu, Juan A Crosby, Jennifer Thomas-Wohlever, Irene Lee, and Carolyn K Suzuki. The ATP-dependent Lon protease of Mus musculus is a DNA-binding protein that is functionally conserved between yeast and mammals. Gene, 306:45–55, 2003.

41. Vieux EF, Wohlever ML, Chen JZ, Sauer RT, and Baker TA. Distinct quaternary structures of the AAA+ Lon protease control substrate degradation. Proc Natl Acad Sci U.S.A., 110(22):E2002–8, 2013.

42. Jonas K, Liu J, Chien P, and Laub MT. Proteotoxic stress induces a cell-cycle arrest by stimulating Lon to degrade the replication initiator DnaA. Cell, 154(3): p. 623-36, 2013.

43. Fu GK, Smith MJ, and Markovitz DM. Bacterial protease Lon is a site-specific DNA-binding protein. J Biol Chem, 272(1): p. 534-8, 1997.

44. Adam C, Picard M, Dequard-Chablat M, Sellem CH, Hermann-Le Denmat S, and Contamine V. Biological roles of the Podospora anserina mitochondrial Lon protease and the importance of its N-domain. PLoS One, 7(5): p. e38138, 2012.

45. Rigas S, Daras G, Laxa M, Marathias N, Fasseas C, Sweetlove LJ, and Hatzopoulos P. Role of Lon1 protease in post-germinative growth and maintenance of mitochondrial function in Arabidopsis thaliana. New Phytol, 181(3): p. 588-600, 2009.

46. Van Dyck L, Pearce DA, and Sherman F. PIM1 encodes a mitochondrial ATP-dependent protease that is required for mitochondrial function in the yeast Saccharomyces cerevisiae. J Biol Chem, 269(1):238–42, 1994.

47. Suzuki CK, Suda K, Wang N, and Schatz G. Requirement for the yeast gene LON in intramitochondrial proteolysis and maintenance of respiration. Science, 264(5161):891, 1994.

48. Wagner I, Van Dyck L, Savel'ev AS, Neupert W, and Langer T. Autocatalytic processingof the ATP-dependent PIM1 protease: crucial function of a pro-region for sorting tomitochondria. EMBO J, 16(24):7317–25, 1997.

49. Wang N, Gottesman S, Willingham MC, Gottesman MM, and Maurizi MR. A human mitochondrial ATP-dependent protease that is highly homologous to bacterial Lon protease, Proc Natl Acad Sci U S A, 90(23): p. 11247-51, 1993.

50. Wang N, Maurizi MR, Emmert-Buck L, and Gottesman MM. Synthesis, processing, and localization of human Lon protease. J Biol Chem, 269(46):29308–13, 1994.

51. AYu A, Petukhova GV, Grigorenko VG, Lykov IP, Yarovoi SV, Lipkin VM, and Gorbalenya AE. Cloning and sequence analysis of cDNA for a human homolog of eubacterial ATP-dependent Lon proteases. FEBS Lett, 340(1-2):25–8, 1994.

52. Iyer LMLeipe DD, Koonin EV, Aravind L. Evolutionary history and higher order classification of AAA+ ATPases. J Struct Biol, 146(1-2): p. 11-31, 2004.

53. Rotanova TV, Botos I, Melnikov EE, Rasulova F, Gustchina A, Maurizi MR, Wlodawer A. Slicing a protease: structural features of the ATP-dependent Lon proteases gleaned from investigations of isolated domains. Protein Sci, 15(8): p. 1815-28, 2006.

54. Ngo JK, Pomatto LC, and Davies KJ. Upregulation of the mitochondrial Lon Protease allows adaptation to acute oxidative stress but dysregulation is associated with chronic stress, disease, and aging. Redox Biol, 1(1): p. 258-64, 2013.

55. Lupas AN and Martin J. AAA proteins. Curr Opin Struct Biol, 12(6): p. 746-53, 2002.

56. Ondrovicova G, Ondrovicová G, Liu T, Singh K, Tian B, Li H, Gakh O, Perecko D, Janata J, Granot Z, Orly J, Kutejová E, Suzuki CK. Cleavage site selection within a folded substrate by the ATP-dependent lon protease. J Biol Chem, 280(26): p. 25103-10, 2005.

57. Amerik A, Petukhova GV, Grigorenko VG, Lykov IP, Yarovoi SV, Lipkin VM, and Gorbalenya AE. Cloning and sequence analysis of cDNA for a human homolog of eubacterial ATP-dependent Lon proteases, FEBS Lett, 340(1-2): p. 25-8, 1994.

58. Bayot A, Basse N, Lee I, Gareil M, Pirotte B, Bulteau AL, Friguet B, Reboud-Ravaux M. Towards the control of intracellular protein turnover: mitochondrial Lon protease inhibitors versus proteasome inhibitors. Biochimie, 90(2): p. 260-9, 2008.

59. Bernstein SH, Venkatesh S, Min L, Lee J, Bin L, Hilchey SP, Morse KM, Metcalfe HM, Skalska J, Andreeff M, Brookes PS, and Suzuki CK. The mitochondrial ATP-dependent Lon protease: a novel target in lymphoma death mediated by the synthetic triterpenoid CDDO and its derivatives. Blood, 119(14):3321–9, 2012.

60. Swamy KH and Goldberg AL. E. coli contains eight soluble proteolytic activities, one being ATP dependent, Nature, 292(5824): p. 652-4, 1981.

61. Fu GK and Markovitz DM. The human LON protease binds to mitochondrial promoters in a single-stranded, site-specific, strand-specific manner. Biochemistry, 37(7):p. 1905-9, 1998.

62. Liu T, Lu B, Lee I, Ondrovicová G, Kutejová E, Suzuki CK.DNA and RNA binding by the mitochondrial lon protease is regulated by nucleotide and protein substrate. J Biol Chem, 279(14): p. 13902-10, 2004.

63. Rep M, van Dijl JM, Suda K, Schatz G, Grivell LA, Suzuki CK.Promotion of mitochondrial membrane complex assembly by a proteolytically inactive yeast Lon. Science, 274(5284): p. 103-6, 1996.

64. Ahmed, E.K., A. Rogowska-Wrzesinska, P. Roepstorff, A.L. Bulteau, and B. Friguet. Protein modification and replicative senescence of WI-38 human embryonic fibroblasts. Aging Cell, 9(2): p. 252-72, 2010.

65. Ngo JK, and Davies KJ. Mitochondrial Lon protease is a human stress protein. Free Radic Biol Med, 46(8): p. 1042-8, 2009.

66. Gibellini L, Pinti M, Boraldi F, Giorgio V, Bernardi P, Bartolomeo R, Nasi M, De Biasi S, Missiroli S, Carnevale G, Losi L, Tesei A, Pinton P, Quaglino D, and Cossarizza A. Silencing of mitochondrial Lon protease deeply impairs mitochondrial proteome and function in colon cancer cells, FASEB J, 28(12):5122-35, 2014.

67. Bota DA, and Davies KJ. Lon protease preferentially degrades oxidized mitochondrial aconitase by an ATP-stimulated mechanism, Nat Cell Biol, 4(9): p. 674-80, 2002.

68. Tian Q, Li T, Hou W, Zheng J, Schrum LW, and Bonkovsky HL. Lon peptidase 1 (LONP1)-dependent breakdown of mitochondrial 5-aminolevulinic acid synthase protein by heme in human liver cells, J Biol Chem, 286(30): p. 26424-30, 2011.

69. Granot Z, Kobiler O, Melamed-Book N, Eimerl S, Bahat A, Lu B, Braun S, Maurizi MR, Suzuki CK, Oppenheim AB, and Orly J. Turnover of mitochondrial steroidogenic acute regulatory (StAR) protein by Lon protease: the unexpected effect of proteasome inhibitors, Mol Endocrinol, 21(9): p. 2164-77, 2007.

70. Lu B, Lee J, Nie X, Li M, Morozov YI, Venkatesh S, Bogenhagen DF, Temiakov D, and Suzuki CK. Phosphorylation of human TFAM in mitochondria impairs DNA binding and promotes degradation by the AAA+ Lon protease, Mol Cell, 49(1): p. 121-32, 2013.

71. Kita K, Suzuki T, and Ochi T. Diphenylarsinic acid promotes degradation of glutaminase C by mitochondrial Lon protease, J Biol Chem, 287(22): p. 18163-72, 2012.

72. Teng H, Wu B, Zhao K, Yang G, Wu L, and Wang R. Oxygen-sensitive mitochondrial accumulation of cystathionine beta-synthase mediated by Lon protease, Proc Natl Acad Sci U S A, 110(31): p. 12679-84, 2013.

73. Gardner PR, Nguyen DD, and White CW. Aconitase is a sensitive and critical target of oxygen poisoning in cultured mammalian cells and in rat lungs. Proc Natl Acad Sci U S A, 91(25): p. 12248-52, 1994.

74. Bota DA, Ngo JK, and Davies KJ. Downregulation of the human Lon protease impairs mitochondrial structure and function and causes cell death. Free Radic Biol Med, 38(5): p. 665-77, 2005.

75. Quiros PM, Espanol Y, Acin-Perez R, Rodriguez F, C. Barcena, K. Watanabe, E. Calvo, M. Loureiro, M.S. Fernandez-Garcia, A. Fueyo, J. Vazquez, J.A. Enriquez, and C. Lopez-Otin. ATP-dependent Lon protease controls tumor bioenergetics by reprogramming mitochondrial activity. Cell Rep, 8(2): p. 542-56, 2014.

76. Fukuda R, Zhang H, Kim JW, Shimoda L, Dang CV, and Semenza GL. HIF-1 regulates cytochrome oxidase subunits to optimize efficiency of respiration in hypoxic cells. Cell, 129(1): p. 111-22, 2007.

77. Goto M, Miwa H, Suganuma K, Tsunekawa-Imai N, Shikami M, Mizutani M, Mizuno S, Hanamura I, and Nitta M. Adaptation of leukemia cells to hypoxic condition through switching

the energy metabolism or avoiding the oxidative stress. BMC Cancer, 14: p. 76, 2014.

78. Ngo JK, Pomatto LC, and Davies KJ. Upregulation of the mitochondrial Lon Protease allows adaptation to acute oxidative stress but dysregulation is associated with chronic stress, disease, and aging. Redox Biol, 1(1):258–264, 2013.

79. Ondrovicová G, Liu T, Singh K, Tian B, Li H, Gakh O, Perecko D, Janata J, Granot Z, Orly J, Kutejová E, and Suzuki CK. Cleavage site selection within a folded substrate by the ATP-dependent lon protease. J Biol Chem, 280(26):25103–10, 2005.

80. Lupas AN and Martin J. AAA proteins. Curr Opin Struct Biol, 12(6):746–53, 2002.

81. Shah IM and Wolf RE. Sequence requirements for Lon-dependent degradation of the Escherichia coli transcription activator SoxS: identification of the SoxS residues critical to proteolysis and specific inhibition of in vitro degradation by a peptide comprised of the N-terminal 21 amino acid residues. J. Mol. Biol., 357(3):718–31, 2006.

82. Kenniston JA, Baker TA, Fernandez JM, and Sauer RT. Linkage between ATP consumption and mechanical unfolding during the protein processing reactions of an AAA+ degradation machine. Cell, 114(4):511–20, 2003.

83. Wang J, Song JJ, Franklin MC, Kamtekar S, Im YJ, Rho SH, Seong IS, Lee CS, Chung CH, and Eom SH. Crystal structures of the HslVU peptidase-ATPase complex reveal an ATP-dependent proteolysis mechanism. Structure, 9(2):177–84, 2001.

84. Lu B, Yadav S, Shah PG, Liu T, Tian B, Pukszta S, Villaluna N, Kutejová E, Newlon CS, Santos JH, Suzuki CK. Roles for the human ATP-dependent Lon protease in mitochondrial DNA maintenance. J Biol Chem, 282(24): p. 17363-74, 2007.

85. Zehnbauer BA, Foley EC, Henderson GW, Markovitz A. Identification and purification of the Lon+ (capR+) gene product, a DNA-binding protein. Proc Natl Acad Sci U S A, 78(4): p. 2043-7, 1981.

86. Matsushima Y, Goto Y, and Kaguni LS. Mitochondrial Lon protease regulates mitochondrial DNA copy number and transcription by selective degradation of mitochondrial transcription factor A (TFAM). Proc Natl Acad Sci U.S.A., 107(43):18410–5, 2010.

87. Luciakova K, Sokolikova B, Chloupkova M, and Nelson BD. Enhanced mitochondrial biogenesis is associated with increased expression of the mitochondrial ATP-dependent Lon protease. FEBS Lett., 444(2-3):186–8, 1999.

88. Howard-Flanders P, Simson E, and Theriot L. The Excision of Thymine Dimers from DNA, Filament Formation and Sensitivity to Ultraviolet Light in Escherichia Coli K-12. Mutat Res, 106: p. 219-26, 1964.

89. Murakami K, Voellmy R, and Goldberg AL. Protein degradation is stimulated by ATP in extracts of Escherichia coli. J Biol Chem, 254(17): p. 8194-200, 1979.

90. Charette MF, Henderson GW, and Markovitz A. ATP hydrolysis-dependent protease activity of the lon (capR) protein of Escherichia coli K-12, Proc Natl Acad Sci U S A, 78(8): p. 4728-32, 1981.

91. Chung CH and Goldberg AL. The product of the lon (capR) gene in Escherichia coli is the ATP-dependent protease, protease La. Proc Natl Acad Sci U S A, 78(8): p. 4931-5, 1981.

92. Ngo JK, Pomatto LC, Bota DA, Koop AL, Davies KJ. Impairment of lon-induced protection against the accumulation of oxidized proteins in senescent wi-38 fibroblasts. J Gerontol A Biol Sci Med Sci, 66:1178-1185, 2011.

93. Pinti M, Gibellini L, De Biasi S, Nasi M, Roat E, O'Connor JE, Cossarizza A. Functional characterization of the promoter of the human Lon protease gene. Mitochondrion, 11:200-206, 2011.

94. Hori O, Ichinoda F, Tamatani T, Yamaguchi A, Sato N, Ozawa K, Kitao Y, Miyazaki M, Harding HP, Ron D, M. Tohyama, M Stern D, and Ogawa S. Transmission of cell stress from endoplasmic reticulum to mitochondria: enhanced expression of Lon protease. J Cell Biol, 157(7): p. 1151-60, 2002.

95. Pinti M, Gibellini L, Guaraldi G, Orlando G, Gant TW, Morselli E, Nasi M, Salomoni P, Mussini C, and Cossarizza A. Upregulation of nuclear-encoded mitochondrial LON protease in HAART-treated HIV-positive patients with lipodystrophy: implications for the pathogenesis of the disease. AIDS, 24(6): p. 841-50, 2010.

96. Gibellini L, Pinti M, Beretti F, Pierri CL, Onofrio A, Riccio M, Carnevale G, De Biasi S, Nasi M, Torelli F, Boraldi F, De Pol A, and Cossarizza A. Sirtuin 3 interacts with Lon protease and regulates its acetylation status. Mitochondrion, 2014.

97. Pavlakis SG, Phillips PC, DiMauro S, De Vivo DC, and Rowland LP. Mitochondrial myopathy, encephalopathy, lactic acidosis, and strokelike episodes: a distinctive clinical syndrome. Ann Neurol, 16(4): p. 481-8, 1984.

98. Wallace DC. Diseases of the mitochondrial DNA. Annu Rev Biochem, 61: p. 1175-212, 1992.

Shoffner JM, Lott MT, Lezza AM, Seibel P, Ballinger SW, and Wallace DC. Myoclonic epilepsy and ragged-red fiber disease (MERRF) is associated with a mitochondrial DNA tRNA(Lys) mutation. Cell, 61(6): p. 931-7, 1990.

99. Felk S, Ohrt S, Kussmaul L, Storch A, and Gillardon F. Activation of the mitochondrial protein quality control system and actin cytoskeletal alterations in cells harbouring the MELAS mitochondrial DNA mutation. J Neurol Sci, 295(1-2): p. 46-52, 2010.

100. Wu SB, Ma YS, Wu YT, Chen YC, and Wei YH. Mitochondrial DNA mutation-elicited oxidative stress, oxidative damage, and altered gene expression in cultured cells of patients with MERRF syndrome. Mol Neurobiol, 41(2-3): p. 256-66, 2010.

101. Hansen J, Corydon TJ, Palmfeldt J, Durr A, Fontaine B, Nielsen MN, Christensen JH, Gregersen N, and Bross P. Decreased expression of the mitochondrial matrix proteases Lon and ClpP in cells from a patient with hereditary spastic paraplegia (SPG13). Neuroscience, 153(2): p. 474-82, 2008.

102. Fukada K, Zhang F, Vien A, Cashman NR, and Zhu H. Mitochondrial proteomic analysis of a cell line model of familial amyotrophic lateral sclerosis. Mol Cell Proteomics, 3(12):1211–23, 2004.

103. Guillon B, Bulteau AL, Wattenhofer-Donze M, Schmucker S, Friguet B, Puccio H, Drapier JC, and Bouton C. Frataxin deficiency causes upregulation of mitochondrial Lon and ClpP proteases and severe loss of mitochondrial Fe-S proteins. FEBS J, 276(4): p. 1036-47, 2009.

104. Pinti M, Salomoni P, and Cossarizza A. Anti-HIV drugs and the mitochondria. Biochim Biophys

Acta, 1757(5-6): p. 700-7, 2006.

105. Ngo JK and Davies KJ. Importance of the lon protease in mitochondrial maintenance and the significance of declining lon in aging. Ann N Y Acad Sci, 1119:78–87, 2007.

106. Hu J, Bianchi F, Ferguson M, Cesario A, Margaritora S, Granone P, Goldstraw P, Tetlow M, Ratcliffe C, Nicholson AG, Harris A, Gatter K, Pezzella F. Gene expression signature for angiogenic and nonangiogenic non-small-cell lung cancer. Oncogene, 24(7): p. 1212-9, 2005.

107. Kita K, Suzuki T, and Ochi T. Diphenylarsinic acid promotes degradation of glutaminase C by mitochondrial Lon protease. J Biol Chem, 2012. 287(22): p. 18163-72.

108. Fraile JM, Quesada V, Rodríguez D, Freije JM, López-Otín C. Deubiquitinases in cancer: new functions and therapeutic options. Oncogene, 31(19): p. 2373-88, 2012.

109. Freije JM, Fraile JM, and Lopez-Otin C. Protease addiction and synthetic lethality in cancer. Front Oncol, 1: p. 25, 2011.

110. Bota DA, Remmen HV, and Davies KJ. Modulation of Lon protease activity and aconitase turnover during aging and oxidative stress. FEBS Lett, 532(1-2): p. 103-6, 2002.

111. Bakala H, Delaval E, Hamelin M, Bismuth J, Borot-Laloi C, Corman B, and Friguet B. Changes in rat liver mitochondria with aging. Lon protease-like reactivity and N(epsilon)-carboxymethyllysine accumulation in the matrix. Eur J Biochem, 270(10): p. 2295-302, 2003.

112. Huang G, Lu H, Hao A, Ng DC, Ponniah S, Guo K, Lufei C, Zeng Q, Cao X. GRIM-19, a cell death regulatory protein, is essential for assembly and function of mitochondrial complex I. Mol Cell Biol, 24(19): p. 8447-56, 2004.

113. Yang H, Brosel S, Acin-Perez R, Slavkovich V, Nishino I, Khan R, Goldberg IJ, Graziano J, Manfredi G, Schon EA. Analysis of mouse models of cytochrome c oxidase deficiency owing to mutations in Sco2. Hum Mol Genet, 2010. 19(1): p. 170-80.

114. Hance N, Ekstrand MI, and Trifunovic A. Mitochondrial DNA polymerase gamma is essential for mammalian embryogenesis. Hum Mol Genet, 14(13): p. 1775-83, 2005.

115. Humble MM, Young MJ, Foley JF, Pandiri AR, Travlos GS, Copeland WC. Polg2 is essential for mammalian embryogenesis and is required for mtDNA maintenance. Hum Mol Genet, 22(5): p. 1017-25, 2013.

116. Larsson NG, Wang J, Wilhelmsson H, Oldfors A, Rustin P, Lewandoski M, Barsh GS, Clayton DA. Mitochondrial transcription factor A is necessary for mtDNA maintenance and embryogenesis in mice. Nat Genet, 18(3): p. 231-6, 1998.

117. Hepple RT, Baker DJ, Kaczor JJ, and Krause DJ. Long-term caloric restriction abrogates the age-related decline in skeletal muscle aerobic function. FASEB J, 19(10): p. 1320-2, 2005.

118. Lanza IR, Short DK, Short KR, Raghavakaimal S, Basu R, Joyner MJ, McConnell JP, and Nair KS. Endurance exercise as a countermeasure for aging. Diabetes, 57(11): p. 2933-42, 2008.

119. Stadtman ER. Protein oxidation and aging. Science, 257(5074): p. 1220-4, 1992.

120. Friguet B, Bulteau AL, and Petropoulos I. Mitochondrial protein quality control: implications in ageing. Biotechnol J, 3(6): p. 757-64, 2008.

121. Delaval E, Perichon M, and Friguet B. Age-related impairment of mitochondrial matrix aconitase and ATP-stimulated protease in rat liver and heart. Eur J Biochem, 271(22): p. 4559-64, 2004.

122. Hoshino A, Okawa Y, Ariyoshi M, Kaimoto S, Uchihashi M, Fukai K, Iwai-Kanai E, and Matoba S. Oxidative post-translational modifications develop LONP1 dysfunction in pressure overload heart failure. Circ Heart Fail, 7(3): p. 500-9, 2014.

123. Hanahan D, Weinberg RA. Hallmarks of cancer: the next generation. Cell, 144:646-674, 2011.

124. Luo J, Solimini NL, Elledge SJ. Principles of cancer therapy: oncogene and non-oncogene addiction. Cell, 136:823-837, 2009.

125. Hanahan D, and Weinberg RA. The hallmarks of cancer. Cell, 100(1): p. 57-70, 2000.

126. Vander Heiden MG. Targeting cancer metabolism: a therapeutic window opens. Nat Rev Drug Discov, 10(9):671–84, 2011.

127. Cairns RA, Harris IS, and Mak TW. Regulation of cancer cell metabolism. Nat. Rev. Cancer, 11(2):85–95, 2011.

128. O WARBURG. On the origin of cancer cells. Science, 123(3191):309–14, 1956.

129. Weinberg F, Hamanaka R, Wheaton WW, Weinberg S, Joseph J, Lopez M, Kalyanaraman B, Mutlu GM, Budinger GR, and Chandel NS. Mitochondrial metabolism and ROS generation are essential for Krasmediated tumorigenicity. Proc Natl Acad Sci U.S.A., 107(19):8788–93, 2010.

130. Lunt SY and Vander Heiden MG. Aerobic glycolysis: meeting the metabolic requirements of cell proliferation. Annu Rev Cell Dev. Biol., 27:441–64, 2011.

131. Weinhouse S. The Warburg hypothesis fifty years later. Z Krebsforsch Klin Onkol Cancer Res Clin Oncol, 87(2):115–26, 1976.

132. Zu XL and Guppy M. Cancer metabolism: facts, fantasy, and fiction. Biochem Biophys Res Commun, 313(3):459–65, 2004.

133. DeBerardinis RJ, Lum JJ, Hatzivassiliou G, and Thompson CB. The biology of cancer: metabolic reprogramming fuels cell growth and proliferation. Cell Metab, 7(1):11–20, 2008.

134. Wallace DC. Mitochondria and cancer. Nat Rev Cancer, 12(10):685–98, 2012.

135. Feron O. Pyruvate into lactate and back: from the Warburg effect to symbiotic energy fuel exchange in cancer cells. Radiother Oncol, 92(3): p. 329-33, 2009.

136. Kennedy KM and Dewhirst MW. Tumor metabolism of lactate: the influence and therapeutic potential for MCT and CD147 regulation. Future Oncol, 6(1): p. 127-48, 2010.

137. Semenza GL. Tumor metabolism: cancer cells give and take lactate. J Clin Invest, 118(12): p. 3835-7, 2008.

138. Hardee ME, Dewhirst MW, Agarwal N, Sorg BS. Novel imaging provides new insights into mechanisms of oxygen transport in tumors. Curr Mol Med, 9(4): p. 435-41, 2009.

139. Tan AS, Baty JW, and Berridge MV. The role of mitochondrial electron transport in tumorigenesis and metastasis. Biochim Biophys Acta, 1840(4):1454–1463, 2014.

140. Lunt SJ, Chaudary N, and Hill RP. The tumor microenvironment and metastatic disease. Clin Exp Metastasis, 26(1):19–34, 2009.

141. Hu Y, Lu W, Chen G, Wang P, Chen Z, Zhou Y, Ogasawara M, Trachootham D, Feng L, Pelicano H, Chiao PJ, Keating MJ, Garcia-Manero G, Huang P. (G12V) transformation leads to mitochondrial dysfunction and a metabolic switch from oxidative phosphorylation to glycolysis. Cell Res, 22(2): p. 399-412, 2012.

142. Wallace DC. A mitochondrial paradigm of metabolic and degenerative diseases, aging, and cancer: a dawn for evolutionary medicine. Annu Rev Genet, 39: p. 359-407, 2005.

143. Goard CA and Schimmer AD. Mitochondrial matrix proteases as novel therapeutic targets in malignancy. Oncogene, 2013.

144. Bayot A, Gareil M, Chavatte L, Hamon MP, L'hermitte-Stead C, Beaumatin F, Priault M, Rustin P, Lombès A, Friguet B, and Bulteau AL. Effect of Lon protease knockdown on mitochondrial function in HeLa cells. Biochimie, 100:38–47, 2014.

145. Nie X, Li M, Lu B, Zhang Y, Lan L, Chen L, and Lu J. Downregulating overexpressed human Lon in cervical cancer suppresses cell proliferation and bioenergetic. PLoS ONE, 8(11):e81084, 2013.

146. Cheng CW, Kuo CY, Fan CC, Fang WC, Jiang SS, Lo YK, Wang TY, Kao MC, and Lee AY. Overexpression of Lon contributes to survival and aggressive phenotype of cancer cells through mitochondrial complex I-mediated generation of reactive oxygen species. Cell Death Dis, 4:e681, 2013.

147. Chen Y, Fu LL, Wen X, Wang XY, Liu J, Cheng Y, and Huang J. Sirtuin-3 (SIRT3), a therapeutic target with oncogenic and tumor-suppressive function in cancer. Cell Death Dis, 5: p. e1047, 2014.

148. Onyango P, Celic I, McCaffery JM, Boeke JD, and Feinberg AP. SIRT3, a human SIR2 homologue, is an NAD-dependent deacetylase localized to mitochondria. Proc Natl Acad Sci U S A, 99(21): p. 13653-8, 2002.

149. Mel'nikov EE, Tsirul'nikov KB, and Rotanova TV. Coupling of proteolysis and hydrolysis of ATP upon functioning of Lon proteinase of Escherichia coli. II. Hydrolysis of ATP and activity of peptide hydrolase sites of the enzyme. Bioorg Khim, 27(2): p. 120-9, 2001.

150. Thomas-Wohlever J and Lee I. Kinetic characterization of the peptidase activity of Escherichia coli Lon reveals the mechanistic similarities in ATP-dependent hydrolysis of peptide and protein substrates. Biochemistry, 41(30): p. 9418-25, 2002.

151. Granot Z, Geiss-Friedlander R, Melamed-Book N, Eimerl S, Timberg R, Weiss AM, Hales KH,. Hales DB, Stocco DM, and Orly J. Proteolysis of normal and mutated steroidogenic acute regulatory proteins in the mitochondria: the fate of unwanted proteins. Mol Endocrinol, 17(12): p. 2461-76, 2003.

152. Adams J. The proteasome: a suitable antineoplastic target. Nat Rev Cancer, 4(5):349–60, 2004.

153. Frase H and Lee I. Peptidyl boronates inhibit Salmonella enterica serovar Typhimurium Lon protease by a competitive ATP-dependent mechanism. Biochemistry, 46(22):6647–57, 2007.

154. Deeb D, Gao X, Arbab AS, Barton K, Dulchavsky SA, and Gautam SC. CDDO-Me: A Novel

Synthetic Triterpenoid for the Treatment of Pancreatic. Cancer Cancers (Basel), 2(4)1779–93, 2010.

155. Ikeda T, Sporn M, Honda T, Gribble GW, Kufe D. The novel triterpenoid CDDO and its derivatives induce apoptosis by disruption of intracellular redox balance. Cancer Res, 63(17)5551–5558, 2003.

156. Gao X, Deeb D, Arbab AS, Dulchavsky SA, Gautam SC. Synthetic triterpenoids inhibit growth, induce apoptosis and suppress Akt, mTOR and NF-κB signaling proteins in colorectal cancer cells. Anticancer Res. 30(3)785–792, 2010.

157. Gao X, Liu Y, Deeb D, Arbab AS, Guo AM, Dulchavsky SA, and Gautam SC. Synthetic oleanane triterpenoid, cddo-me, induces apoptosis in ovarian cancer cells by inhibiting prosurvival akt/nf-κb/ mtor signaling. Anticancer Res, 31(11)3673–3681, 2011.

158. Liby KT and Sporn MB. Synthetic oleanane triterpenoids: multifunctional drugs with a broad range of applications for prevention and treatment of chronic disease. Pharmacol ReV, 64(4)972–1003, 2012.

159. Gibellini L, Pinti M, Bartolomeo R, De Biasi S, Cormio A, Musicco C, Carnevale G, Pecorini S, Nasi M, De Pol A, Cossarizza A. Inhibition of Inhibition of Lon protease by triterpenoids alters mitochondria and is associated to cell death in human cancer cells. Oncotarget, 6(28):25466-83, 2015.

160. Shanmugam MK, Dai X, Kumar AP, Tan BK, Sethi G, and Bishayee A. Oleanolic acid and its synthetic derivatives for the prevention and therapy of cancer: Preclinical and clinical evidence. Cancer Lett, 346(2):206–16, 2014.

161. Gao X, Liu Y, Deeb D, Liu P, Liu A, Arbab AS, and Gautam SC. ROS mediate proapoptotic and antisurvival activity of oleanane triterpenoid CDDO-Me in ovarian cancer cells. Anticancer Res, 33(1):215–21, 2013.

162. Deeb D, Gao X, Jiang H, Janic B, Arbab AS, Rojanasakul Y, Dulchavsky SA, Gautam SC. Oleanane triterpenoid CDDO-Me inhibits growth and induces apoptosis in prostate cancer cells through a ROS-dependent mechanism. Biochem Pharmacol, 79(3)350–360, 2010.

163. Brookes PS, Morse K, Ray D, Tompkins A, Young SM, Hilchey S, Salim S, Konopleva M, Andreeff M, Phipps R, and Bernstein SH. The triterpenoid 2-cyano-3,12-dioxooleana-1,9-dien-28-oic acid and its derivatives elicit human lymphoid cell apoptosis through a novel pathway involving the unregulated mitochondrial permeability transition pore. Cancer Res, 67(4):1793–802, 2007.

164. Wang HM, Cheng KC, Lin CJ, Hsu SW, Fang WC, Hsu TF, Chiu CC, Chang HW, Hsu CH, and Lee AY. Obtusilactone A and (-)-sesamin induce apoptosis in human lung cancer cells by inhibiting mitochondrial Lon protease and activating DNA damage checkpoints, Cancer Sci, 101(12): p. 2612-20, 2010.

165. Kikuchi M, Hatano N, Yokota S, Shimozawa N, Imanaka T, and Taniguchi H. Proteomic analysis of rat liver peroxisome: presence of peroxisome-specific isozyme of Lon protease. J Biol Chem, 279(1): p. 421-8, 2004.

166. Okumoto K, Kametani Y, and Fujiki Y. Two proteases, trypsin domain-containing 1 (Tysnd1) and peroxisomal lon protease (PsLon), cooperatively regulate fatty acid beta-oxidation in

peroxisomal matrix. J Biol Chem, 286(52): p. 44367-79, 2011.

167. Omi S, Nakata R, Okamura-Ikeda K, Konishi H, and Taniguchi H. Contribution of peroxisome-specific isoform of Lon protease in sorting PTS1 proteins to peroxisomes. J Biochem, 143(5): p. 649-60, 2008.

168. Pinti M, Gibellini L, Liu Y, Xu S, Lu B, Cossarizza A. Mitochondrial Lon protease at the crossroads of oxidative stress, ageing and cancer. Cell Mol Life Sci, 72(24):4807-24, 2015.

169. Quaglino D, Boraldi F, Barbieri D, Croce A, Tiozzo R, Pasquali Ronchetti I. Abnormal phenotype of *in vitro* dermal fibroblasts from patients with Pseudoxanthoma elasticum (PXE). Biochim Biophys Acta, 1501:51–62, 2000.

170. Addis MF, Tanca A, Pagnozzi D, Crobu S, Fanciulli G, Cossu-Rocca P, Uzzau S. Generation of high-quality protein extracts from formalin-fixed, paraffin-embedded tissues. Proteomics, 9(15): 3815-23, 2009.

171. Galluzzi L, Pinti M, Guaraldi G, Mussini C, Troiano L, Roat E, Giovenzana C, Nemes E, Nasi M, Orlando G, Salomoni P, Cossarizza A. Altered mitochondrial RNA production in adipocytes from HIV-infected individuals with lipodystrophy. Antivir Ther, 10 Suppl 2: p. M91-9, 2005.

172. Cossarizza A, Riva A, Pinti M, Ammannato S, Fedeli P, Mussini C, Esposito R, Galli M. Increased mitochondrial DNA content in peripheral blood lymphocytes from HIV-infected patients with lipodystrophy. Antivir Ther, 8(4): p. 315-21, 2003.

173. Cossarizza A, Baccarani-Contri M, Kalashnikova G and Franceschi C. A new method for the cytofluorimetric analysis of mitochondrial membrane potential using the J-aggregate forming lipophilic cation 5,5',6,6'-tetrachloro-1,1',3,3'-tetraethylbenzimidazolcarbocyanine iodide (JC-1). Biochem Biophys Res Commun, 197(1):40-45, 1993.

174. Troiano L, Ferraresi R, Lugli E, Nemes E, Roat E, Nasi M, Pinti M, and Cossarizza A. Multiparametric analysis of cells with different mitochondrial membrane potential during apoptosis by polychromatic flow cytometry. Nat Protoc, 2(11):2719–27, 2007.

175. Barbieri D, Abbracchio MP, Salvioli S, Monti D, Cossarizza A, Ceruti S, Brambilla R, Cattabeni F, Jacobson KA and Franceschi C. Apoptosis by 2-chloro-2'-deoxy-adenosine and 2-chloro-adenosine in human peripheral blood mononuclear cells. Neurochem Int, 32(5-6):493-504, 1998.

176. Salvioli S, Dobrucki J, Moretti L, Troiano L, Fernandez MG, Pinti M, Pedrazzi J, Franceschi C and Cossarizza A. Mitochondrial heterogeneity during staurosporine-induced apoptosis in HL60 cells: analysis at the single cell and single organelle level. Cytometry, 40(3):189-197, 2000.

177. Hoffstrom BG, Kaplan A, Letso R, Schmid RS, Turmel GJ, Lo DC, and Stockwell B R. Inhibitors of protein disulfide isomerase suppress apoptosis induced by misfolded proteins. Nat Chem Biol 6, 900-906, 2010.

178. Inwald EC, Klinkhammer-Schalke M, Hofsta¨dter F, Zeman F, Koller M, Gerstenhauer M, Ortmann O. Ki-67 is a prognostic parameter in breast cancer patients: results of a large population-based cohort of a cancer registry. Breast Cancer Res Treat 139:539–552, 2013.

179. Breier G, Grosser M, Rezaei M. Endothelial cadherins in cancer. Cell Tissue Res, 355(3):523-7, 2014.

180. Lee S, Tak E, Lee J, Rashid MA, Murphy MP, Ha J, Kim SS. Mitochondrial H2O2 generated from electron transport chain complex I stimulates muscle differentiation. Cell Res, 21:817–834, 2011.

181. Zhou Y, Hileman EO, Plunkett W, Keating MJ, Huang P. Free radical stress in chronic lymphocytic leukemia cells and its role in cellular sensitivity to ROS-generating anticancer agents. Blood, 101:4098–4104, 2003.

182. Chen Y, McMillan-Ward E, Kong J, Israels SJ, Gibson SB. Oxidative stress induces autophagic cell death independent of apoptosis in transformed and cancer cells. Cell Death Differ, 15:171–182, 2008.

183. Lee HC, Yin PH, Chi CW, Wei YH. Increase in mitochondrial mass in human fibroblasts under oxidative stress and during replicative cell senescence. J Biomed Sci, 9:517–526, 2002.

184. Apostolova N, Gomez-Sucerquia LJ, Moran A, Alvarez A, Blas-Garcia A, Esplugues JV. Enhanced oxidative stress and increased mitochondrial mass during efavirenz-induced apoptosis in human hepatic cells. Br J Pharmacol, 160:2069–2084, 2010.

ACKNOWLEDGEMENTS

At the end of my PhD course I would like to thank all those people who made this thesis possible and an unforgettable experience for me.

First of all I would like to express my sincere gratitude to my Tutor Prof. Andrea Cossarizza for the continuous support of my PhD study and research, for his motivation, enthusiasm, and immense knowledge.

Special thanks to Prof. Marcello Pinti for the absolute support to my research. I thank him for the systematic guidance and for giving me precious advices.

My sincere thanks also goes to Dr. Lara Gibellini, for her continuous advice and encouragement throughout the course of these three years. Her guidance helped me in all the time of research and writing of this thesis.

I also wish to thank Dr. Sara De Biasi, Dr. Milena Nasi, Elena Bianchini and Simone Pecorini for the support and encouragement whenever I was in need, and for their precious friendship.

Last but not the least, I would like to express a special thank to my family: my parents, my grandparents, my sister, Danilo and Mirko, for supporting me spiritually throughout my life. Their encouragement and love are my power.